

QUASI-ISOLATED HIGHWAY BRIDGES:
INFLUENCE OF BEARING ANCHORAGE STRENGTH ON SEISMIC PERFORMANCE

BY

JESSICA REVELL

THESIS

Submitted in partial fulfillment of the requirements
for the degree of Master of Science in Civil Engineering
in the Graduate College of the
University of Illinois at Urbana-Champaign, 2013

Urbana, Illinois

Advisers:

Associate Professor James M. LaFave
Assistant Professor Larry A. Fahnestock

ABSTRACT

The Illinois Department of Transportation (IDOT) commonly uses elastomeric bearings to accommodate thermal deformations in bridges, and these bearings also have potential utility in seismic events. IDOT has developed an earthquake resisting system (ERS) using the displacement capacity of typical bearings to achieve a structural response similar to isolation. Earlier research at the University of Illinois comprised full-scale laboratory tests of bearings, and computational models capturing full-bridge seismic response. This prior research validated the quasi-isolated ERS, demonstrated that most bridges in Illinois would not experience severe damage during a 75-year design life, and indicated calibration of fuse capacities might improve overall bridge response. Current research focused on the potential for bearing anchorage capacity to calibrate bridge response in the longitudinal and transverse directions. A suite of 24 bridges was created with variables that included superstructure type, pier height, and anchorage strength. A set of ten synthetic ground motions from the New Madrid Seismic Zone were scaled to match the AASHTO seismic design spectra for Cairo, Illinois, and applied in the longitudinal and transverse directions during a total of 480 nonlinear dynamic analyses conducted in OpenSees. Based on the sensitivity study, longitudinal response was largely insensitive to anchor bolt diameter, but transverse response displayed sensitivity and offered potential for performance calibration. Bridges with short piers and light superstructures were most responsive to anchor bolt calibration, and the use of smaller anchor bolts was effective at reducing column damage. The bearing sliding that followed anchor bolt fracture led to larger superstructure displacements, but never led to unseating or a risk of span loss.

ACKNOWLEDGEMENTS

Many thanks are due my advisors, Dr. James LaFave and Dr. Larry Fahnestock, for the opportunity to be part of this project. Thanks also to Dr. Doug Foutch, who so willingly took the time to provide guidance, review papers, and share his knowledge of bridge design. To graduate students Joshua Steelman and Evgueni Filipov - it was only by standing on your shoulders that this thesis came to fruition. Lastly, my thanks and admiration go out to Dr. Dan Tobias and Mark Shaffer at IDOT. Without their enthusiasm and commitment to Illinois infrastructure, I suspect this project would never have been.

TABLE OF CONTENTS

CHAPTER 1 - INTRODUCTION.....	1
CHAPTER 2 - PRIOR RESEARCH	6
CHAPTER 3 - SENSITIVITY STUDY	23
CHAPTER 4 - DYNAMIC ANALYSES.....	31
CHAPTER 5 - RESULTS.....	55
CHAPTER 6 - CONCLUSIONS.....	80
REFERENCES	83
APPENDIX A - NUMERICAL RESULTS	86
APPENDIX B - GROUND MOTIONS	100

CHAPTER 1

INTRODUCTION

1.1 MOTIVATION FOR RESEARCH PROJECT

The 2009 AASHTO seismic provisions increased the design earthquake return period from 500 to 1000 years, leading to higher bridge design and construction costs. Such code updates have been guided primarily by the seismic practices in the western United States, and have focused on bridge configurations where energy is dissipated by either plastic deformation of the piers, or a specially designed and constructed seismic isolation device placed between the superstructure and substructure.

The Illinois Department of Transportation (IDOT) has identified the potential to adapt concepts underpinning this second 'classical isolation' approach to formulate a cost-effective 'quasi-isolation' alternative, targeted to the seismic hazard and typical bridge configurations in Illinois. The quasi-isolated earthquake resisting system uses conventional elastomeric bearing elements, but deviates from conventional seismic design requirements by allowing bearing anchorages to fracture during a design earthquake and relies on the subsequent bearing deformation and sliding to accommodate seismic demands. Sufficient seat width is provided to allow bearing sliding, and as a tertiary level of redundancy, the piers can be used to dissipate additional energy.

IDOT joined with the Illinois Center for Transportation and the University of Illinois at Urbana-Champaign to complete ICT Project R27-070, *Calibration and Refinement of Illinois' Earthquake Resisting System Bridge Design Methodology*. The objective of Project R27-070 was to facilitate implementation of the quasi-isolated seismic design concept through a combined experimental and analytical program at the University of Illinois at Urbana-Champaign. IDOT Type I and II elastomeric bearings were tested in the laboratory along with retainers and fixed bearings. Nonlinear numerical bearing models were then developed based on this experimental data and incorporated into 3D finite element bridge models to explore the system-level response of typical IDOT bridges.

The experimental program demonstrated that elastomeric bearings are extremely resilient, and able to accommodate displacements many times in excess of the shear strains conventionally allowed by AASHTO for bearing design. Based on the global bridge analyses most bridges in

Illinois would not experience severe damage during a 75-year design life. However, the fixed bearings and retainers did not always fuse as intended, and moderate pier damage was often recorded. Overall, ICT R27-070 indicated the quasi-isolated ERS has potential but would benefit from further calibration.

This thesis looks at the potential to calibrate the quasi-isolated ERS via bearing anchorage strength. A sensitivity study of the superstructure to substructure connecting elements (i.e. retainers and fixed bearings) was devised to determine which components are the most critical and to seek improved system behavior. The primary task was to assess the influence of fusing component force-capacity on peak sliding displacement of the superstructure and peak strains in the column plastic hinge zone. Sensitivity of response to input ground motion was also considered, providing data that may be used to envelope force and displacement demands as part of developing a simplified design method. The research presented in this report builds upon the results of ICT R27-070 and should assist IDOT in further developing a consistent bridge design approach that can balance structural safety with design methodologies and construction practices appropriate for the state of Illinois.

1.2 REPORT ORGANIZATION

The primary goal of this research has been to investigate bearing anchorage strength as a calibration method for the quasi-isolated ERS, focusing on seismic hazards and bridge configurations appropriate for Illinois. Following is a brief summary of the contents.

Chapter 1 discusses the motivation for the research, and provides an overview of the state-of-practice for the design of bridge bearings and bridge seismic design.

Chapter 2 discusses the methodology and key results of the earlier research that provided the foundation and impetus for the current sensitivity study.

Chapter 3 explains the methodology of the sensitivity study.

Chapter 4 presents results of the dynamic analyses.

Chapter 5 presents results of the overall sensitivity study.

Chapter 6 discusses key observations and conclusions.

1.3 STATE-OF-PRACTICE REVIEW

1.3.1 Bridge Bearings

In conventional (i.e. thermal expansion) applications, steel-reinforced elastomeric bearings must be designed to resist loads and accommodate movement at the service and strength limit states. Failure of the bearing is generally due to gradual deterioration over many cycles rather than sudden failure under a single load, and the AASHTO specifications are written with an eye to controlling compressive stress, uplift, buckling, and fatigue over the design life of the bearing (Roeder and Stanton 1991).

The AASHTO specifications allow two distinct methods for elastomeric bearing design. Both methods require bearings to be checked at limit states governed by compression stress, combined compression and rotation, buckling stability, shear, and stress on the internal reinforcing. Method A is the older, simpler, and more conservative method. This design approach allows shear modulus to be approximated from hardness measurements. By comparison, Method B requires laboratory testing to verify shear modulus, but compensates for the additional material testing with less stringent stress and deformation limits (AASHTO 2008). This method is the more rigorous of the two, and requires significantly more effort on the part of the designer, but may result in a bearing that uses less material.

The criteria employed by IDOT for elastomeric bearings are summarized below and generally align with AASHTO Method A (IDOT 2012).

- The total elastomer height must be at least twice the total movement for a Type I bearing and equal to the total movement for a Type II bearing, effectively limiting shear strain to roughly 50% in order to control bearing fatigue.
- The width of the bearing parallel to the direction of movement must be at least three times the total elastomer height in order to ensure stability of the bearing under service loads.
- The average compression stress from dead load must be between 200 and 500 psi.
- The average compression stress from dead load and live load (without impact) must be between 200 and 800 psi. This is more conservative than the AASHTO criteria, which would allow up to 1,250 psi average compression stress.

IDOT has augmented these provisions with tabular and graphical design aids that incorporate the design parameters and limitations, and simplify the elastomeric bearing selection process for ordinary highway bridges.

1.3.2 Seismic Design

In bridge seismic design, the Earthquake Resisting System (ERS) controls the seismic displacements and provides the load path for transmitting seismically induced forces down into the ground. In the AASHTO Guide Specifications for LRFD Seismic Bridge Design, there are three recognized ERS categories (AASHTO 2009):

- Type I – A ductile substructure with essentially elastic superstructure. This is the conventional seismic design approach, and is representative of the way that many IDOT bridges are currently designed for seismic effects.
- Type II – An essentially elastic substructure with ductile superstructure. This less common approach applies only to steel superstructures with specially detailed ductile cross-frames.
- Type III – An elastic superstructure and substructure with a fusing mechanism in between. This approach is characteristic of traditional seismic isolation, and is also representative of the philosophy IDOT is targeting with the quasi-isolated ERS concept.

A Type I ERS generally employs a capacity design approach, wherein the substructure is specially detailed for a ductile response, and the foundation and superstructure are provided with sufficient strength to remain essentially elastic while plastic hinges form in the substructure. In high seismic zones, this requires designers to complete involved analyses, and the labor-intensive detailing requirements can inflate construction costs.

Bridges designed with traditional seismic isolation utilize a Type III ERS, and a vertical load-carrying component that also functions as a seismic isolator is placed between the superstructure and substructure. This isolation device is designed to carry the bulk of the seismic displacement and provides sufficient lateral flexibility to lengthen the period of the system. This period elongation can significantly reduce seismic forces, but there is generally a concomitant reduction in stiffness that leads to increased displacements, as illustrated conceptually in Figure 1.1 and Figure 1.2 (Buckle et al. 2006). In order to limit displacements to practical magnitudes, it

is necessary to introduce additional energy dissipation into the isolation system by way of hysteretic or viscous damping. The isolation system should also have some means of ensuring lateral rigidity under service loads such as wind and truck-braking.

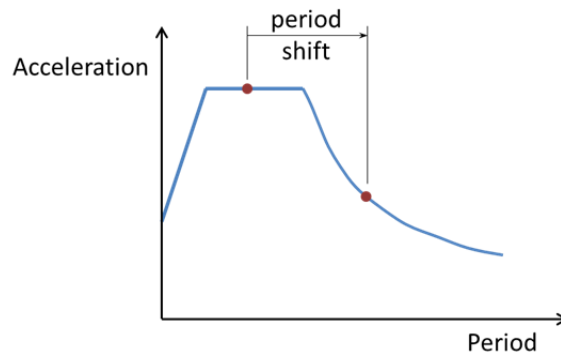


Figure 1.1. Effect of Period Shift on Acceleration.

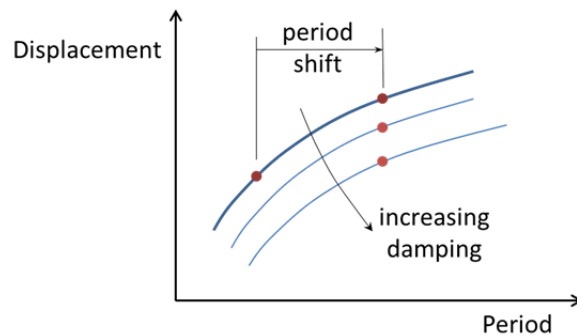


Figure 1.2. Effect of Period Shift and Damping on Displacement Response.

CHAPTER 2

PRIOR RESEARCH

2.1 OVERVIEW OF PRIOR RESEARCH

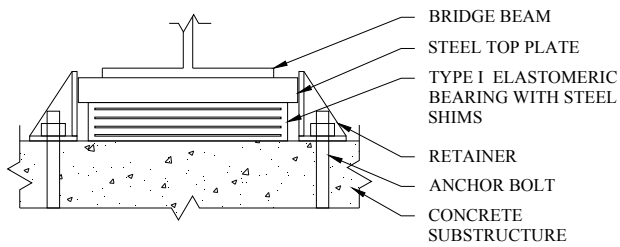
Prior research consisted of ICT Project R27-070, *Calibration and Refinement of Illinois' Earthquake Resisting System Bridge Design Methodology* (LaFave et al. 2013a, 2013b), a combined experimental and analytical program conducted at the University of Illinois at Urbana-Champaign from 2009 to 2012. Typical IDOT bearing components were tested in the UIUC laboratory to characterize bearing performance at large displacements. Nonlinear numerical bearing models were developed based on this experimental data and incorporated into finite element bridge models to explore the system-level response of typical IDOT bridges. The project served to investigate and validate the IDOT ERS strategy, focusing on the specific seismic hazard and bridge structural characteristics appropriate for Illinois. The new research presented in this document follows directly from the existing work and thus, this chapter provides essential background information.

2.2 BEARING TESTS AND PHENOMENOLOGICAL MODELS

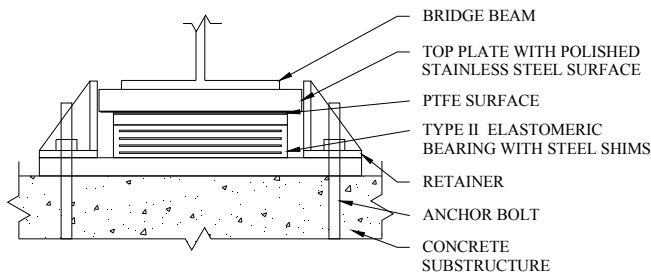
Full-scale bearing tests were conducted from 2009 to 2012 at the Newmark Structural Engineering Laboratory using a customized test setup designed to represent field conditions. Bearings were installed on a concrete pad with broom-finished surface, vertical load was applied with a pair of 100 kip actuators, and lateral displacements were imposed with a 30 in stroke, 220 kip actuator. The following subsections summarize key experimental outcomes based on details of experimental protocols and test results reported elsewhere (Steelman et al. 2012; LaFave et al. 2013a).

The bearing types included in the experimental program are shown in Figure 2.1, via a schematic drawing on the left and a test photo on the right. Type I bearings use steel reinforced elastomer vulcanized to a plate attached to the bridge girder. The bottom of the elastomer bears directly on the concrete substructure and this defines the sliding interface. Type II bearings also use steel reinforced elastomer, but it is vulcanized to both a top and bottom plate and the bottom plate is anchored to the concrete substructure. The top plate features a layer of PTFE that creates a sliding interface with a stainless steel sheet attached to the bridge girder. In the transverse

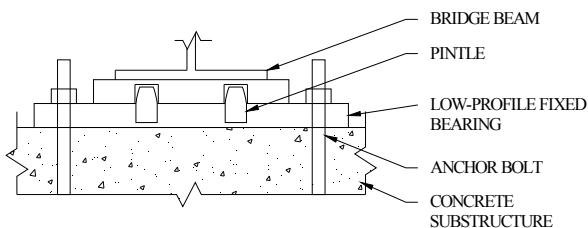
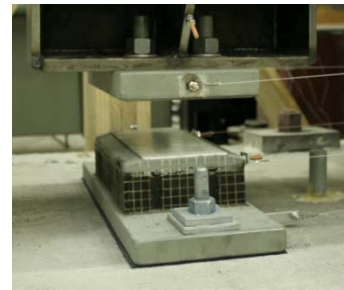
direction, both Type I and Type II bearings feature L-shaped retainers anchored to the substructure. These retainers are meant to prevent transverse bridge movement under service loads but to break off and permit bearing sliding during an earthquake. Fixed bearings consist of a bottom plate anchored to the substructure that mates with a curved top plate via two pintles.



Type I Bearing



Type II Bearing



Low-Profile Fixed Bearing



Figure 2.1. Examples of IDOT Bearings Included in the Testing Program (LaFave et al. 2013a)

The experimental results were used to develop and validate nonlinear elements capable of capturing the experimentally observed bearing behaviors. The following subsections contain a brief description of bearing element characteristics based on details of bearing element formulation reported elsewhere (Filipov et al. 2013a; Filipov 2012).

2.2.1 IDOT Type I and Type II Bearings

Tests of Type I bearings were conducted at 200 psi, 500 psi and 800 psi bearing pressures. Bearings began sliding between 125% and 250% shear strain, and initial coefficients of friction were between 0.25 and 0.5. An increase in bearing pressure delayed the onset of sliding and decreased the coefficient of friction. During the early sliding cycles the bottom surface of the elastomer was abraded by the roughened concrete substructure and a layer of elastomer was ground into the concrete, reducing the surface roughness. After a few cycles, the coefficient of friction stabilized at approximately 0.1 to 0.15 below the initial coefficient. Note that most data was obtained from tests conducted at very low strain rates (0.003 in./sec) and a limited subset of tests conducted at higher strain rates (4 in./sec) showed an estimated 33% increase in the breakaway friction – an observation that informed the selection of friction parameters for the computational models.

Type II bearings were all tested at higher strain rates (0.6 to 2.5 in./sec) and the coefficients of friction for the PTFE/stainless steel sliding interface ranged from 0.13 to 0.15. While the PTFE interface did not produce the pronounced degradation or stick-slip behavior observed at the Type I concrete interface, the overall response was similar and thus the same phenomenological model could be used for both Type I and Type II bearings.

A nonlinear bi-directional sliding bearing element, similar to Constantinou et al (1990), was developed to capture elastomeric bearing response in the global bridge models. The model could represent the initial static breakoff coefficient (μ_{SI}), the kinetic coefficient (μ_k), and the post-slip breakoff (μ_{SP}) sometimes observed when the sliding direction reversed. Element response was also a function of the instantaneous vertical load on the bearing. A conceptual sketch of the bearing model is provided in Figure 2.2, and Figure 2.3 shows a comparison of experimental results with the behavior predicted by the numerical model. The specific Type I and Type II parameters summarized in Table 2.1 were based on the experimental data.

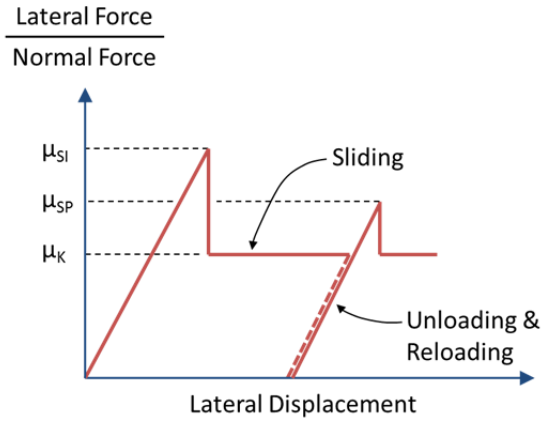


Figure 2.2. Sliding Bearing Force-Disp. Model

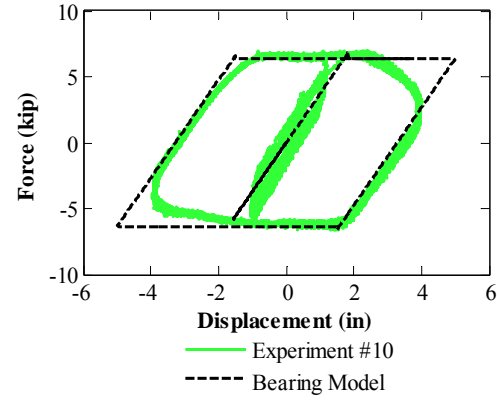


Figure 2.3. Experimental and Numerical Response for a Type II Bearing

Table 2.1. Bearing Model Parameters for Type I and Type II Bearings

Property		Type I	Type II
G	Shear Modulus	85 psi	85 psi
μ_{SI}	Initial static coefficient of friction	0.60	0.16
μ_K	Kinetic coefficient of friction	0.45	0.15
μ_{SP}	Stick-slip coefficient of friction	0.50	0.15

2.2.2 Retainers

Typical IDOT retainers are stiffened L-shaped brackets positioned adjacent to Type I and Type II bearings and secured to the concrete substructure with anchor bolts. These retainers restrict transverse bearing motion under service conditions but rupture and allow sliding in a seismic event. By current IDOT design provisions, retainers are intended to rupture at a lateral load equal to 20% of the dead load (IDOT 2012). Experimental testing of individual retainers and retainer-bearing assemblies showed marked variation in retainer response, complex failure mechanisms, and failure loads significantly in excess of 20% dead load (LaFave et al. 2013b).

The response generally began with elasto-plastic deformation of the anchor followed by localized concrete crushing around the anchor and the retainer toe, and finally anchor bolt fracture by a tension-shear mechanism. A discussion of retainer response and suggestions for capacity estimation have been presented elsewhere (LaFave et al. 2013a and 2013b). For numerical modeling, the simplified force displacement model shown in Figure 2.4 captured the basic observed behavior entirely through elasto-plastic response of the anchor bolt followed by

failure at a user-defined ultimate displacement (Filipov et al. 2013a). Figure 2.5 illustrates that this simple approach provided reasonable correlation with experimental results of individual retainer tests. The values selected for elastic stiffness, plastic stiffness, yield displacement, and ultimate displacement were based on data from the experimental program.

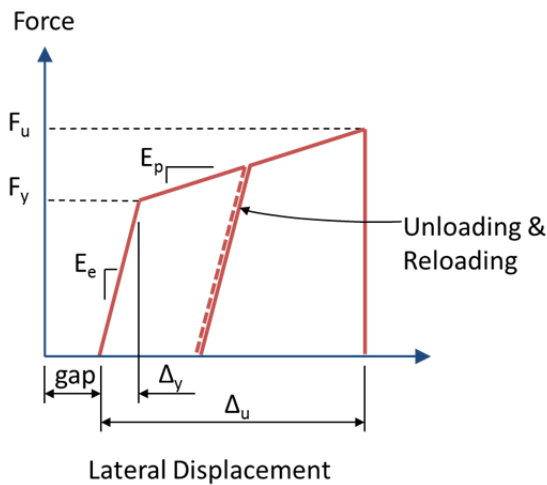


Figure 2.4. Retainer Force-Disp. Model

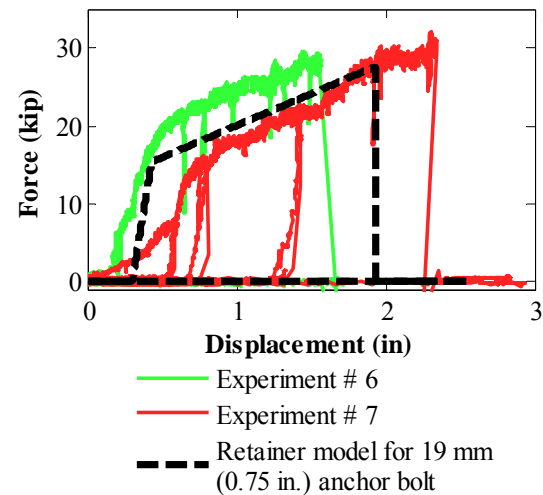


Figure 2.5. Experimental and Numerical Pushover Response for Retainer (Filipov et al. 2013a)

2.2.3 IDOT Low-Profile Fixed Bearings

Low-profile fixed bearings are generally placed on a 0.125 in. neoprene leveling pad and secured to the concrete substructure with anchor bolts. In tests, fixed bearing response was controlled by shear rupture of the concrete anchors, and the steel bottom plate subsequently slid on the neoprene leveling pad with an observed coefficient of friction between 0.2 and 0.35.

A bi-directional nonlinear element based on research by Ibarra (2005) modeled anchor bolt behavior via an elasto-plastic response with variable pinching followed by fracture at a predefined displacement (Filipov et al. 2013a). This anchor bolt element was coupled with a sliding bearing element that captured the friction between the bottom plate and leveling pad. Model parameters for the fixed bearing element were calibrated against test data, and Figure 2.6 shows a comparison of observed response with the behavior predicted by the numerical model.

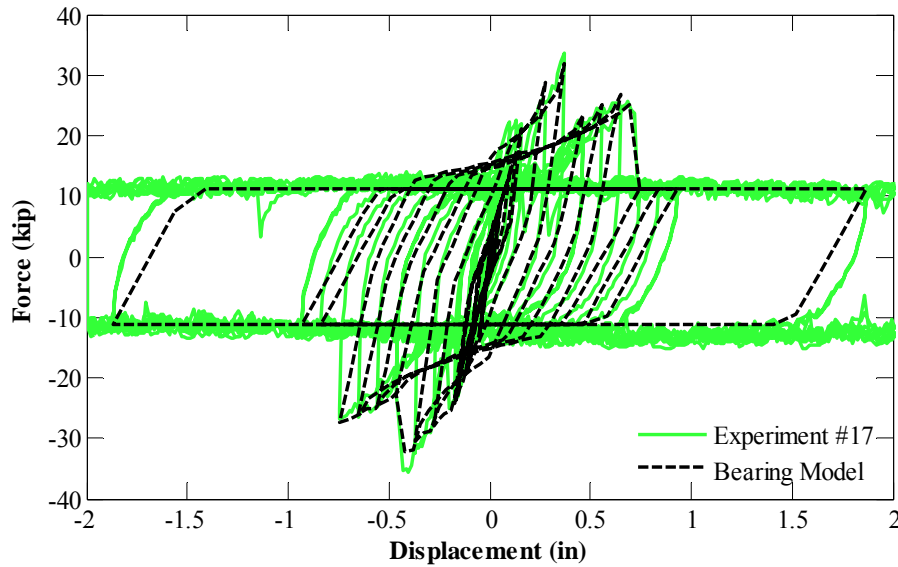


Figure 2.6. Experimental and Numerical Response for a Fixed Bearing

2.3 GLOBAL BRIDGE MODELING

In the analytical study, component-level bearing models were incorporated into 3-D finite element bridge models to explore the system-level response of typical IDOT bridges. A prototype bridge model was formulated with the ability to capture a variety of nonlinear behaviors potentially exhibited under earthquake loading. Variations of the model were then developed to envelope a range of bridge systems encountered in practice. The suite of 48 bridges was analyzed as part of a parametric study using the open source nonlinear seismic analysis program, OpenSees (McKenna et al., 2011).

The prototype bridge, shown in Figure 2.7, featured a three-span continuous steel I-girder superstructure supported on multi-column concrete piers and stub abutments. All components were proportioned in accordance with the IDOT Bridge Manual (2012). The 42 ft superstructure width accommodated two lanes of traffic and consisted of six W27x84 girders composite with an 8 in. cast-in-place concrete deck. All superstructure elements were modeled as linear-elastic.

Low-profile fixed bearings were installed at Pier 2, while Type I elastomeric bearings were used at Pier 1 and the abutments. The multi-column piers had a 15 ft clear height and were modeled using beam-column elements with fiber sections in the plastic hinge zones to capture material nonlinearities in the concrete and steel reinforcement. Foundations were modeled as fixed, representing bearing on rock. The abutment backwalls incorporated a 2 in. gap to simulate an expansion joint along with a rotational plastic hinge, and backfill response was captured with

nonlinear springs. A detailed discussion of the bridge modeling is presented by Filipov et al. (2013a).

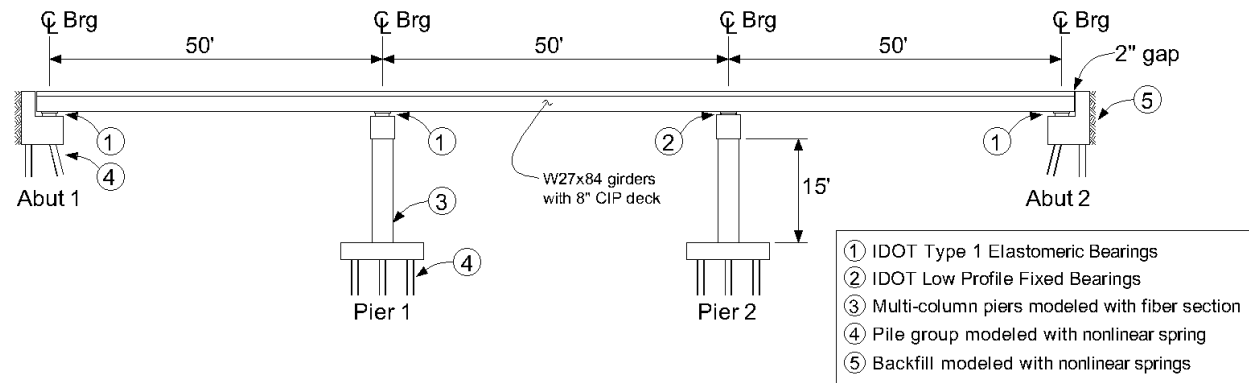


Figure 2.7. Prototype Bridge Model

The bridges selected for the parametric study incorporated variations in superstructure type (**Ss** short steel, **Sl** long steel, **Cs** precast concrete), substructure type (**C** column pier, **W** wall pier), substructure height (**15** ft, **40** ft), elastomeric bearing type (**T1** Type I IDOT bearings, **T2** Type II IDOT bearings), and foundation type (**F** fixed/rock, **S** flexible boundary condition). Individual bridge models were named with a series of letters and numbers to indicate selected parameters. For example, the prototype bridge was named SsC15T1F – a short steel superstructure with 15 ft column piers, Type I bearings, and fixed foundations. Note that Pier 2 always used low-profile fixed bearings, and the foundation boundary condition was an independent variable from the ground motion parameters discussed subsequently.

On the basis of studies of the New Madrid Seismic Zone (NMSZ), researchers have developed various synthetic earthquake records capable of modeling soil characteristics in the Mississippi embayment (Fernandez and Rix, 2008). A rock site was represented by Cape Girardeau, Missouri records (CG), based on a 10-m soil column. Paducah, Kentucky records (Pa), based on a 120-m soil column, were selected to represent a soil site. Each location supplied a set of ten synthetic records that modeled a risk of 7% in 75 years (1000-year event). Vertical accelerations were not included because southern Illinois is far enough from the New Madrid fault zone that this near-field phenomenon is not expected to be significant.

A least-squares methodology (Somerville et al., 1997) was used to fit the synthetic ground motions to the AASHTO design spectrum for Cairo, Illinois. The CG rock records were

normalized to a Site Class B hazard, while the Pa soil records were normalized to Site Class D. Figure 2.8 shows the normalized ground motion spectra at the design hazard, referred to as Scale Factor (SF) 1.0. The SF = 1.0 ground motions were then linearly scaled to encompass different hazard levels. The study used a total of six scale factors (0.5; 0.75; 1.0 = design; 1.25; 1.5; 1.75) to create a coarse incremental dynamic analysis (Vamvatsikos and Cornell, 2002).

Current design provisions (AASHTO, 2009) conservatively recommend accounting for the directional uncertainty of earthquake motions. However, only unidirectional ground motions were available for the geographic region of interest so this research focused on orthogonal ground motion application. For completeness, the SsC15T2S bridge was subjected to 45° incident angle excitation, but the system response was less critical than under unidirectional ground motion application. Recent research also suggests incidence angle may have negligible impact on the response of symmetric highway bridges (Mackie et al., 2011).

Transient dynamic analyses were performed for the parametric study bridges using OpenSees (McKenna et al., 2011). A single analysis “run” was uniquely defined by the bridge model, the ground motion, the direction of application of that ground motion, and the scale factor applied to the accelerogram. This resulted in a total of nearly 12,000 dynamic analysis runs. In all runs, stiffness and mass-proportional viscous damping of 5% was used for the first (elastic) mode, and additional energy was dissipated through nonlinear hysteretic behavior of components in the model. Force and displacement data were recorded for key model elements at each time step in a run and used to quantify bridge performance.

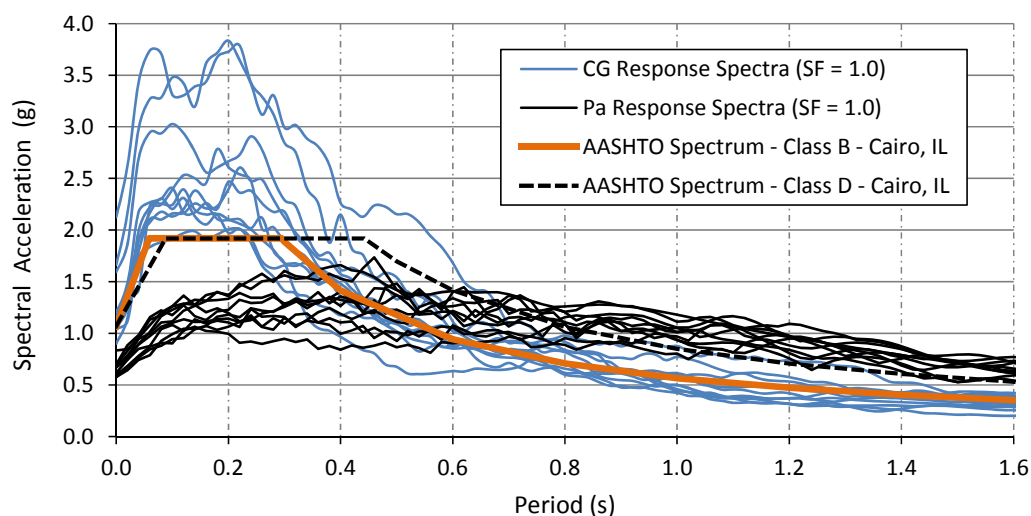


Figure 2.8. Response Spectra

2.4 MODAL ANALYSIS

Modal analysis was performed in OpenSees for all 48 bridge variants, and periods of vibration were recorded for the first eight modes. The eigenvectors were used to plot the deformed bridge shape in each mode and used for visual identification of the fundamental longitudinal and transverse modes.

Two distinct modeling cases were considered for the modal analysis. The elastic case used the elastic response of all bearings, including the fixed bearings, along with the elastic response of the retainers in the transverse direction. This represents the initial elastic response of the bridge. By comparison, in the fused case, the fixed bearings and retainers were removed and only the elastomeric bearings remained at the superstructure-substructure interface. This fused case represents the response of the bridge later in the earthquake record, when retainers and fixed bearings have fused, and when the elastomeric bearings are in a static configuration, but can deform elastically. Note that if all bearings were to slide simultaneously, the effective period would be infinite.

Table 2.2 summarizes the fundamental longitudinal and transverse periods of vibration for the short steel superstructure variants. A visualization of the period shift that occurs from the elastic case to the fused case is provided in Figure 2.9. In the longitudinal direction, tall bridge variants had noticeably longer periods than short pier variants, but the elastic and fused cases produced similar modal responses. The opposite was true in the transverse direction, where the fused bridges had longer periods than the elastic bridges and pier height was not particularly influential. Figure 2.9 also shows the periods of vibration in relation to the Pa and CG response spectra scaled to $SF = 1.0$.

Table 2.2. Periods of Vibration for Short Steel (Ss) Bridge Variants

			Longitudinal Period (s)				Transverse Period (s)			
			Short (15 ft)		Tall (40 ft)		Short (15 ft)		Tall (40 ft)	
			Elast.	Fused	Elast.	Fused	Elast.	Fused	Elast.	Fused
Column Pier	Type I Bearings	Fixed base	0.65	0.73	1.32	1.32	0.24	0.80	0.33	0.96
		Soft soil	0.73	0.80	1.35	1.35	0.33	0.82	0.41	1.01
	Type II Bearings	Fixed base	0.63	0.70	1.19	1.20	0.24	0.73	0.33	0.91
		Soft soil	0.71	0.76	1.22	1.22	0.33	0.75	0.41	0.95
Wall Pier	Type I Bearings	Fixed base	0.37	0.58	0.93	0.95	0.19	0.78	0.19	0.78
		Soft soil	0.58	0.69	1.07	1.08	0.33	0.81	0.41	0.82
	Type II Bearings	Fixed base	0.37	0.57	0.89	0.90	0.19	0.71	0.19	0.71
		Soft soil	0.57	0.66	1.01	1.02	0.33	0.74	0.41	0.75

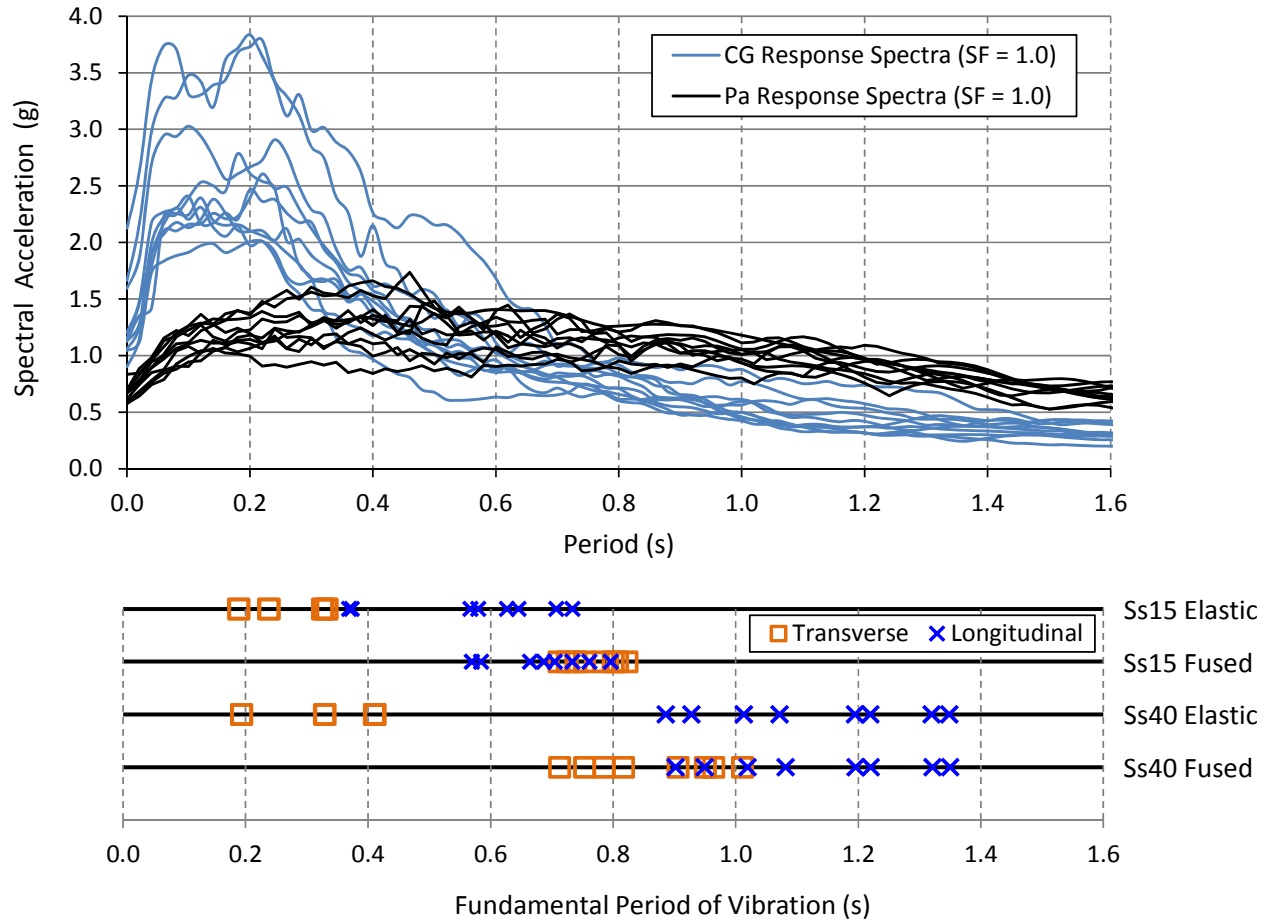


Figure 2.9. Fundamental Periods of Vibration for Ss Bridge Variants

2.5 EFFECT OF BEARING TYPE ON GLOBAL BRIDGE RESPONSE

Elastomeric bearings (either Type I or II) were modeled at the abutments and Pier 1, and low-profile fixed bearings were modeled at Pier 2. For elastomeric bearings, relative bearing displacement was calculated by subtracting elastic deformation from total deformation to obtain a sliding displacement at either the elastomer-on-concrete-cap interface (Type I) or top-plate-on-PTFE pad interface (Type II) as shown in Figure 2.10. Displacements for fixed bearings were reported directly because the elastic deformation was negligible.

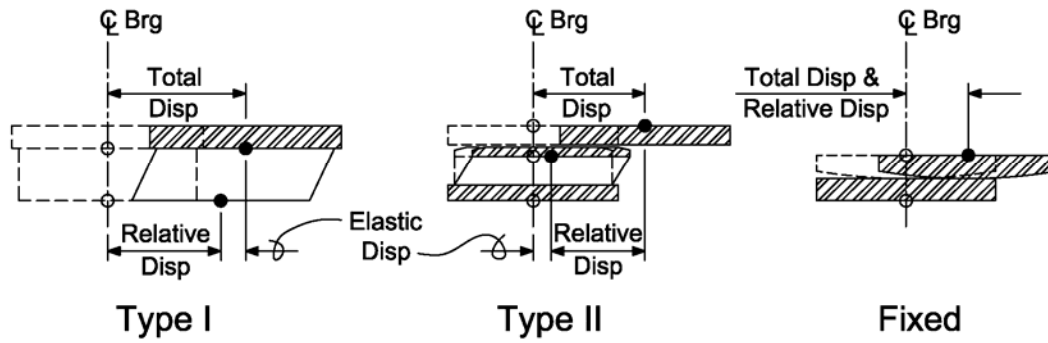


Figure 2.10. Definitions of Relative Bearing Displacement

The critical limit state for Type I and II bearings was bearing unseating, empirically defined as the displacement at which the bearing system was likely to become unstable and the computational models were unable to capture the true response (Figure 2.11). Type I bearing unseating was assumed to occur when the leading edge of the bearing moved to the edge of the support. Type II unseating was assumed to occur when the contact length between the top and bottom plate became less than 3 in.

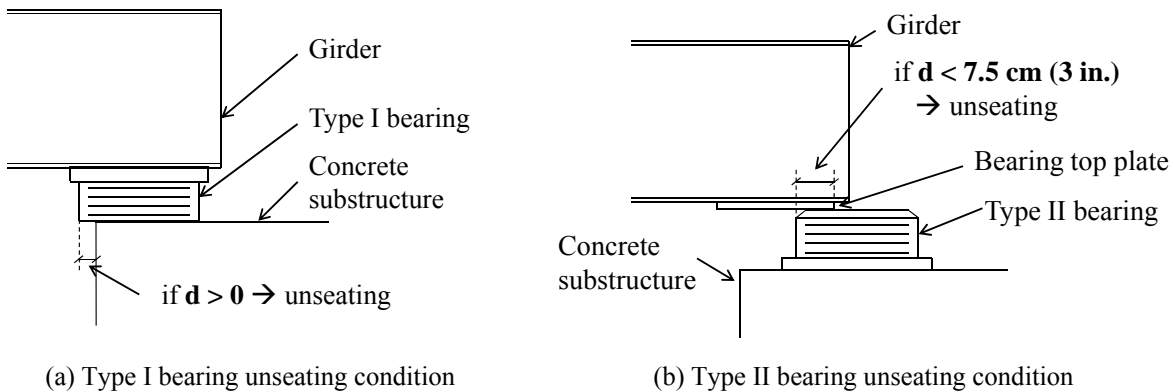


Figure 2.11. Assumed Bearing Unseating Conditions (Filipov et al. 2013b)

Bearing displacements at Pier 1 were most influenced by bearing type (Figure 2.12). At $SF = 1.0$, Type II bearings at Pier 1 always fused, while Type I bearings often did not fuse because of their comparatively high coefficient of static friction. Thus, Type II bearings experienced significantly larger displacements on average than Type I bearings.

Bearing displacements at Pier 2 were most influenced by substructure type (Figure 2.13). Fixed bearings installed on wall piers experienced larger deformations on average than those

installed on column piers. In both the longitudinal and transverse directions, the wall piers had greater strength and stiffness than the column piers, which led to earlier fixed bearing fusing and thus larger fixed bearing displacements. In the longitudinal direction, this meant the difference between the fixed bearings remaining elastic (column piers) and fusing (wall piers). In the transverse direction the earlier fusing meant fixed bearings at wall piers were more likely to reach bearing unseating, and also correlated with significantly increased variability in peak displacement.

The larger Type II displacements coupled with their more stringent unseating criteria, caused Type II systems to reach the bearing unseating limit state at much lower hazard levels than bridges with Type I bearings. The scale factor at which peak bearing displacement (when averaged over the 10 Pa ground motions) first exceeded the bearing unseating limit is reported in Table 2.3 and Table 2.4. For both longitudinal and transverse Pa ground motions, bridges with tall substructures and Type II bearings often unseated at or before design earthquake ($SF = 1.0$). Type I bearing systems, on the other hand, performed much better, with no unseating recorded for longitudinal excitation, and no transverse unseating recorded at the design earthquake.

Table 2.3. Scale Factor at which Longitudinal Bearing Unseating Occurs (Pa Ground Motions)

			Steel short (Ss) superstructure		Steel long (Sl) superstructure		Concrete (Cs) superstructure	
			Short (15 ft)	Tall (40 ft)	Short (15 ft)	Tall (40 ft)	Short (15 ft)	Tall (40 ft)
Column pier substructure	Type I Bearings	Fixed base	NA	NA	NA	NA	NA	NA
		Soft soil	NA	NA	NA	NA	NA	NA
	Type II Bearings	Fixed base	1.25	0.75	1.25	0.75	1.25	1.00
		Soft soil	1.25	0.75	1.00	0.75	1.25	1.00
Wall pier substructure	Type I Bearings	Fixed base	NA	NA	NA	NA	NA	NA
		Soft soil	NA	NA	NA	NA	NA	NA
	Type II Bearings	Fixed base	1.25	0.75	1.25	0.75	1.50	1.00
		Soft soil	1.25	0.75	1.25	0.75	1.25	1.00

Table 2.4. Scale Factor at which Transverse Bearing Unseating Occurs (Pa ground motions)

			Steel short (Ss) superstructure		Steel long (Sl) superstructure		Concrete (Cs) superstructure	
			Short (15 ft)	Tall (40 ft)	Short (15 ft)	Tall (40 ft)	Short (15 ft)	Tall (40 ft)
Column pier substructure	Type I Bearings	Fixed base	1.75	NA	1.75	NA	1.75	NA
		Soft soil	1.75	NA	1.50	NA	1.75	NA
	Type II Bearings	Fixed base	1.25	1.00	1.00	1.00	1.25	0.75
		Soft soil	1.25	1.00	1.00	0.75	1.00	0.75
Wall pier substructure	Type I Bearings	Fixed base	1.75	NA	1.75	NA	1.75	NA
		Soft soil	1.50	1.50	1.50	1.50	1.50	1.50
	Type II Bearings	Fixed base	1.25	1.25	1.25	1.25	1.25	1.25
		Soft soil	1.00	1.00	1.00	0.75	1.00	1.00

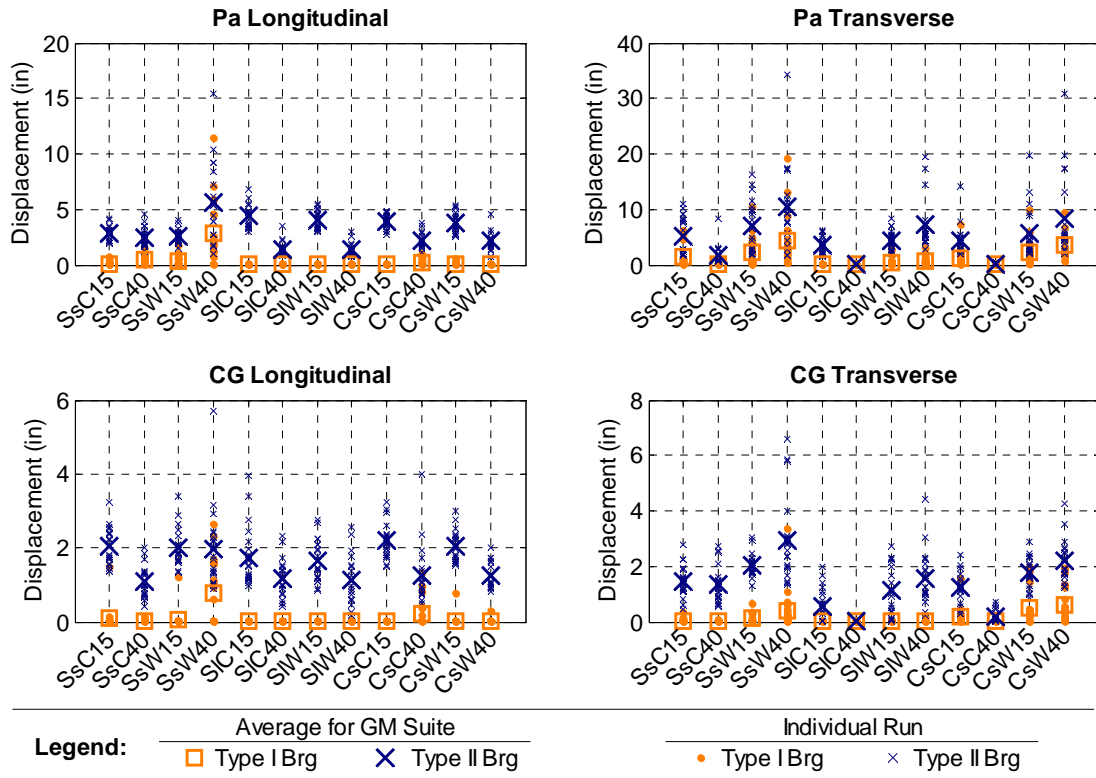


Figure 2.12. Pier 1 Bearing Displacements Grouped by Bearing Type (SF = 1.0)

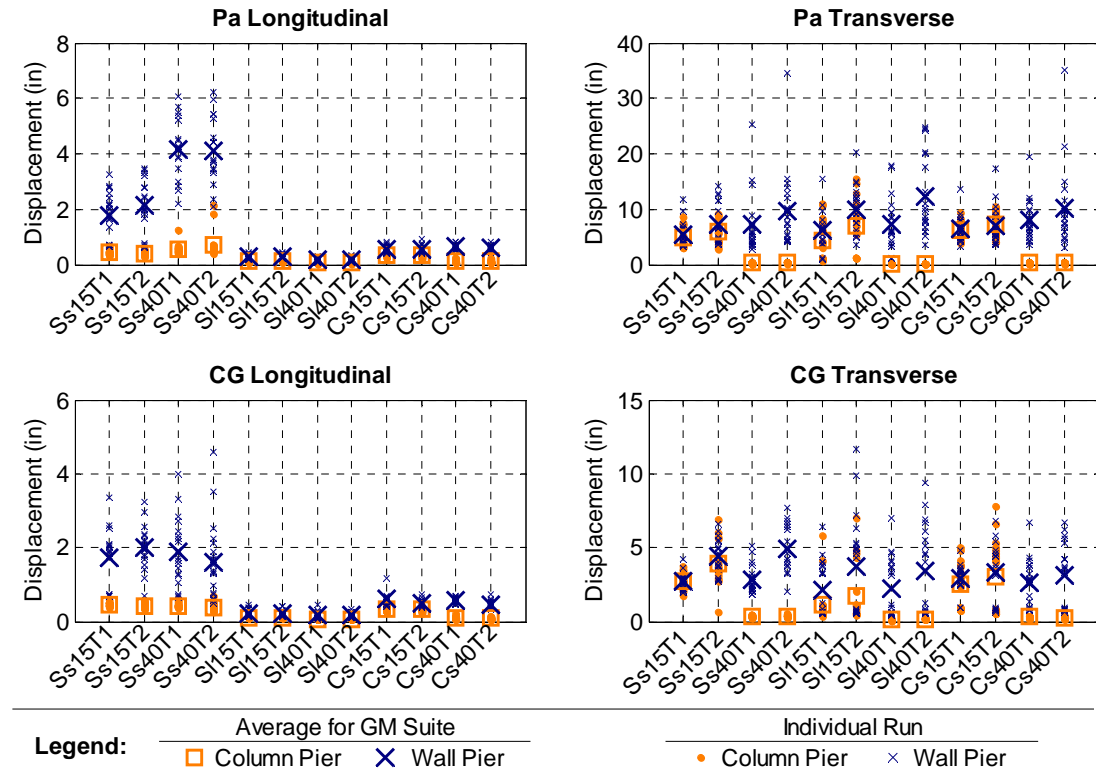


Figure 2.13. Pier 2 Bearing Displacements Grouped by Pier Type (SF = 1.0)

2.6 EFFECT OF PIER TYPE ON GLOBAL BRIDGE RESPONSE

Relative pier displacement (Figure 2.14) was reported as the top-of-pier displacement relative to bottom-of-pier displacement minus any translation caused by rotation of the foundation element or the pier cap element.

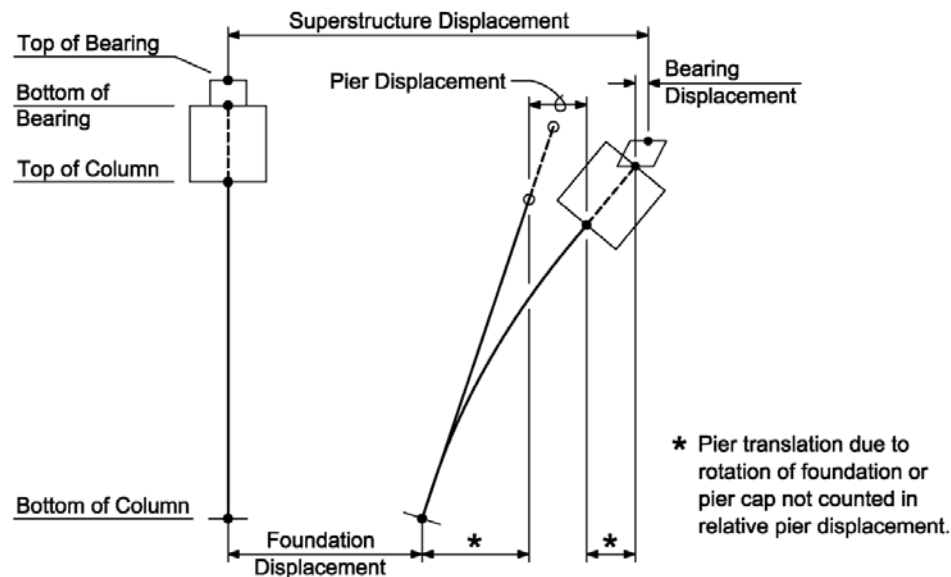


Figure 2.14. Definition of Relative Pier Displacement

Displacements were most influenced by pier height, with tall piers displacing more than short piers (Figure 2.15). In the transverse direction, the substructure type was also significant in determining pier response because wall piers were essentially rigid and column piers experienced more deformation (Figure 2.16).

In the quasi-isolated ERS, pier yielding is not ideal but is allowed to function as a secondary structural fuse after the bearings have fused. Thus, a bridge with a sequence of damage where the bearings fuse and then the piers yield could still be considered quasi-isolated. A bridge where pier yielding dominates the inelastic response, preventing the bearings from fusing or resulting in severe damage to the substructure would not be considered quasi-isolated. To help make this distinction, drift ratios were used to assess substructure damage. Pier drift ratios (peak substructure displacement divided by the substructure clear height of 15 ft or 40 ft) between 2% and 4% were correlated with moderate damage, and ratios in excess of 4% were considered to represent severe substructure damage (Building Seismic Safety Council, 2000).

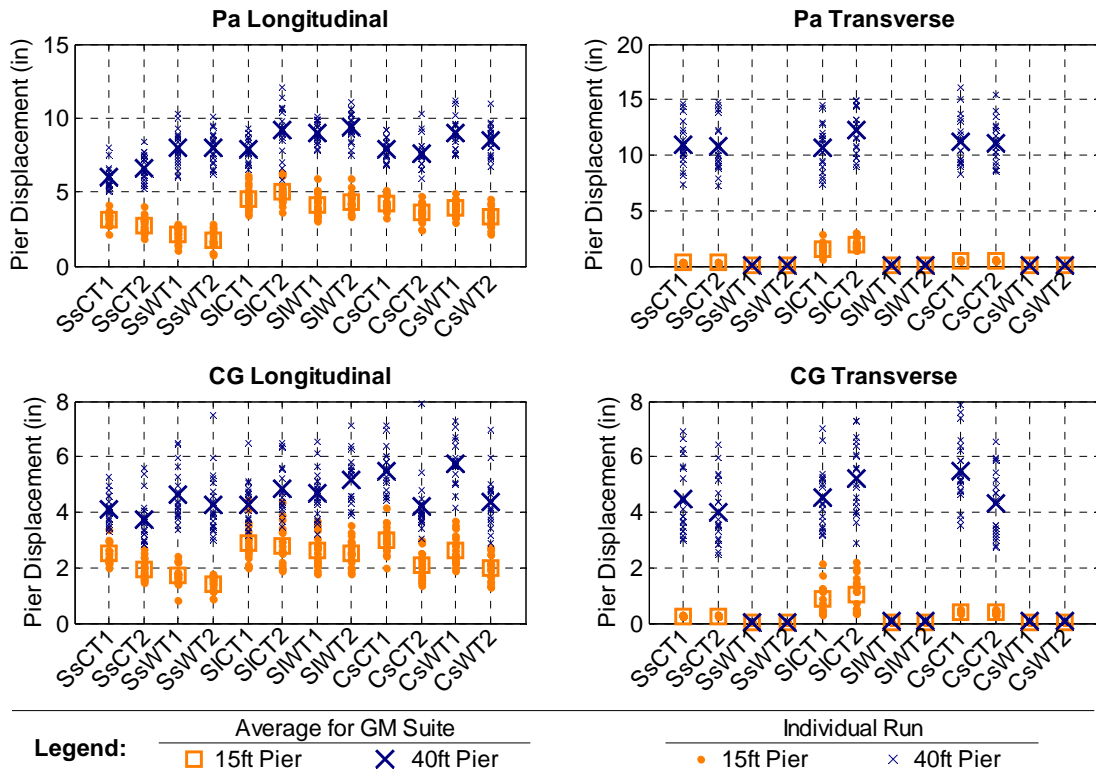


Figure 2.15. Pier 2 Displacements Grouped by Pier Height (SF = 1.0)

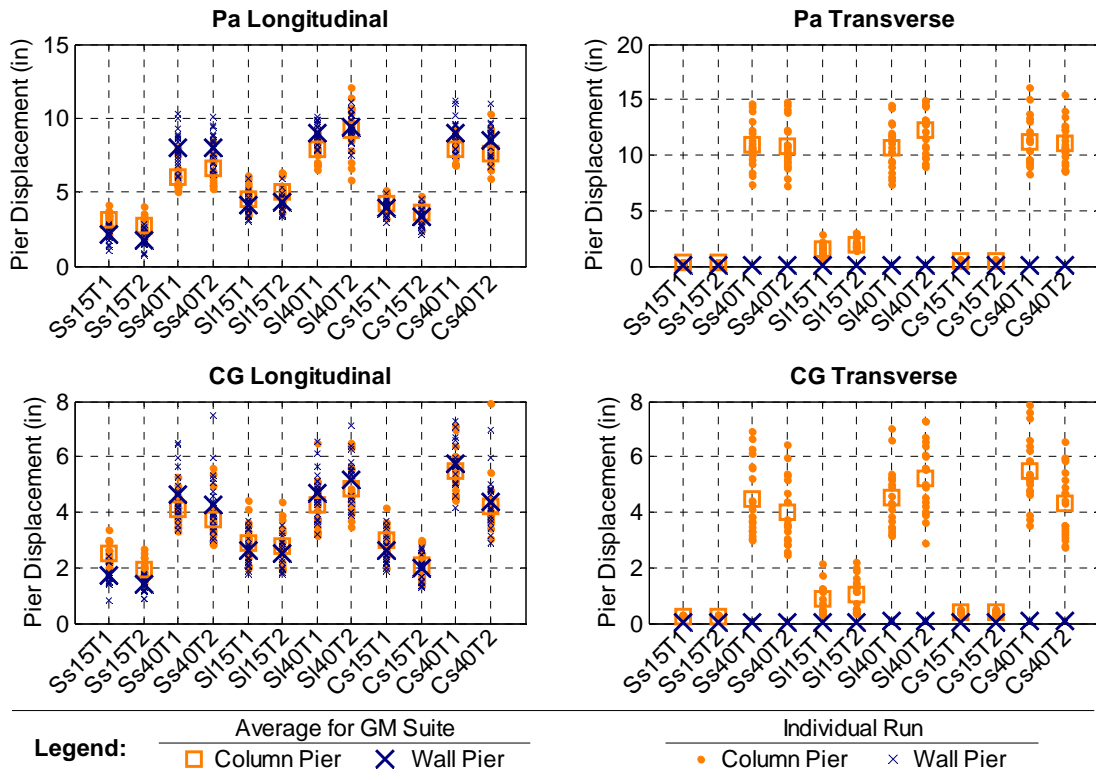


Figure 2.16. Pier 2 Displacements Grouped by Pier Type (SF = 1.0)

At SF = 1.0 severe damage never occurred, but moderate damage occurred in roughly 15% of longitudinal Pa runs and 25% of transverse Pa runs, distributed across the bridge variants as indicated in Table 2.5 and Table 2.6. In the vast majority of CG runs, pier drifts remained below 2%. For wall piers in the transverse direction, onset of damage would be expected well before the 2% limit selected for column piers and out-of-plane wall piers. However, recorded in-plane wall pier displacement demands were nearly zero, no damage was anticipated at SF = 1.0, and unique drift limits were therefore considered unnecessary.

Table 2.5. Number of Longitudinal Runs with Moderate Pier Damage (2% - 4% Drift)

			Ss Superstructure				SI Superstructure				Cs Superstructure			
			Short (15 ft)		Tall (40 ft)		Short (15 ft)		Tall (40 ft)		Short (15 ft)		Tall (40 ft)	
			Pier 1	Pier 2	Pier 1	Pier 2	Pier 1	Pier 2	Pier 1	Pier 2	Pier 1	Pier 2	Pier 1	Pier 2
Column Pier	Type I Brg	Fixed base	NA	2	NA	NA	NA	10	3	NA	NA	10	2	NA
		Soft soil	NA	1	NA	NA	NA	8	3	NA	NA	9	3	NA
	Type II Brg	Fixed base	NA	1	NA	NA	NA	10	2	2	NA	7	NA	NA
		Soft soil	NA	NA	1	NA	NA	10	8	5	NA	4	1	1
Wall Pier	Type I Brg	Fixed base	NA	NA	2	2	NA	9	5	3	NA	9	3	NA
		Soft soil	NA	NA	5	NA	NA	6	8	3	NA	6	7	4
	Type II Brg	Fixed base	NA	NA	2	1	NA	10	5	4	NA	4	1	NA
		Soft soil	NA	NA	5	NA	NA	7	7	4	NA	2	5	2

Table 2.6. Number of Transverse Runs with Moderate Pier Damage (2% - 4% Drift)

			Ss Superstructure				SI Superstructure				Cs Superstructure			
			Short (15 ft)		Tall (40 ft)		Short (15 ft)		Tall (40 ft)		Short (15 ft)		Tall (40 ft)	
			Pier 1	Pier 2	Pier 1	Pier 2	Pier 1	Pier 2	Pier 1	Pier 2	Pier 1	Pier 2	Pier 1	Pier 2
Column Pier	Type I Brg	Fixed base	NA	NA	5	8	1	NA	7	8	NA	NA	7	7
		Soft soil	NA	NA	5	8	NA	NA	5	5	NA	NA	5	5
	Type II Brg	Fixed base	NA	NA	3	8	NA	NA	9	9	NA	NA	7	8
		Soft soil	NA	NA	3	5	NA	NA	8	9	NA	NA	6	7
Wall Pier	Type I Brg	Fixed base	NA	NA	NA	NA	NA	NA	NA	NA	NA	NA	NA	NA
		Soft soil	NA	NA	NA	NA	NA	NA	NA	NA	NA	NA	NA	NA
	Type II Brg	Fixed base	NA	NA	NA	NA	NA	NA	NA	NA	NA	NA	NA	NA
		Soft soil	NA	NA	NA	NA	NA	NA	NA	NA	NA	NA	NA	NA

2.7 KEY CONCLUSIONS FROM PRIOR RESEARCH

The full-scale bearing tests in the experimental program confirmed that typical IDOT bridge bearings can be used as sliding isolation components. The elastomeric components demonstrated excellent resistance when subjected to multiple large displacement cycles, and tests of retainers and fixed bearings showed these components can be designed to fuse at prescribed capacities.

The dynamic parametric analyses in the analytical program supported the feasibility of the IDOT ERS concept and indicated that most structures in Illinois would not experience severe damage during a 75 year design life. Type I bearings never unseated at the design earthquake, promoting a reliable no-collapse response. Type II bearings were more prone to unseating, and while this does not necessarily represent span loss, it is an unstable behavior that may lead to local or global collapse. Designers should therefore consider the potential for bearing unseating when selecting bearing type and sizing bearing surfaces. The sequence of damage for most bridge structures indicated yielding of the piers for small earthquakes, which is not the ideal response for quasi-isolation. Calibration of fuse component capacities may improve the sequence of damage for many of these bridge systems, and this motivated the sensitivity study that is the focus of the remainder of this thesis.

CHAPTER 3

SENSITIVITY STUDY

3.1 OBJECTIVE

Prior research (Chapter 2) investigated the seismic performance of typical bearings and bridge configurations currently used in Illinois. The analytical component of the program provided initial data to characterize the response of global bridge systems during an earthquake. In the earlier research, bridge response appeared sensitive to bearing type and substructure parameters, and bearing assemblies often remained elastic while energy was dissipated through pier yielding. This suggested the potential to calibrate and refine the ERS by adjusting the superstructure-to-substructure connecting elements (i.e. retainers and fixed bearings). Varying anchorage strengths produced a range of fusing behaviors and made it possible to investigate the influence of fusing component force-capacity on peak superstructure sliding displacement and peak strains in the column plastic hinge zone. The sensitivity study described in this chapter is a direct extension of the previous analytical research (Filipov et al 2013b) and supports continued refinement of the IDOT ERS.

3.2 BRIDGE MODELING

Aside from a few minor adjustments, the sensitivity study used the same bearing component models and finite element bridge models developed for earlier research. The size of bearing anchorages and the column fiber section properties were modified as discussed in Sections 3.2.4 and 3.2.5, but in all other particulars the bridge models were exactly as described in Chapter 2 and Filipov et al. (2013a).

3.2.1 Bridge Variants

In the earlier parametric study, bridge variables included superstructure type, substructure type and height, bearing type, and foundation fixity, resulting in the 48 unique bridges described in Chapter 2. For the sensitivity study, only four of these bridges were used. Superstructure type was limited to Short Steel (**Ss**) or Long Steel (**SI**) and substructures used column piers (**C**) with clear heights of 15 or 40 ft (**15, 40**). Fixed bearings were used at Pier 2, and to minimize the probability of bearing unseating only Type I bearings (**T1**) were considered at the other supports.

Finally, all bridges were modeled with fixed foundations (**F**). Thus, the four basic bridge configurations carried over from the parametric study were SsC15T1F, SsC40T1F, SlC15T1F and SlC40T1F. Anchor bolt size was then introduced as a system variable, creating the suite of 24 bridges for the sensitivity study (Table 3.1). Bolt diameters of 1.25 in., 1.0 in., 0.75 in., and 0.5 in. were considered along with a 0.0 in. 'no anchor bolts' case, and a given bridge used the same size anchor bolts at all supports for both retainers and fixed bearings. In practice, fixed bearings would never be installed without anchor bolts, but this last case still provides valuable conceptual information about bridge response and serves as a point of comparison for a 'floating bridge' case where the Pier 2 fixed bearings were swapped out for Type I bearings and no retainers were used at any support. Individual bridge cases are identified by appending the anchor bolt size to the parametric study name. For example, the Short Steel bridge with 15 ft piers and 1 in. diameter anchor bolts at all supports is SsC15T1F_100, and the floating bridge case is SsC15T1F_NFB indicating 'no fixed bearings'. Basic bridge parameters are summarized in Table 3.2 and discussed further in the subsequent subsections.

3.2.2 Superstructure and Foundations

Superstructure modeling was the same as in the earlier parametric study. A grid model (Chang and White 2008; Barth and Wu 2006) captured superstructure stiffness in three dimensions and provided the ability to represent the transverse and vertical mass distributions that affect breakaway behavior of the bearings (Filipov et al. 2013a). All superstructure components were modeled with linear elastic elements because the quasi-isolated ERS concept features an essentially elastic superstructure.

All bridge variants used fixed foundations intended to represent H-piles founded on rock. In the parametric study, bridges were modeled with both fixed foundations and a flexible foundation condition represented by nonlinear springs. However, foundation fixity did not have a clear impact on bridge response, and for simplicity only fixed foundations were used in the sensitivity study.

Table 3.1. Bridge Variations Selected for Sensitivity Study

Bridge Characteristic	Parametric Study Alternatives	Additional Variable for Sensitivity Study	
Superstructure Configuration	Ss (50 ft-50 ft-50 ft)	Anchor Bolt Dia (in.)	1.25
	SI (80 ft-120 ft-80 ft)		1.00
	Cs (60 ft-60 ft-60 ft)		0.75
Pier Type	Multi-Column		0.50
	Wall		0.00
Pier Height	Short 15 ft Tall 40 ft		0.00NFB ²
Elastomeric Bearing Type ¹	Type I	Total: 24 Bridges for Sensitivity Study	
	Type II		
Foundation	Fixed	Highlighted alternatives included in sensitivity study	
	Flexible		

Notes

1. Elastomeric bearings at the Abutments and Pier 1, fixed bearings at Pier 2 except as in Note 2, below.
2. NFB = No Fixed Bearings; substitute elastomeric bearings for the fixed bearings at Pier 2.

Table 3.2 Bridge Properties

Superstructure	Steel Short (Ss)		Steel Long (Sl)	
Girder Size	W27x84		W40x183	
Span Lengths	50 - 50 - 50 ft		80 - 120 - 80 ft	
Superstructure Wt.	6.28 kip/ft		6.85 kip/ft	
Abutment Bearings				
Type I	9-b		15-e	
Retainer Bolt Dia	varies		varies	
Pier Bearings				
Type I	11-a		15-b	
Retainer Bolt Dia	varies		varies	
Fixed Bearing Bolt Dia	varies		varies	
Column Piers				
Column Clear Height	15 ft	40 ft	15 ft	40 ft
Column Diameter	3 ft	3 ft	3 ft	3 ft
Reinforcement	#9 tot 11	#9 tot 11	#9 tot 15	#9 tot 15

3.2.3 Abutment Backwall

The abutment backwall and backfill were modeled exactly as in the earlier parametric study. Abutment backwalls were positioned to provide a 2 in. expansion joint gap from the end of the bridge deck. Under seismic excitation, superstructure displacements close this gap and there is a nonlinear response from both the backwall and backfill that can have a significant effect on global response (Wilson and Elgamal 2010). Calculations indicated shear friction capacity at the cold joint between backwall and pile cap significantly exceeded flexural capacity, and the backwall structural response was therefore captured through a rotational plastic hinge. Nonlinear backfill response was defined per Shamsabadi, Rollins, and Kapuskar (2007) and modeled using the OpenSees hyperbolic gap material (McKenna et al. 2011). This material traces a hyperbolic force-displacement relationship for the backfill up to a user-defined peak passive resistance (Filipov et al. 2013a).

3.2.4 Bearing Assembly Fuse Capacities

The bearings were modeled with the OpenSees elements developed for the earlier parametric study, as discussed in Chapter 2. Type I bearing assemblies used a sliding bearing element to capture elastomer response and included retainer elements in the transverse direction. Fixed bearing assemblies used a sliding bearing element to capture the effect of the 0.125 in. neoprene leveling pad and a fixed bearing element to represent the two anchor bolts. Total fuse capacity for a bearing included both friction force from the elastomer and rupture capacity of the anchor bolts. Table 3.3 summarizes the friction coefficients used for bearings in the sensitivity study and Table 3.4 provides the estimated capacity developed through friction at a given bridge support (i.e. the total for all six bearings at a support).

Table 3.3. Modeled Properties for Type I Bearings and Fixed Bearing Leveling Pads

	Property	Type I	Fixed
G	Shear Modulus	85 psi	85 psi
μ_{SI}	Initial static coefficient of friction	0.60	0.31
μ_K	Kinetic coefficient of friction	0.45	0.30
μ_{SP}	Stick-slip coefficient of friction	0.50	0.305

Table 3.4. Estimated Capacity Developed Through Friction

		Short Steel (Ss) Bridges		Long Steel (Sl) Bridges	
		Abut	Pier	Abut	Pier
Superstructure Dead Load Reaction	(kips)	128	342	184	775
Type I Breakaway Horiz. Friction Force	(kips)	77	205	110	465
Fixed Bearing Friction Force	(kips)	n/a	103	n/a	233

The retainers had complex failure mechanisms involving concrete crushing and tension-shear anchor rupture, but the retainer capacity was simply estimated as the ultimate tensile capacity of the anchor, as shown in Equation (3-1). The factor of 0.8 accounts for reduced area due to anchor bolt threads. By comparison, the fixed bearing anchors generally failed in pure shear so fixed bearing anchor capacity was based on shear rupture of the two anchors, as shown in Equation (3-2). The 0.6 factor accounts for reduced strength in shear and the 0.8 factor again accounts for area reduction due to anchor bolt threads. An ultimate strength, f_u , of 60 ksi and a phi-factor of 1.0 were used for both anchor types. Table 3.5 summarizes the estimated anchor capacities for all cases included in the sensitivity study. The tabulated values represent total capacity at a support with six bearings, meaning six retainer anchors or 12 fixed bearing anchors were engaged.

$$F_{ult} = \phi 0.8 A_{bolt} f_u, \phi = 1.00 \quad (3-1)$$

$$F_{ult} = \phi(0.6)(0.8)A_{bolt} f_u, \phi = 1.00 \quad (3-2)$$

Table 3.5. Estimated Capacity Developed Through Anchor Rupture

Bolt Dia (in.)	Tot Anchor Capacity (kips)	
	Retainer	Fixed Brg
1.25	353	424
1	226	271
0.75	127	153
0.5	57	68
0	0	0

3.2.5 Substructure

Bridges in the sensitivity study used multi-column pier substructures with clear heights of either 15 or 40 ft. While the pier cap could reasonably be modeled as linear elastic, it was important to model the columns in a way that would capture nonlinear responses such as cracking and flexural yielding. Thus, the columns were modeled with the distributed plasticity model (Scott and Fences 2006) that was previously implemented and validated for the parametric study (Filipov et al. 2013a). Figure 3.1 explains that fiber sections similar to that shown in Figure 3.2 were used to capture material nonlinearity in the plastic hinge regions of the column. Outside the plastic hinge regions, the column was modeled with an elastic beam-column element with a gross moment of inertia about both axes multiplied by 0.7 to account for initial cracking. Plastic hinge length was estimated by Equation (3-3) where L was taken as the column clear height, and both f_y and d_b pertained to the longitudinal reinforcement (Berry, Lehman, and Lowes 2008). Plastic hinge lengths were set at 18 in. for the 15 ft columns and 33 in. for the 40 ft columns.

$$l_p = 0.05L + \frac{0.008 f_y d_b}{\sqrt{f'_c} \text{ (in psi)}} \quad (3-3)$$

All column piers featured four 36 in. diameter columns spaced at 10.75 ft on center. Transverse reinforcing was assumed sufficient to prevent longitudinal bar buckling and column shear failure. The Short Steel and Long Steel bridges used 11 and 15 #9 longitudinal bars, respectively, with 2 in. clear cover. Longitudinal steel was modeled with the OpenSees Steel02 material assuming 68 ksi yield stress and a strain hardening ratio of 0.09. A tensile rupture strain of 0.12 was enforced using an OpenSees MinMax material, defining the backbone curve shown in Figure 3.3. The columns used normal-weight concrete with a specified 14-day strength of 3500 psi. However, based on the AASHTO recommendations for seismic modeling (AASHTO 2009), peak concrete strength was factored up by 1.3 and modeled as 4550 psi. For the confined core, peak strength increased to 6140 ksi based on the Mander model (Mander, Priestly, and Park 1988), and spalling strain for the unconfined concrete was estimated as 0.005. Both confined and unconfined concrete fibers were modeled with the OpenSees Concrete 02 material previously used for the parametric study for which the cyclic response had already been validated against

available literature (Filipov et al. 2013a). The backbone curves for confined and unconfined concrete are shown in Figure 3.4.

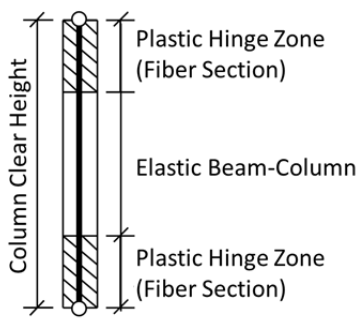


Figure 3.1. Beam-Column with Hinges

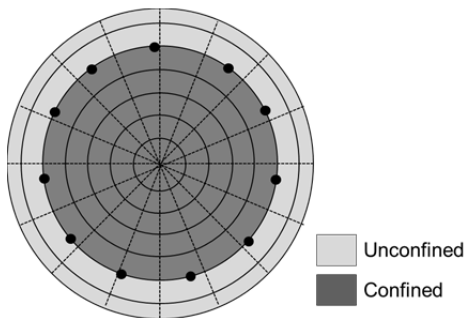


Figure 3.2. Fiber Section

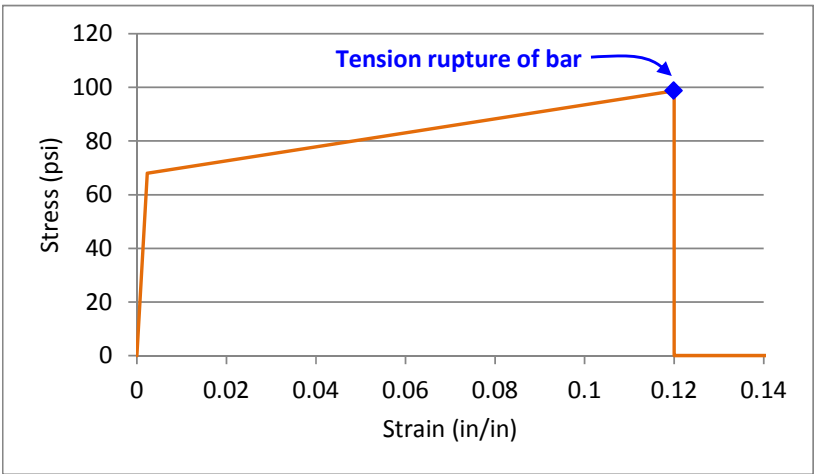


Figure 3.3. Steel 02 Backbone

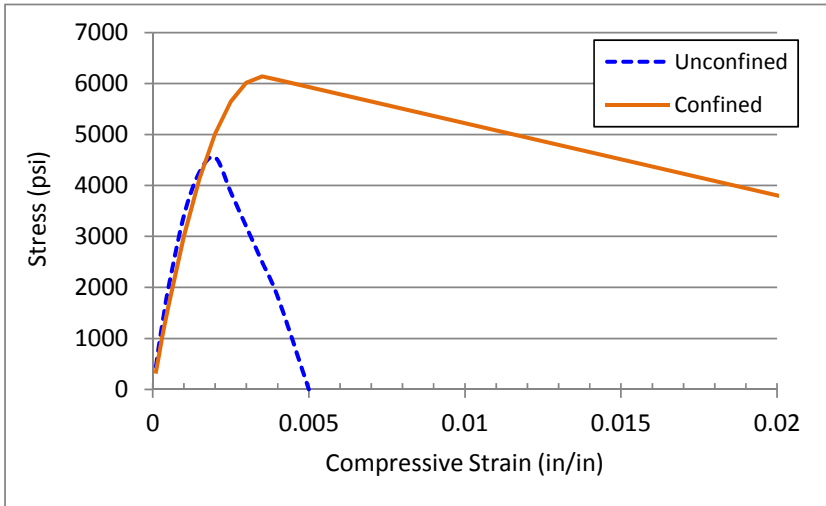


Figure 3.4. Concrete 02 Backbone

3.2.6 Seismic Hazard

As discussed in Chapter 2, in the earlier parametric study two synthetic ground motion suites considered representative of the New Madrid Seismic Zone (Fernandez and Rix 2008) were normalized to fit the 1000 year spectra for Cairo, Illinois (AASHTO 2009). Once normalized and adjusted for site class, the two sets of ten ground motions were considered representative of the design seismic hazard for rock and soil conditions, respectively. The soil ground motions typically produced higher responses in comparison to rock ground motions of similar intensity, but general bridge response characteristics were similar for the two ground motion suites. Thus, for the sensitivity study the rock ground motions were discarded and the soil condition was again represented by the normalized Paducah, Kentucky records (Pa). Records were applied in the longitudinal and transverse directions, and only the design earthquake was considered (identified as Scale Factor $SF = 1.0$ in prior research).

The earlier parametric study had considered non-orthogonal ground motion directionality in addition to pure longitudinal and pure transverse excitation. However, the study results indicated non-orthogonal excitation was no more critical than orthogonal excitation. Recent research also suggests incidence angle may have negligible impact on the response of symmetric highway bridges (Mackie et al., 2011). The sensitivity study therefore focused exclusively on pure longitudinal and transverse application of the ground motions.

CHAPTER 4

DYNAMIC ANALYSES

Nonlinear time-history analyses were conducted for the sensitivity study bridges using OpenSees, an open source earthquake engineering simulation software package (McKenna, Mazzoni, and Fenves 2011). The suite of ten ground motions was applied to each model in the pure longitudinal and pure transverse directions, resulting in a total of 480 analysis runs. In all analysis runs, stiffness and mass proportional viscous damping of 5% was used for the first longitudinal and transverse modes, and additional energy was dissipated through hysteretic response of nonlinear elements such as the bearings and pier columns. At each time step in a run, force and displacement data were recorded for all nonlinear bridge elements, and fiber section response was also recorded for the column plastic hinge zones. While this chapter does present some numerical results, the focus is on qualitative response characterization for the Ss and Sl bridge groups. After looking at each bridge group individually, Chapter 5 then extends the discussion into numerical results and trends for the sensitivity study as a whole.

4.1 LIMIT STATES

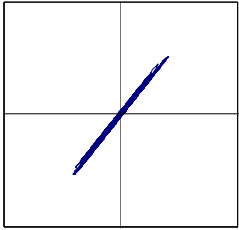
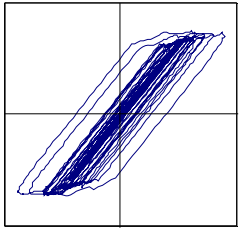
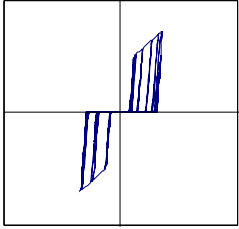
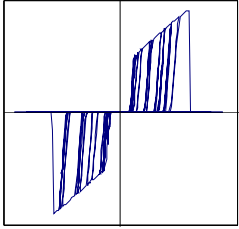
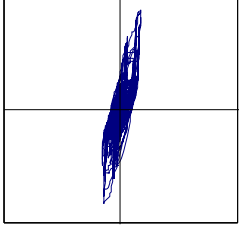
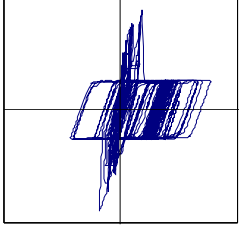
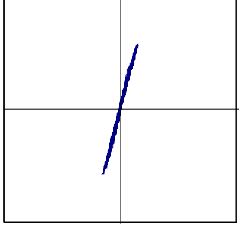

Typical limit states for the sensitivity study are summarized in Table 4.1, and match those used in the earlier parametric study. In the remainder of this document, the two letter limit state abbreviations from this table will sometimes be employed as a shorthand notation.

Hysteretic force-displacement curves for each bridge component were the most conceptually straightforward method of determining whether a limit state had occurred because the hysteresis provided an intuitive connection between the numerical data and the physical state of the structure. Several force-displacement plots in Table 4.2 illustrate this approach.

Table 4.1. Typical Limit States Observed in the Sensitivity Study

Acceptable for quasi-isolation	Acceptable as secondary fuse
EA - Elastomeric bearings slide at abutment	P1 - Pier 1 columns yield
EP - Elastomeric bearings slide at Pier 1	P2 - Pier 2 columns yield
RA - Retainer anchors rupture at abutment	
RP - Retainer anchors rupture at Pier 1	Discouraged for quasi-isolation
Fb - Fixed bearing anchors rupture	UA - Bearings unseat at abutment
Bw - Backwall yields	UP - Bearings unseat at pier

Table 4.2. Methods of Determining Whether a Limit State Occurred

Limit State	Example Hysteresis When Limit State Has: Not Occurred Occurred		Quantitative Limit State Criteria
Bearing Sliding			Relative bearing displacement (as defined in Figure 2.10) is nonzero.
Retainer Anchor Rupture			Transverse bearing displacement (including elastic deformation) exceeds a pre-defined ultimate displacement that is a function of bolt diameter.
Fixed Bearing Anchor Rupture			Fixed bearing displacement exceeds a pre-defined ultimate displacement.
Pier Yielding			Based on strain data: the point where the first reinforcing bar yields in tension ($\epsilon = 0.0023$) or the core concrete reaches a maximum compression strain of 0.002.

However, these force-displacement plots are primarily useful when assessing the response to a single ground motion, and a suite of ten ground motions must be considered in the sensitivity study. Thus, a more efficient approach was to establish displacement-based limit state criteria that could easily be compared against average peak displacements for the ground motion suite. Table 4.2 summarizes some of the criteria used for nonlinear elements in the sensitivity study.

For both retainer anchor rupture and fixed bearing anchor rupture, the ultimate displacement was defined based on related testing and research (Chapter 2). For fixed bearing anchors, ultimate displacement was equal to the bolt diameter, and for retainer anchors it was approximately 2.23 times the square of the bolt diameter. Bearing unseating limit states were more empirical, but as discussed in Section 2.5, they were similarly based on displacement criteria. When relative bearing displacement at a support exceeded the limits set in Table 4.3, the bearing was said to have unseated, indicating the bearing system was likely to become unstable and the computational models were unable to capture the true response.

Table 4.3. Seat Widths and Bearing Unseating Criteria

		Ss Bridges		SI Bridges	
		Abut	Pier	Abut	Pier
Seat Width (in.)	15 ft Pier	23	23	27	27
[Pier Cap Width = 2* Seat Width]	40 ft Pier	32	32	35	35
Longitudinal Bearing Displacement	15 ft Pier	18.5	17.5	19.5	19.5
at Bearing Unseating (in.)	40 ft Pier	27.5	26.5	27.5	27.5
Transverse Bearing Displacement at	15 ft Pier	17	15	15	15
Bearing Unseating (in.)	40 ft Pier	26	24	23	23

Yielding of the piers is not ideal for quasi-isolation, but it is still permitted to function as a secondary structural fuse after the bearings have fused. Thus, a bridge with a sequence of damage where the bearings fuse, and then the piers yield, could still be considered quasi-isolated. A bridge where pier yielding dominates the inelastic response, preventing the bearings from fusing or resulting in severe damage to the substructure, would not be considered quasi-isolated. To help make this distinction, fiber section deformations were recorded in the column plastic hinge zones, and used to calculate peak strains for the reinforcing bars and the core concrete. For purposes of identifying limit states, onset of yielding was defined as the point where the first longitudinal reinforcing bar yielded in tension ($\epsilon = 0.0023$) or the maximum compression strain in the core concrete exceeded 0.002 (Elwood and Eberhard 2006). Beyond yielding, the performance limits shown in Table 4.4 were established (Kowalsky 2000). Between the yield and serviceability limits, the column was considered lightly damaged with no post-earthquake repair required. The serviceability limit marked the onset of concrete crushing and residual crack widths greater than 1 mm. From this point up through the damage control limit the column was considered damaged but repairable, and the damage control limit marked the onset of non-

repairable damage. When discussing column performance in this document, columns with strains below yield are termed "essentially elastic," and those with strains between the yield point and the serviceability limit are denoted "serviceable" or "lightly damaged". For strains between the serviceability and damage control limits, columns are identified as "damaged," and columns with higher strains than the damage control limit are indicated as "severely damaged".

Table 4.4. Performance Limit States for Pier Columns (Kowalski 2000)

Performance Limit	Concrete Strain Limit (compression)	Steel Strain Limit (tension)
Serviceability	0.004	0.015
Damage Control	0.018	0.060

4.2 CHARACTERIZING SEISMIC RESPONSE

Seismic bridge performance was assessed based on key response parameters, such as superstructure displacement, relative bearing displacement, relative pier displacement, and base shear. In order to distill the 480 time history runs into summary tables and graphics, representative values of these response parameters were obtained for each bridge via a series of approximations:

- i. At each time step in an individual time-history analysis, bearing displacement at a support was calculated by averaging the response of the six bearings. Similarly, displacement of the multi-column piers was calculated by averaging the response of the four columns. Backwall displacement was conservatively reported as the peak displacement across the eight backwall interaction nodes. Force response was always reported as the total for a support, e.g., the summation of forces for all six bearings.
- ii. For each time history run, the peak force and displacement responses were extracted and then an average was calculated for the ten ground motions. Note that in some instances only eight or nine runs were successfully completed, due to computational difficulties associated with achieving convergence during nonlinear time-history analyses of sliding systems with small tangent stiffness. According to the AASHTO Guide Specification for LRFD Seismic Bridge Design (AASHTO 2009), use of the mean response is acceptable when averaging over at least seven time histories.

The following sections contain descriptions of longitudinal and transverse seismic behavior of the Ss and SI bridge groups. Figure 4.7 through Figure 4.10 at the end of the chapter show peak force, displacement, and strain responses for various bridge components during individual runs, as well as average responses for the ground motion suite. These figures are meant to complement and clarify the commentary presented in the main text. The abscissa of all plots corresponds to the anchor bolt diameter variations included in the sensitivity study, and "AB" is adopted as a shorthand reference for this in the remainder of the document. For example, the 0.75 in. diameter anchor bolt case is referenced as $AB = 0.75$.

4.2.1 Short Steel Bridges Subjected to Longitudinal Excitation

The longitudinal response of the Ss bridges was not particularly sensitive to anchor bolt variation because under longitudinal excitation the retainers were not engaged, and thus fixed bearing strength was the only parameter affected by anchor bolt variation. Additionally, the abutment backwalls provided a degree of longitudinal restraint that limited the potential impact of fixed bearing strength on system behavior.

The abutment bearing force and displacement responses shown in Figure 4.1 were insensitive to anchor bolt variation. While abutment bearing sliding occurred in every run, the displacements were not large enough to cause bearing unseating. At Pier 1, many ground motions produced no bearing sliding at all, and average peak sliding displacements of the Type I bearings were less than 0.5 in. The fixed bearing response at Pier 2 was comparatively sensitive to anchor bolt variation, and exhibited a range of fusing behavior. Anchorages remained elastic at $AB = 1.25$, but began to experience inelastic deformation by $AB = 0.75$, and finally fractured at $AB = 0.50$. Following anchor failure, the fixed bearing bottom plate slid on the neoprene leveling pad and reached peak displacements between 2 and 4 in.

Column pier response was a function of both pier height and anchor bolt diameter, though Figure 4.2 suggests pier height was the more significant variable. At Pier 1, the 40 ft piers showed a constant force response for varying displacements, suggesting the columns were past yield. The 15 ft piers exhibited the opposite trend, suggesting little or no yielding had occurred for these columns.

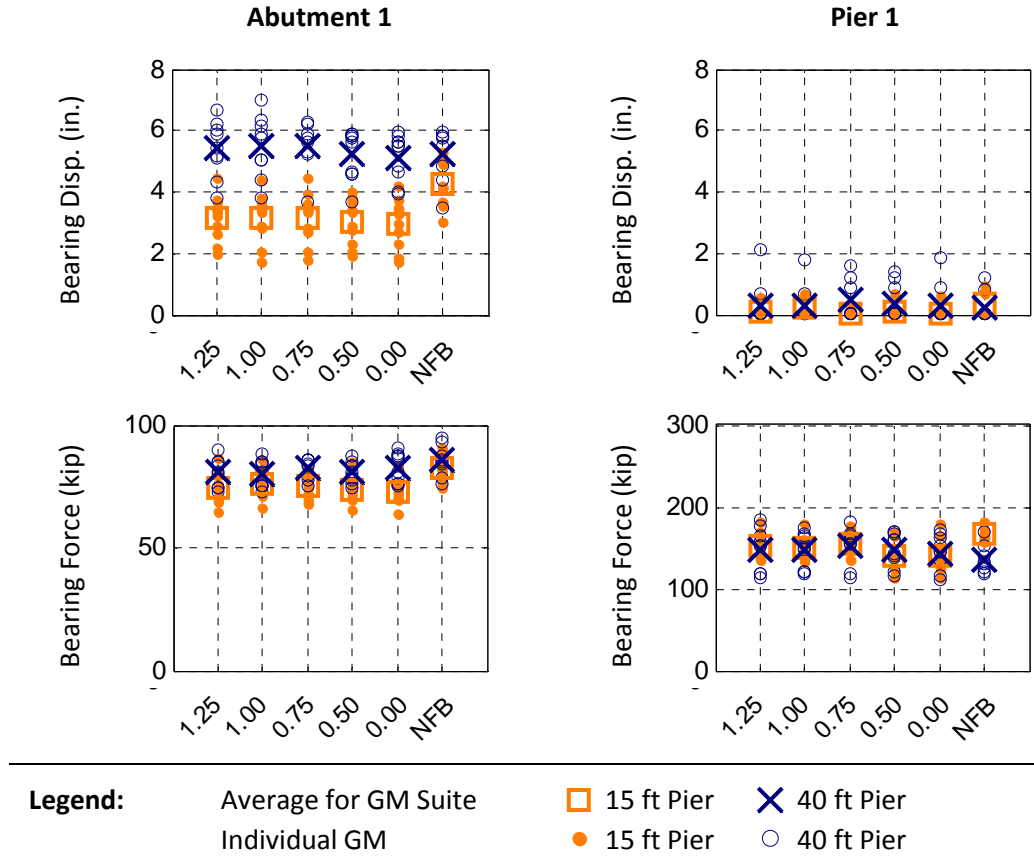


Figure 4.1. Bearing Response for Ss Bridges Subjected to Longitudinal Excitation

At Pier 2, the 15 ft columns yielded in cases where the fixed bearing anchor bolts did not fracture. Upon transitioning to smaller diameter bolts, anchor fracture occurred, pier displacement was significantly reduced, and there was little or no column yielding. In 40 ft pier bridges, the Pier 2 columns yielded regardless of whether the fixed bearing anchors fractured.

The superstructure displacement (i.e., the total displacement of a point on the deck relative to a fixed point on the ground) was not influenced by anchor bolt diameter, and displacement was roughly constant along the length of the bridge, indicating there was no appreciable twisting of the superstructure or deformation of superstructure elements. Base shear at each support was likewise insensitive to anchor bolt diameter, and the distribution of base shear between supports revealed that the abutment backwalls were critical components in the system response. The base shears in Figure 4.3 indicate the reaction at Abutment 1 was three to five times larger than that at Pier 1. Given that abutment base shear is approximately the sum of bearing force and backwall force, and taking bearing forces from Figure 4.1, abutment backwall forces account for as much as 80% of the total base shear.

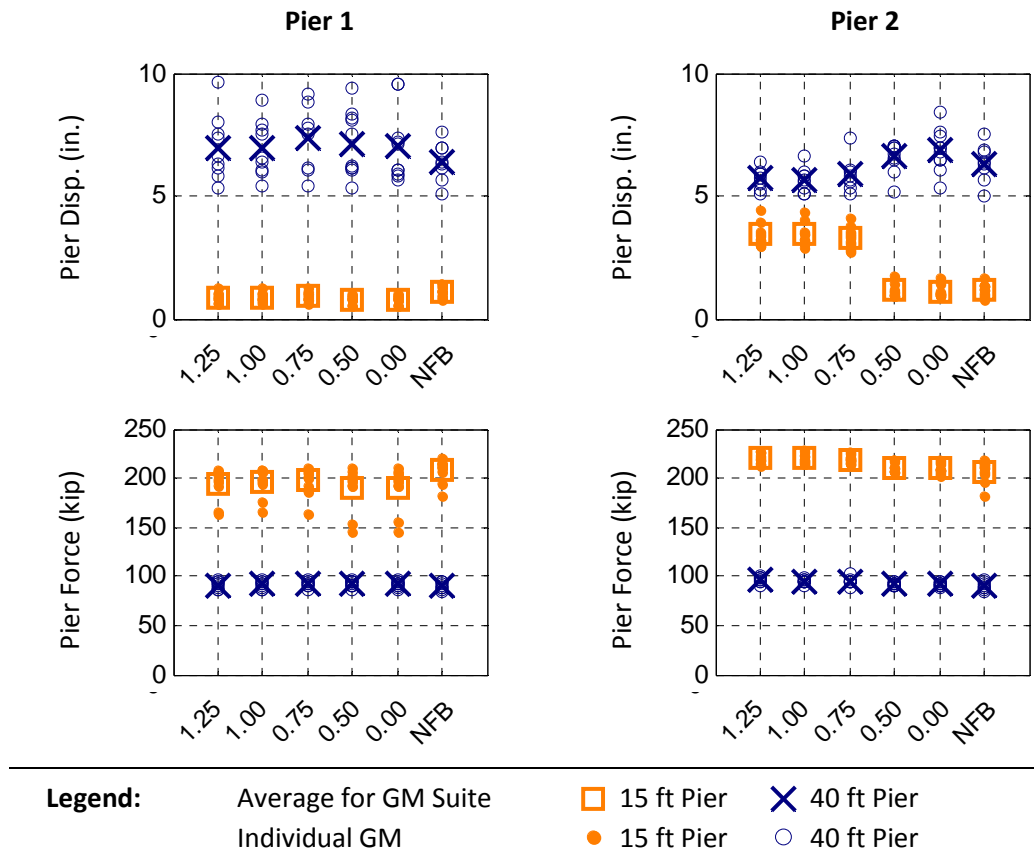


Figure 4.2. Pier Response for Ss Bridges Subjected to Longitudinal Excitation

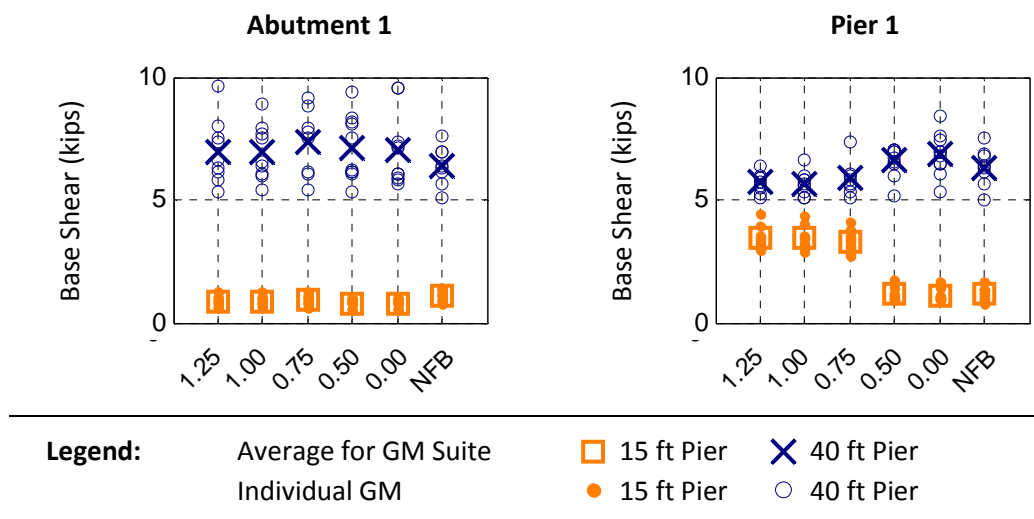


Figure 4.3. Base Shear for Ss Bridges Subjected to Longitudinal Excitation

4.2.2 Short Steel Bridges Subjected to Transverse Excitation

The transverse response of the Ss bridges was much more affected by anchor bolt variation than the longitudinal response. Under transverse excitation, all retainer and fixed bearing anchorages were engaged, making bolt diameter a significant variable in the response of individual bridge components as well as the global bridge system.

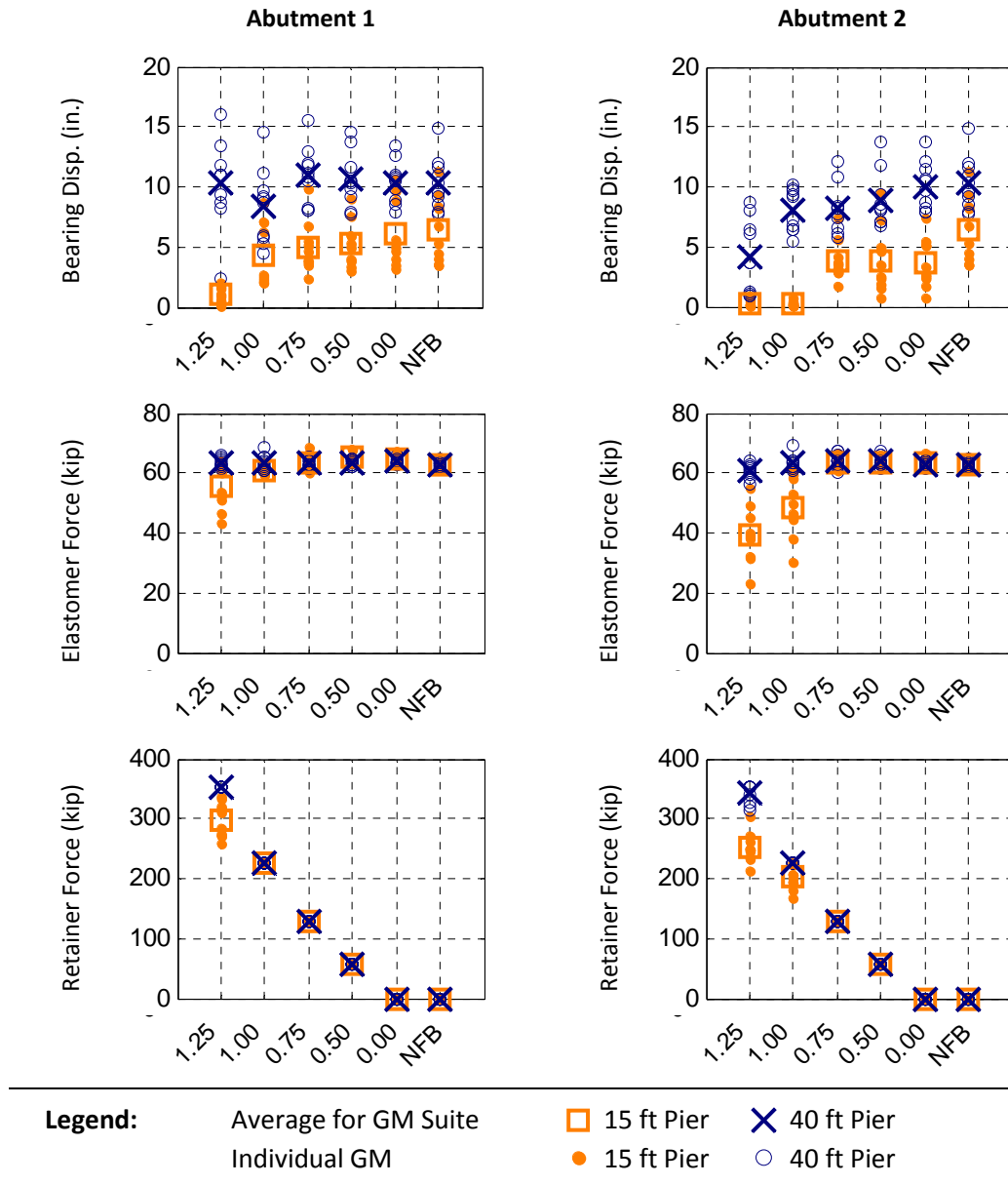


Figure 4.4. Abutment Bearing and Retainer Response for Ss Bridges Subjected to Transverse Excitation

Abutment elastomer and retainer responses, shown in Figure 4.4, were somewhat influenced by the retainer anchor bolt diameter, particularly in bridges with 15 ft piers. In these

bridges, the nature of bearing assembly response varied with bolt diameter. At $AB = 1.25$ neither abutment experienced retainer rupture or bearing sliding, and at $AB = 1.00$ only Abutment 1 reached these limit states. This difference in abutment bearing response at $AB = 1.00$ suggests the superstructure was twisting about a vertical axis. Bridges with 40 ft piers exhibited retainer rupture and bearing sliding at both abutments for all runs. Interestingly, at $AB = 1.25$ the bearing displacement at Abutment 1 was approximately twice that at Abutment 2, and this suggests superstructure twisting similar to that observed with the 15 ft piers. As the anchor bolt size decreased, this twisting behavior abated.

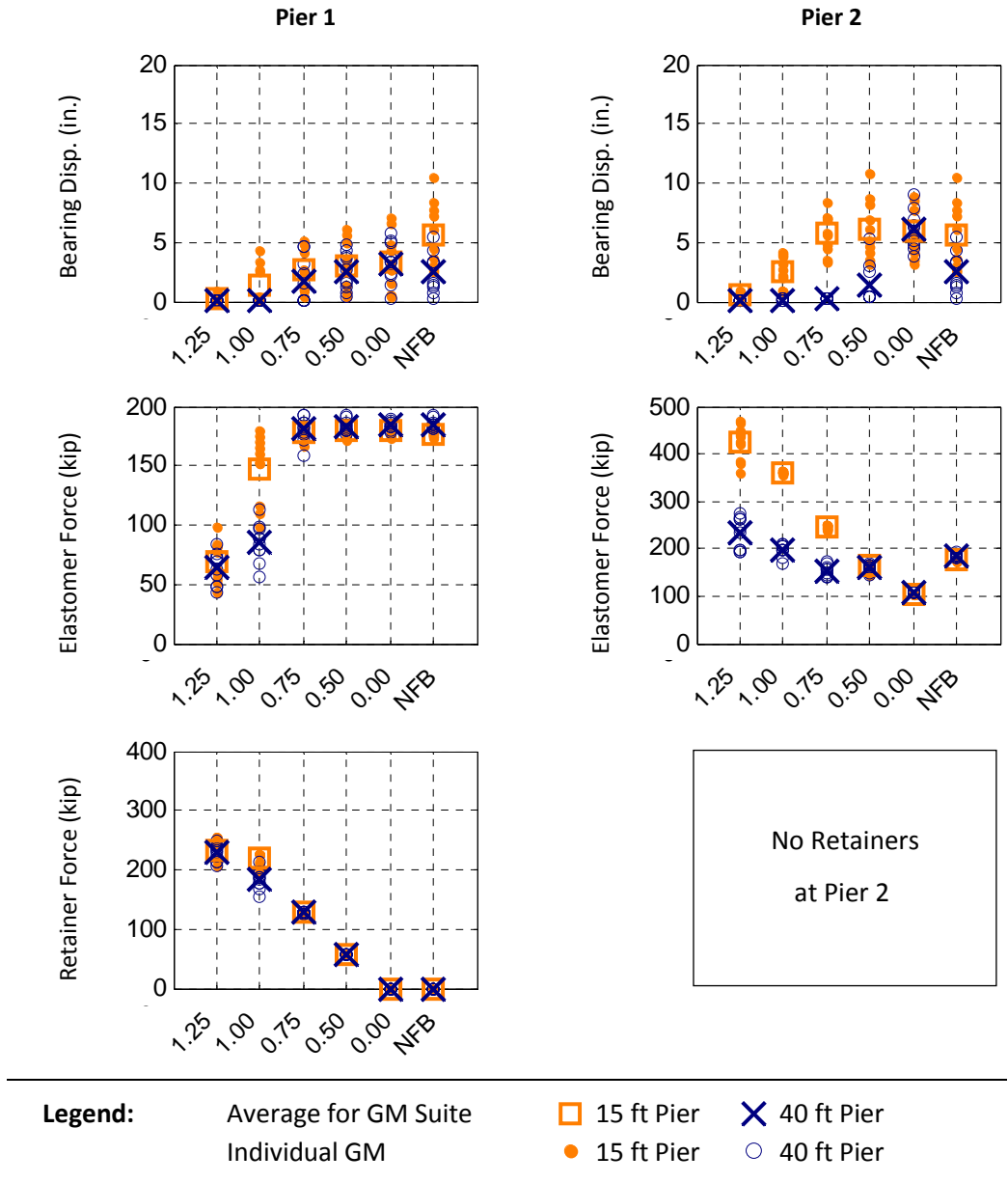


Figure 4.5. Pier Bearing and Retainer Response for Ss Bridges Subjected to Transverse Excitation

In contrast to the abutments, elastomer and retainer responses at Pier 1 were similar for 15 ft and 40 ft pier bridges. Retainers did not rupture at $AB = 1.25$ or $AB = 1.00$, and this generally prevented the bearings from sliding.

At Pier 2, the response sensitivity to anchor bolt diameter was more pronounced for bridges with 15 ft piers than for those with 40 ft piers, but the observed trends in fixed bearing behavior were similar. As anchor bolt size decreased, bolt strength eventually became lower than pier yield strength. In this configuration, the anchors became the critical ERS component and generally fractured during the time-history analysis. As shown in Figure 4.5, this first occurred at $AB = 1.00$ for the 15 ft pier bridges and at $AB = 0.50$ for the 40 ft pier bridges. When anchor bolt size was further decreased, peak sliding displacement increased.

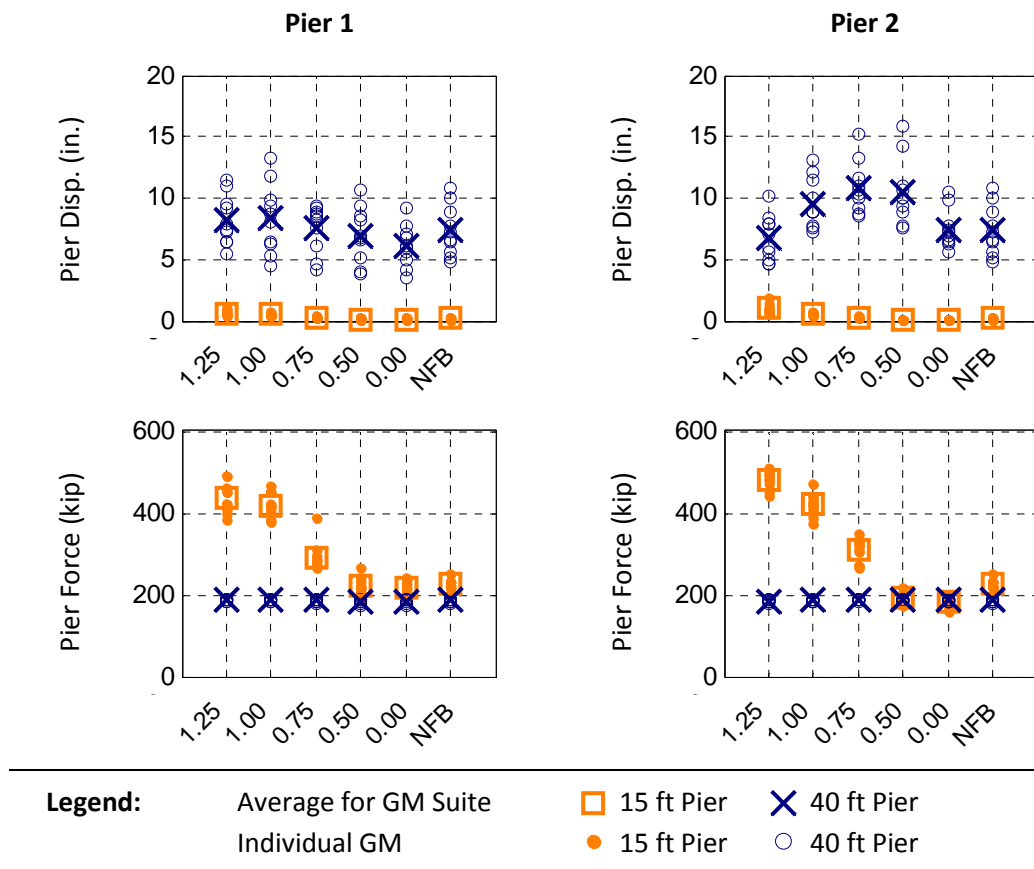


Figure 4.6. Pier Response for Ss Bridges Subjected to Transverse Excitation

As illustrated in Figure 4.6, the transverse column pier responses of Pier 1 and Pier 2 were extremely similar. In bridges with 40 ft piers, the pier response was largely insensitive to anchor bolt variation and pier yielding occurred in all runs. The 15 ft piers were quite stiff in the

transverse direction, and pier displacement was less than 1 in. for all runs. The $AB = 1.25$ case exhibited a small degree of pier yielding, but in the remaining cases, retainer fracture and bearing sliding capped the pier force demands at a level below pier strength. Note that the peak pier force was generally slightly higher than the peak bearing force, most likely due to the acceleration of the column and pier cap mass.

4.2.3 Long Steel Bridges Subjected to Longitudinal Excitation

Longitudinal behavior of the SI bridges was quite similar to that of the Ss bridges. Variations in response were generally attributed to increased breakaway and sliding friction forces developed at the bearings as a consequence of the higher SI superstructure dead load. Regardless of anchor bolt diameter, the abutment bearings slid and the Pier 1 bearings did not. For the fixed bearings, decreasing the anchor bolt size produced inelastic anchor deformation at $AB = 0.75$ and anchor rupture at $AB = 0.5$. However, the response was limited by frictional resistance between the bearing and neoprene pad such that for $AB = 0.00$, peak fixed bearing force and displacement were approximately the same as for $AB = 0.5$. The response of pier columns at Pier 1 and Pier 2 was not influenced by the anchor bolt variations, and both piers yielded for all runs.

Under longitudinal excitation it is therefore not feasible to modify or calibrate the seismic performance of SI bridges via anchor bolt diameter because the columns remain the critical ERS component regardless of anchor bolt strength.

4.2.4 Long Steel Bridges Subjected to Transverse Excitation

Retainer rupture and bearing sliding occurred at both abutments for all bridges with 40 ft piers, and at nearly all bridges with 15 ft piers. The lone exception was the response at Abutment 2 for $AB = 1.25$, where the retainers deformed but did not actually rupture. The 40 ft pier bridges show a fairly similar response at Abutment 1 and Abutment 2, but the dissimilar abutment bearing displacements observed for the 15 ft pier bridges suggest the same superstructure twisting previously noted in the Ss bridge responses. At Pier 1, the bridges with 15 ft piers recorded retainer rupture in all runs and bearing sliding for all but $AB = 1.25$. The 40 ft pier bridges, by comparison, did not achieve retainer rupture until the bolt diameter was reduced to 0.75 in., and bearing sliding never occurred. At Pier 2, the fixed bearing fused in all runs

featuring 15 ft pier bridges. The 40 ft pier bridges were largely insensitive to anchor bolt size, and even with the anchor bolts removed, displacements were less than 1 in.

In the S1 bridge group, the transverse responses of Pier 1 and Pier 2 were extremely similar, and followed the same trends observed for the Ss bridge group. In bridges with 40 ft piers, the pier response was largely insensitive to anchor bolt variation and pier yielding occurred in all runs. The 15 ft piers were quite stiff in the transverse direction, and pier displacement was less than 1 in. for all runs. The piers did yield at $AB = 1.25$, but in the remaining cases retainer fracture and bearing sliding capped the pier force demands at a level below pier yield strength.

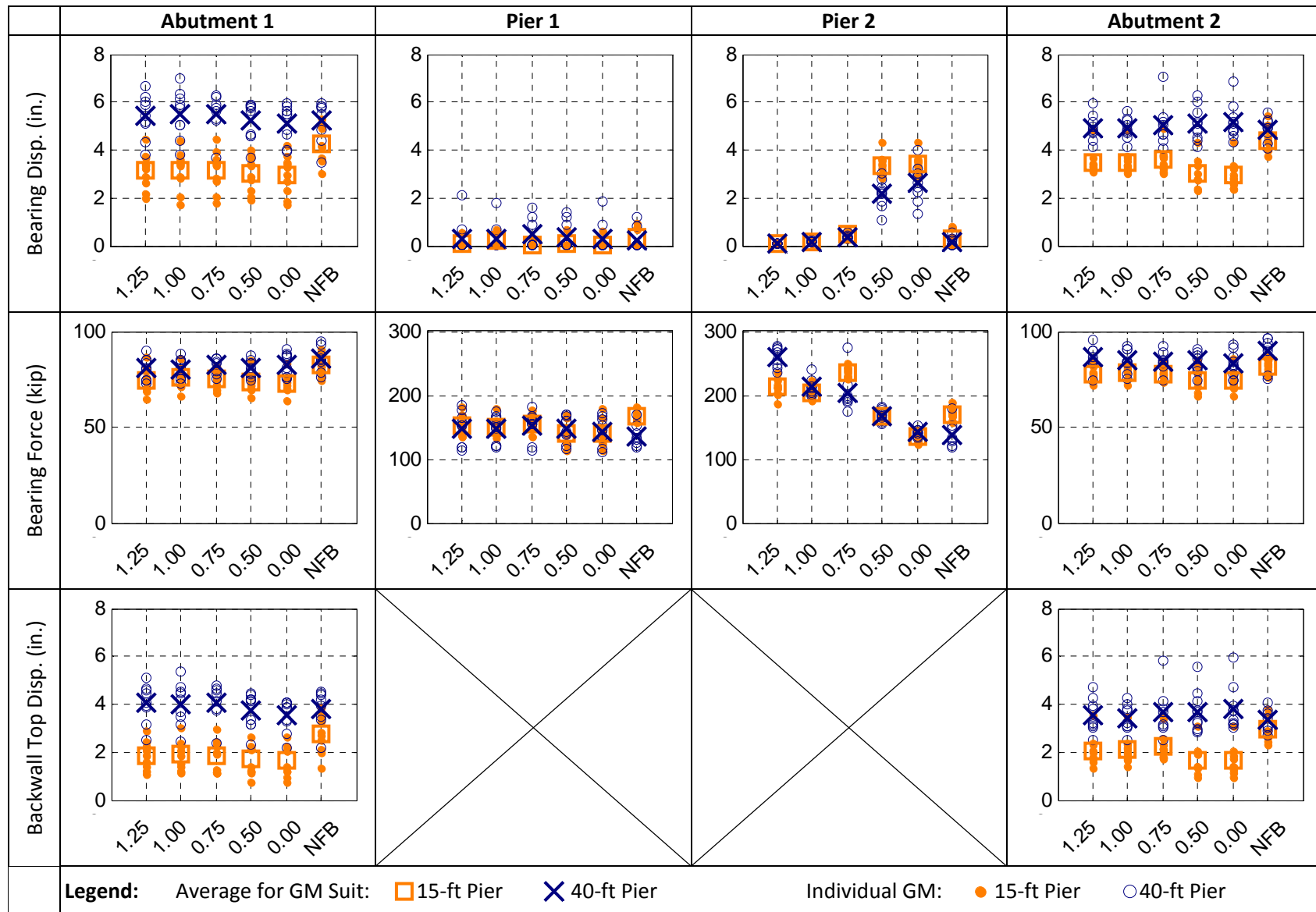


Figure 4.7. Response of Ss Bridge Variants Subjected to Pure Longitudinal Excitation

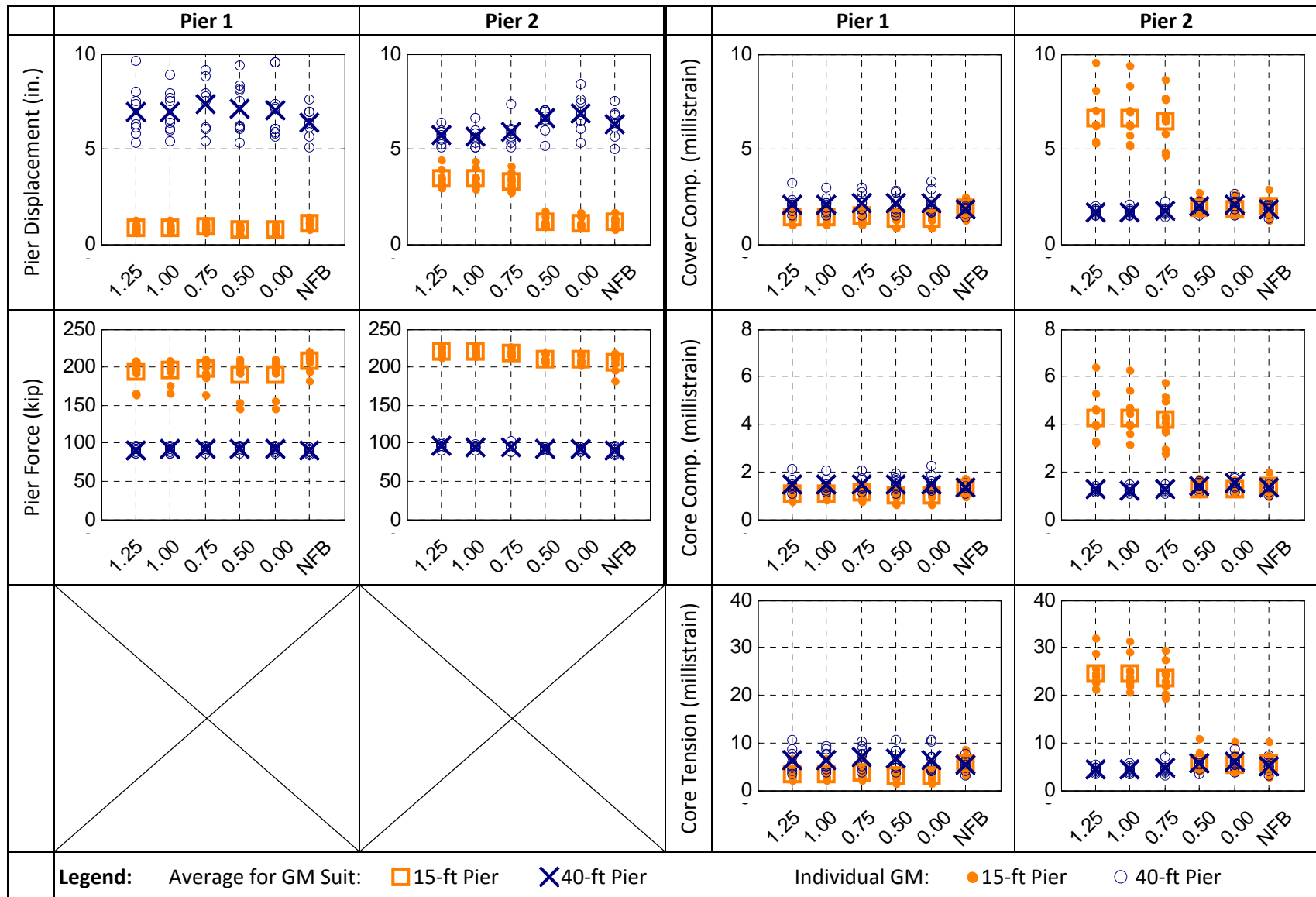


Figure 4.7. Response of Ss Bridge Variants Subjected to Pure Longitudinal Excitation (cont.)

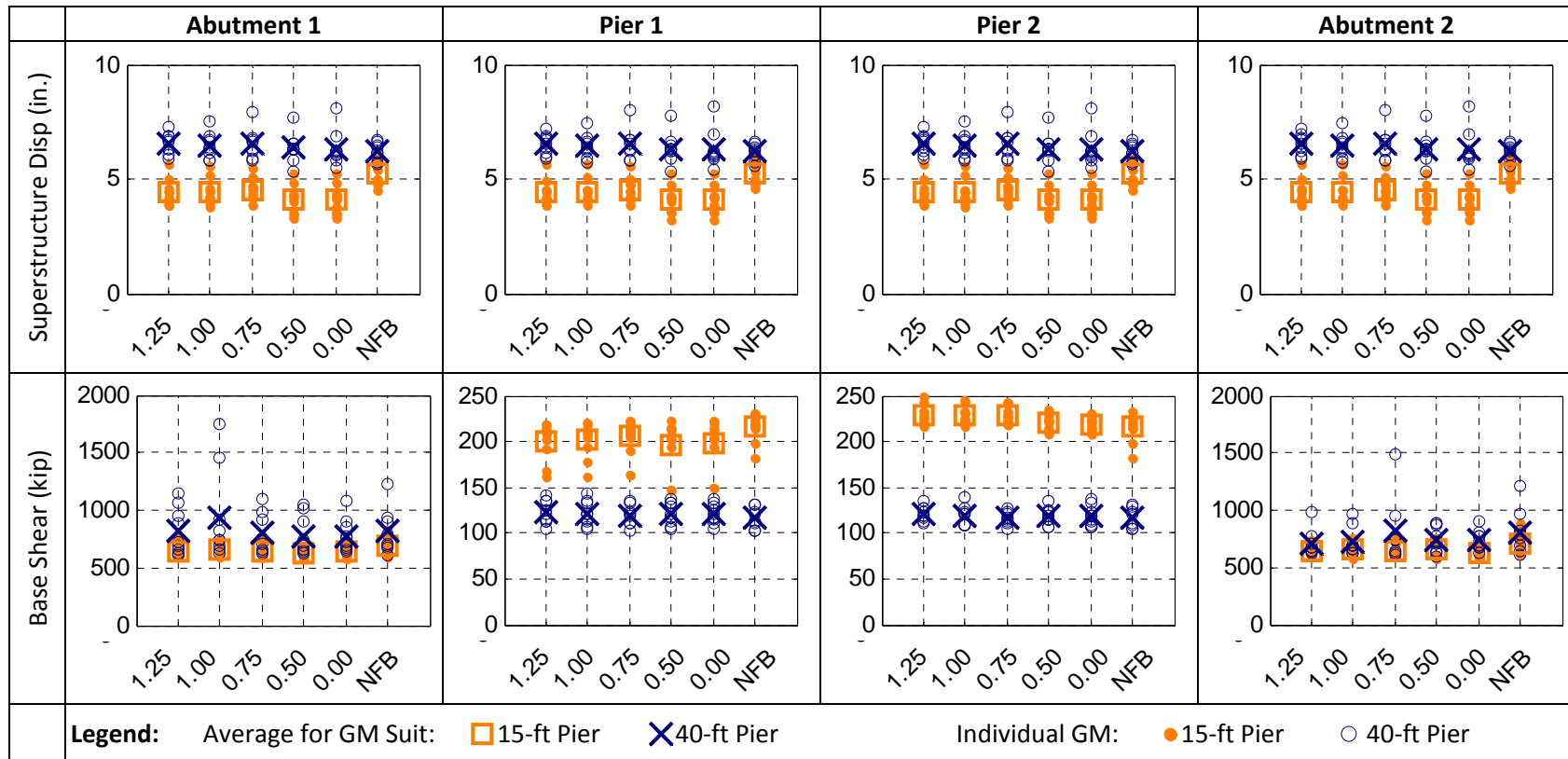


Figure 4.7. Response of Ss Bridge Variants Subjected to Pure Longitudinal Excitation (cont.)

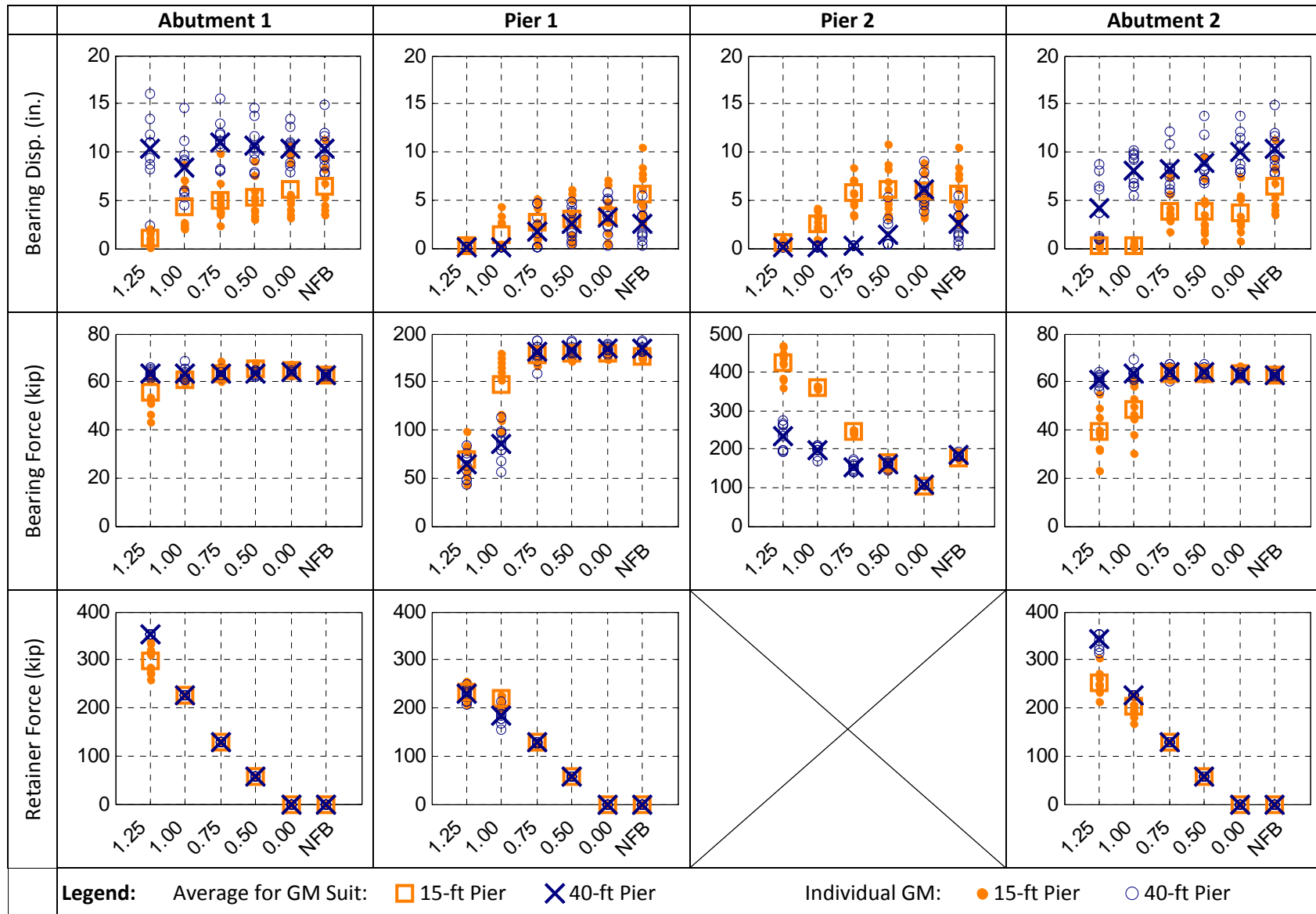


Figure 4.8. Response of Ss Bridge Variants Subjected to Pure Transverse Excitation

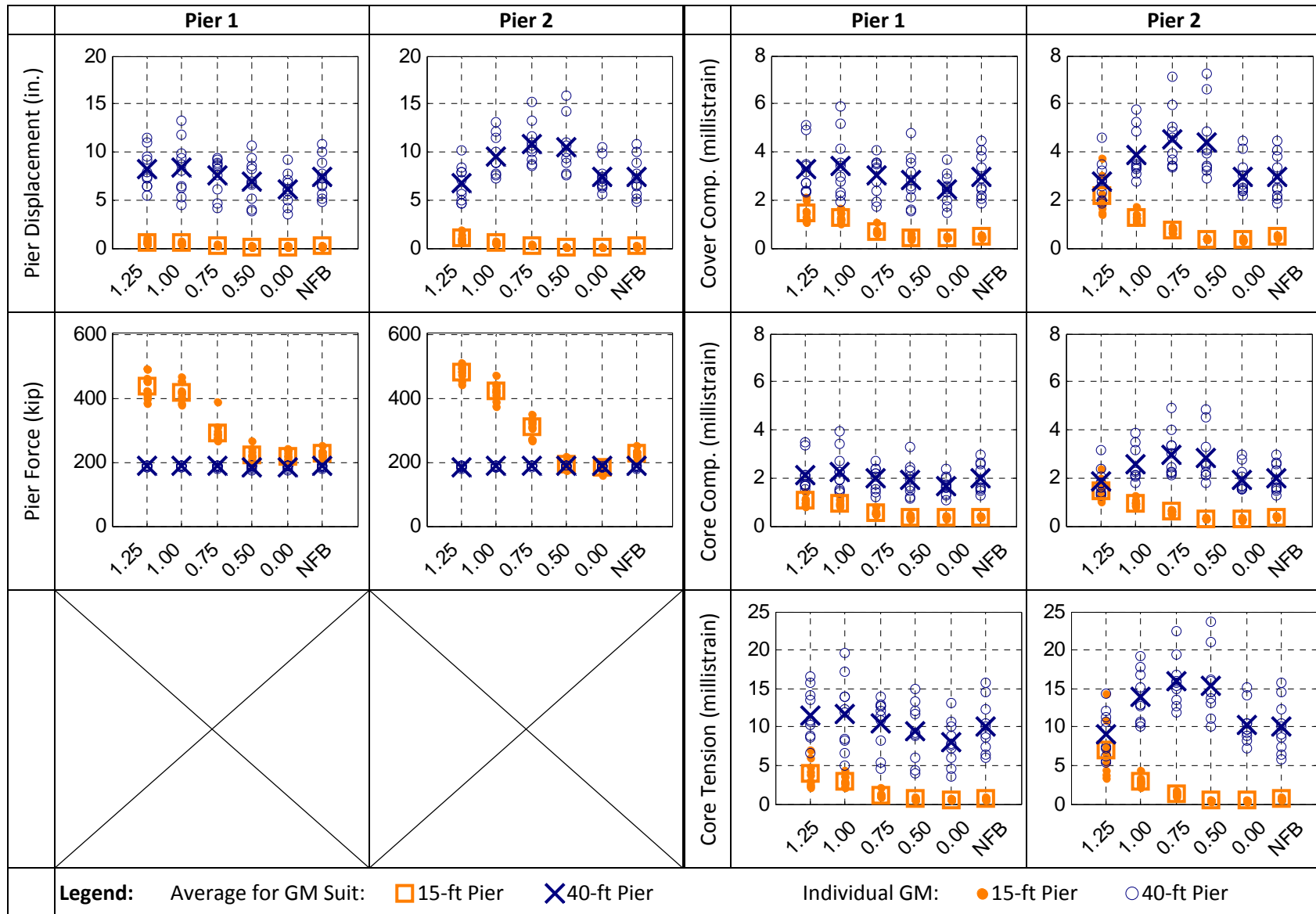


Figure 4.8. Response of Ss Bridge Variants Subjected to Pure Transverse Excitation (cont.)

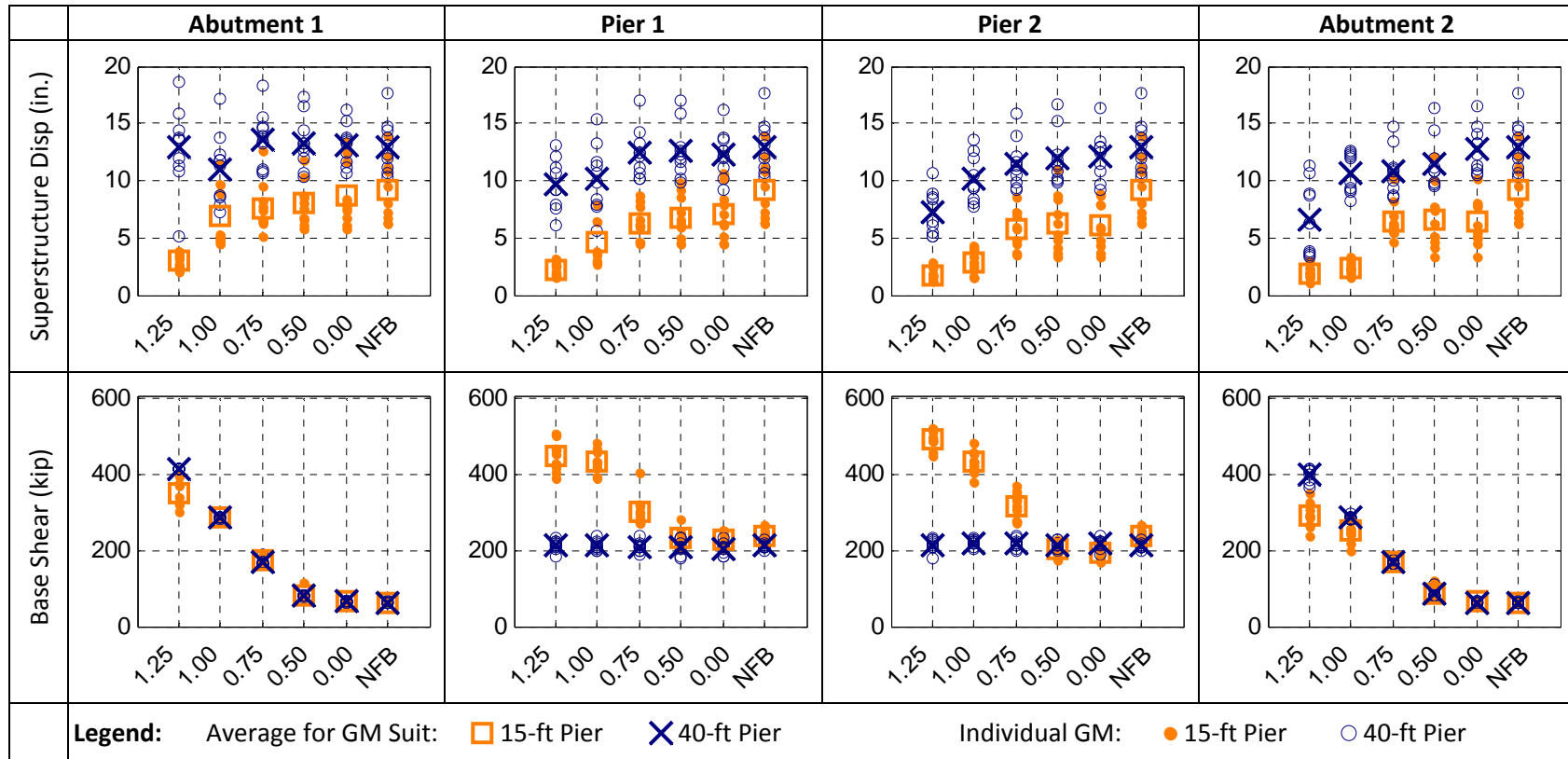


Figure 4.8. Response of Ss Bridge Variants Subjected to Pure Transverse Excitation (cont.)

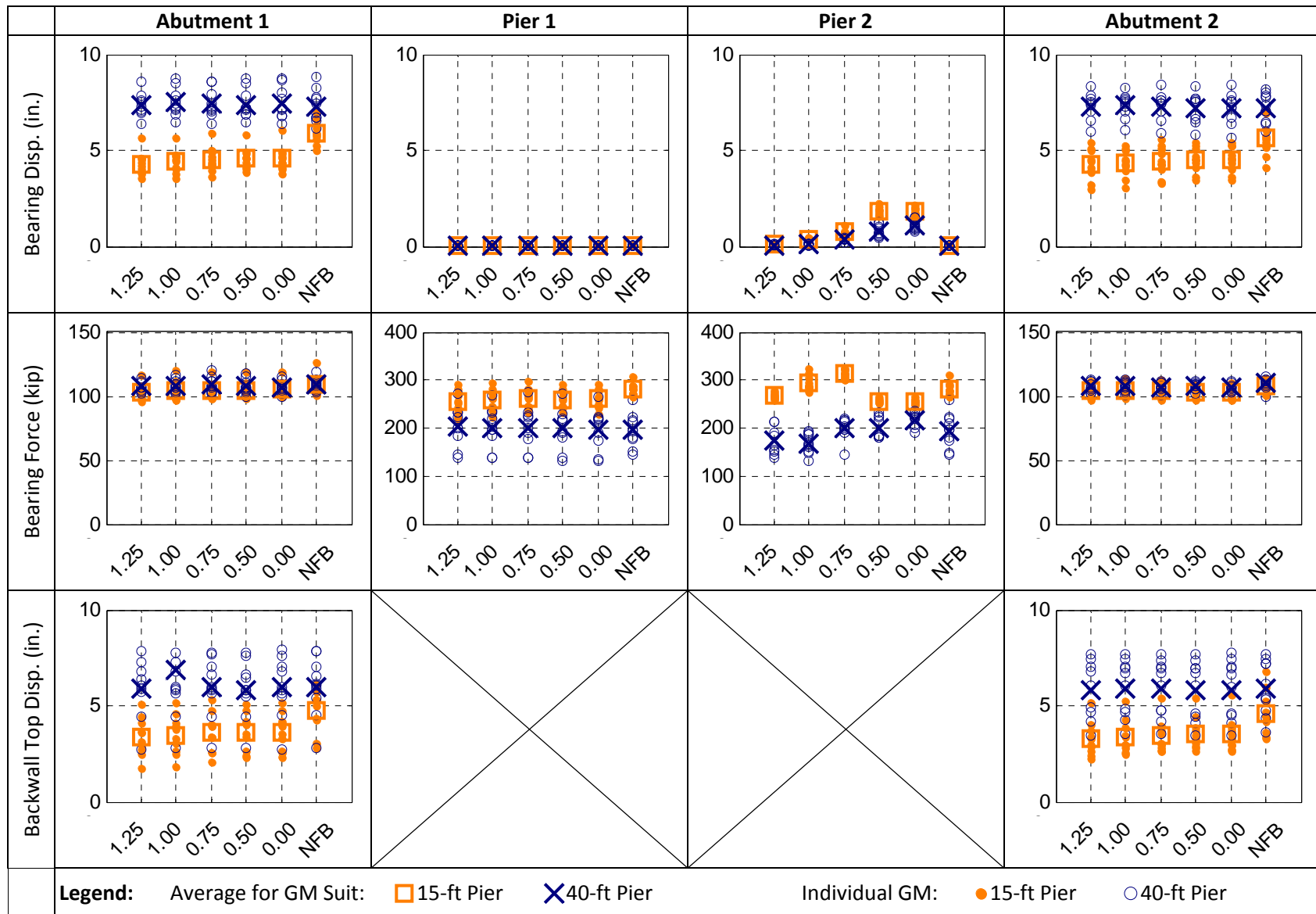


Figure 4.9. Response of SI Bridge Variants Subjected to Pure Longitudinal Excitation

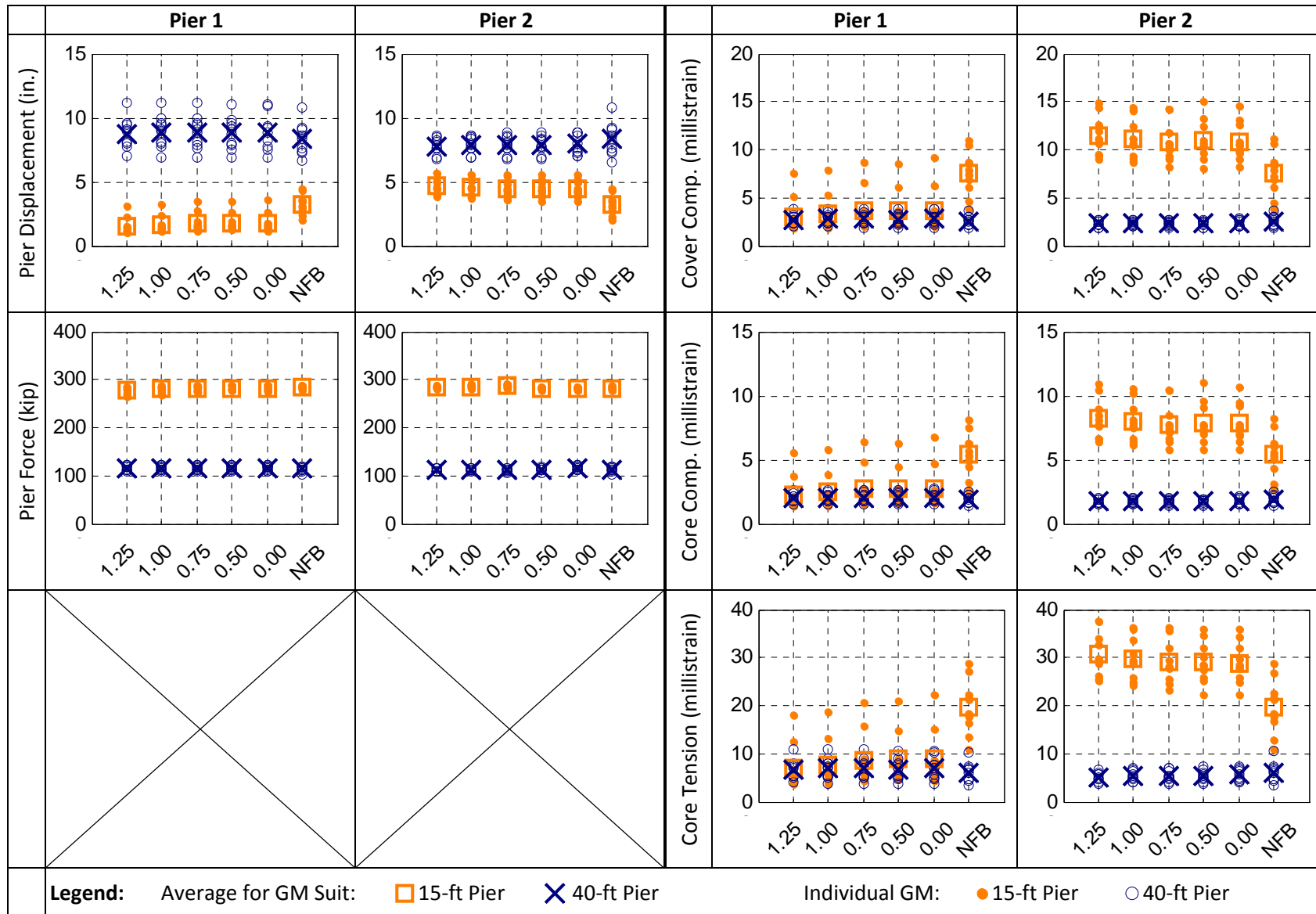


Figure 4.9. Response of SI Bridge Variants Subjected to Pure Longitudinal Excitation (cont.)

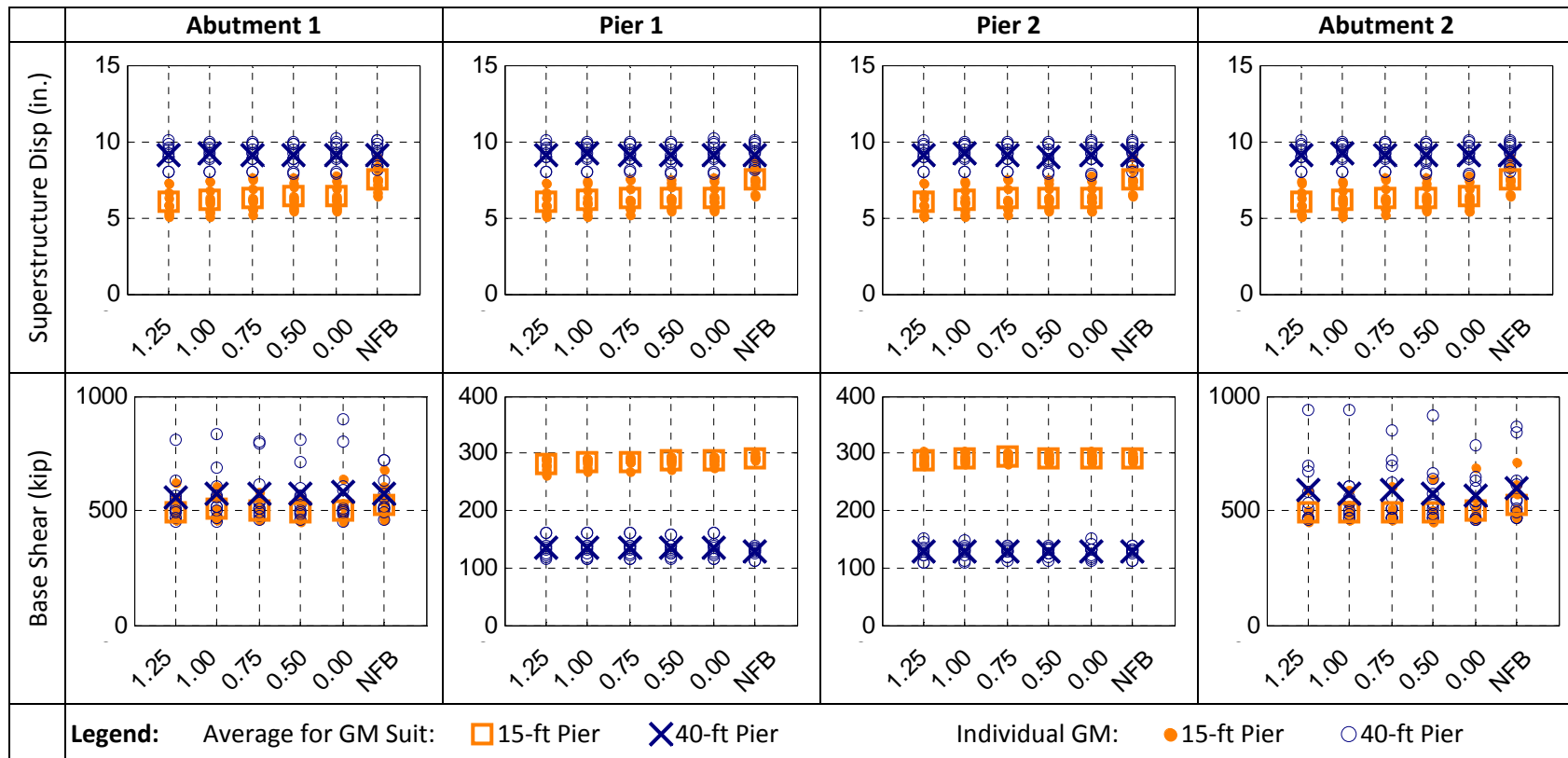


Figure 4.9. Response of SI Bridge Variants Subjected to Pure Longitudinal Excitation (cont.)

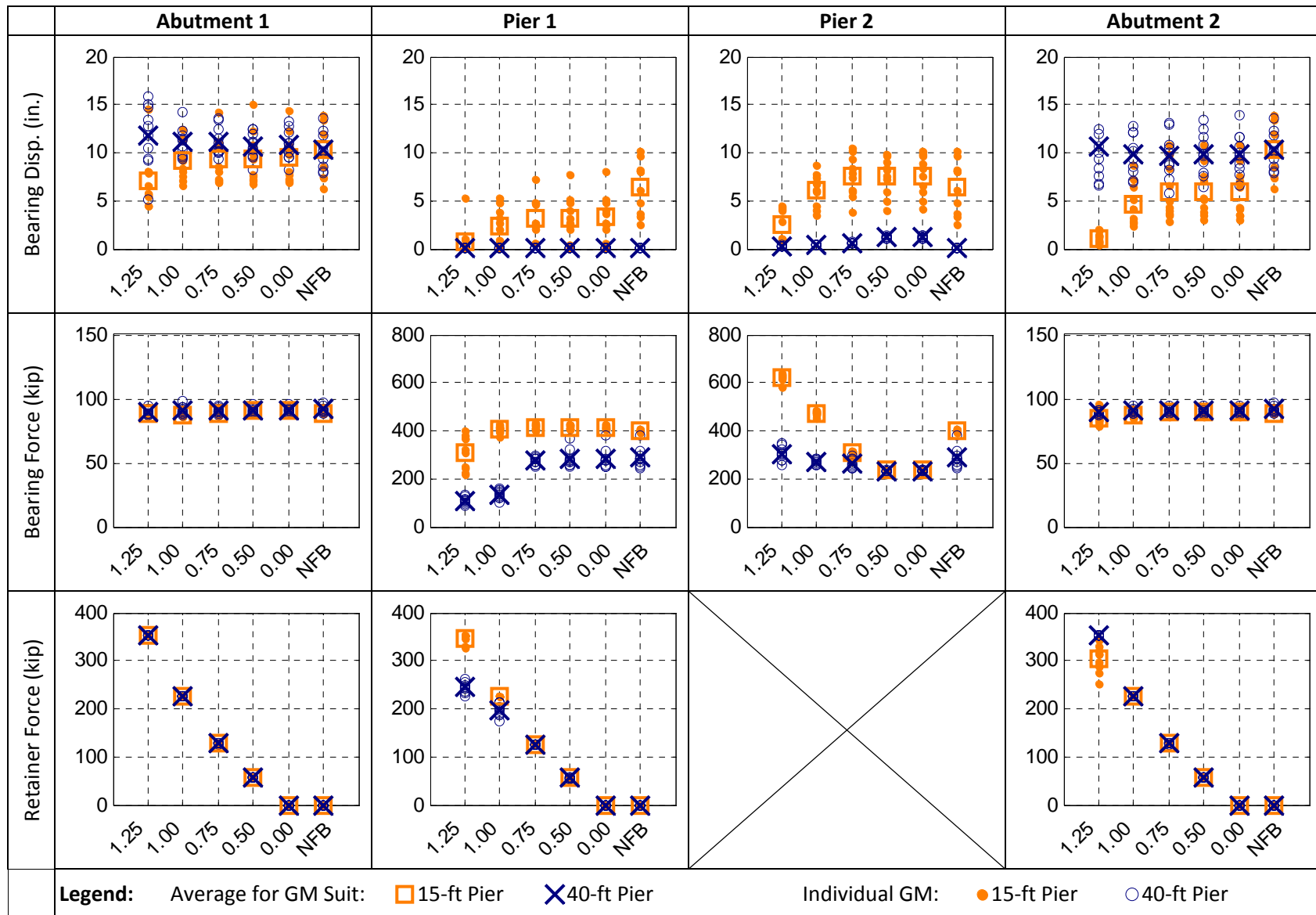


Figure 4.10. Response of SI Bridge Variants Subjected to Pure Transverse Excitation

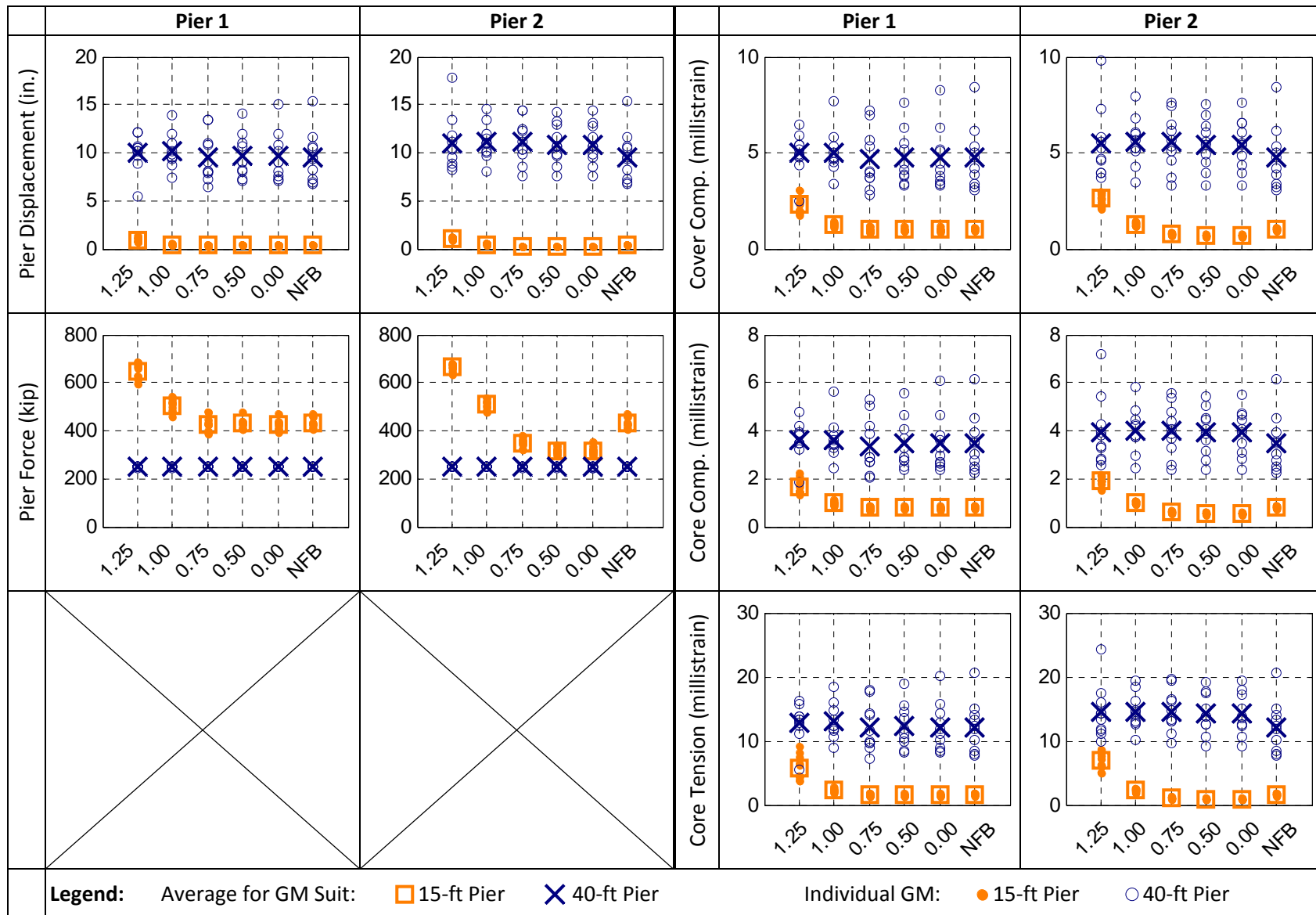


Figure 4.10. Response of SI Bridge Variants Subjected to Pure Transverse Excitation (cont.)

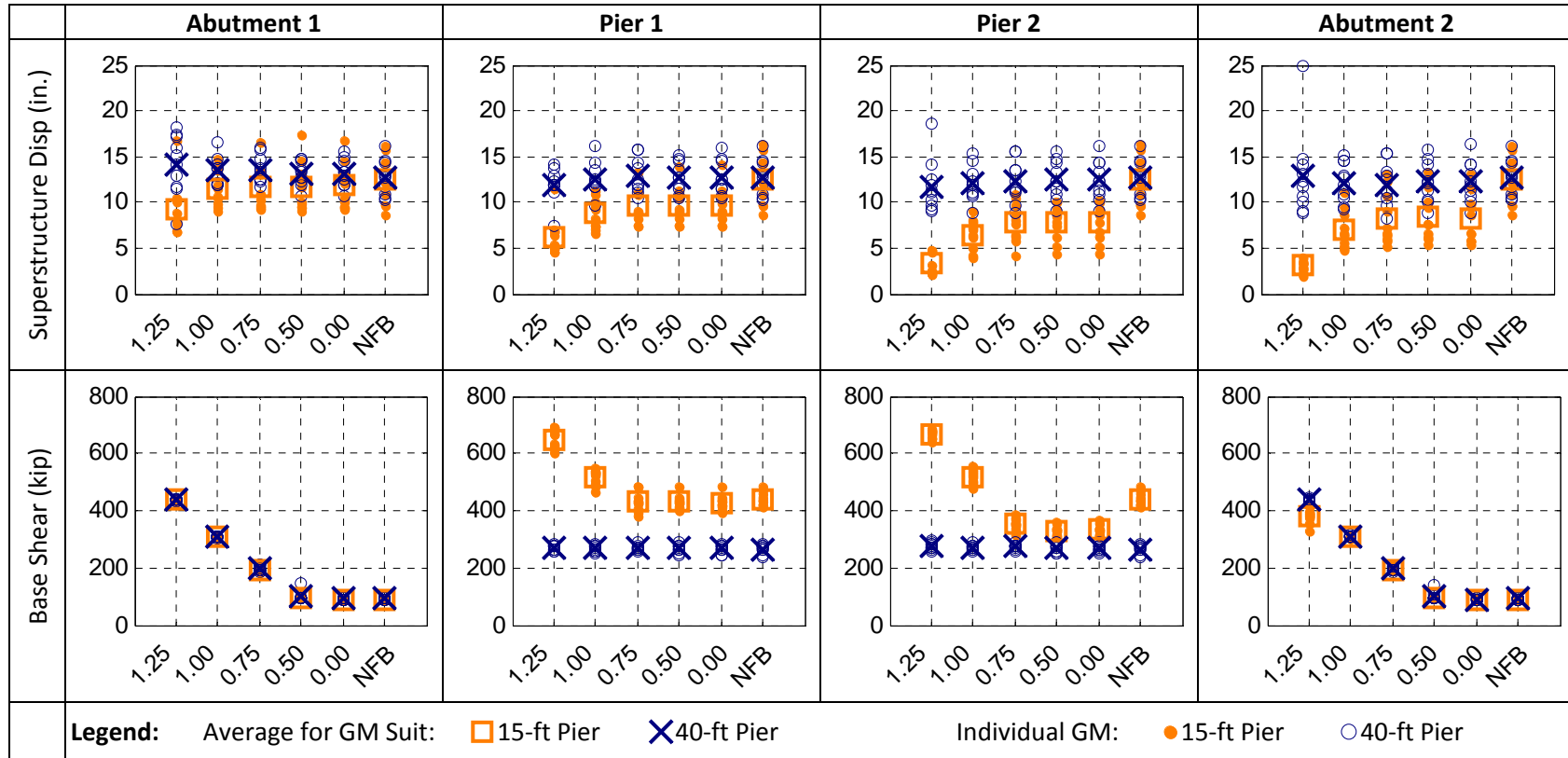


Figure 4.10. Response of SI Bridge Variants Subjected to Pure Transverse Excitation (cont.)

CHAPTER 5

RESULTS

5.1 LONGITUDINAL RESPONSE

5.1.1 Global Longitudinal Response

The longitudinal response of the overall bridge system was assessed through peak base shears at the supports and peak displacements of the deck relative to a fixed point on the ground. Peak global base shears and superstructure displacements are summarized in Table 5.1 and Table 5.2, respectively. Both of these global indices were unaffected by variations in anchor bolt diameter, as illustrated by the constancy of response in Figure 5.1 and Figure 5.2 with respect to bolt diameter.

Recall that retainers were not engaged under longitudinal excitation, meaning the fixed bearing anchors at Pier 2 were the only bridge parameter impacted by anchor bolt variation. This partially accounts for the lack of global response sensitivity. Additionally, the abutment backwalls dominated the longitudinal response, and further limited the extent to which local changes in fixed bearing behavior were reflected in global response. Figure 5.1 compares the peak base shear at a support with the peak base shear for the entire bridge (Table 5.1), and shows that under longitudinal excitation the abutments drew the majority of the base shear. For this base shear distribution to occur, the backwalls must have been contributing significant strength and stiffness to the system. Note that peak support base shear and peak global base shear were achieved at different points in the time-history record, and therefore the ratios should not be expected to sum to 1.0 over the four supports.

These base shears demonstrate the importance of capturing the backwall response as accurately as possible. Underestimation of backwall strength or stiffness may result in unexpectedly high demands on the abutment foundations, while overestimation may result in higher displacements and pier demands than anticipated by the designer. Capturing the detailed nonlinear response of backwall, wingwalls, approach slab, and backfill is beyond the capabilities of the current finite element model, and is a topic that would benefit from future research.

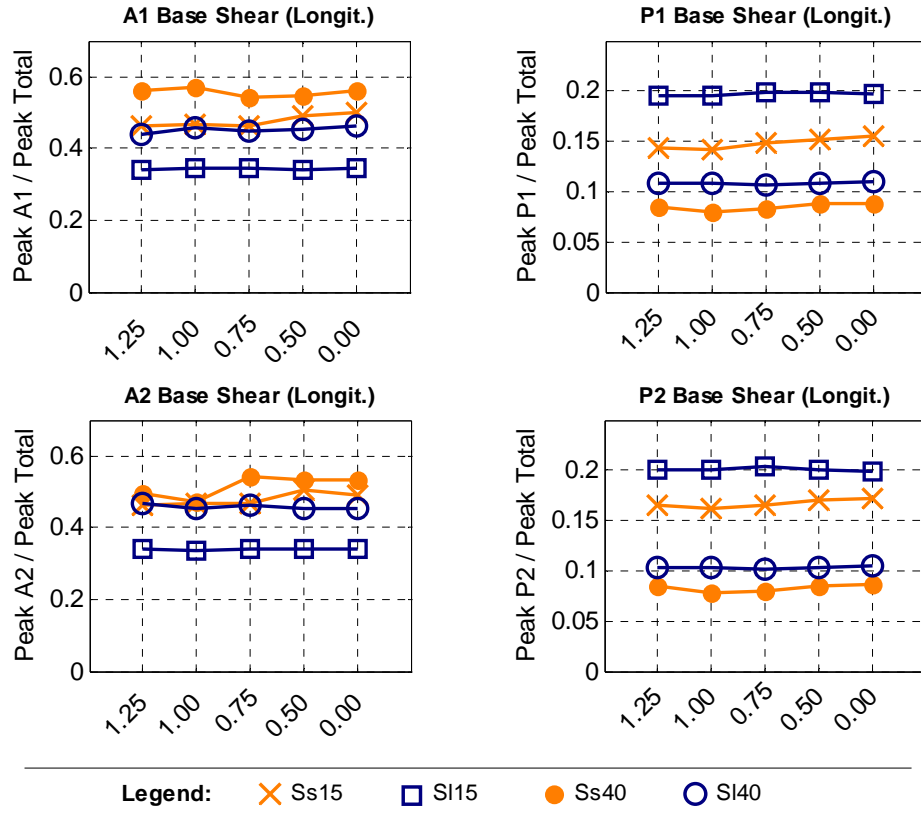


Figure 5.1. Variations in Ratio of Peak Support Base Shear to Peak Global Base Shear

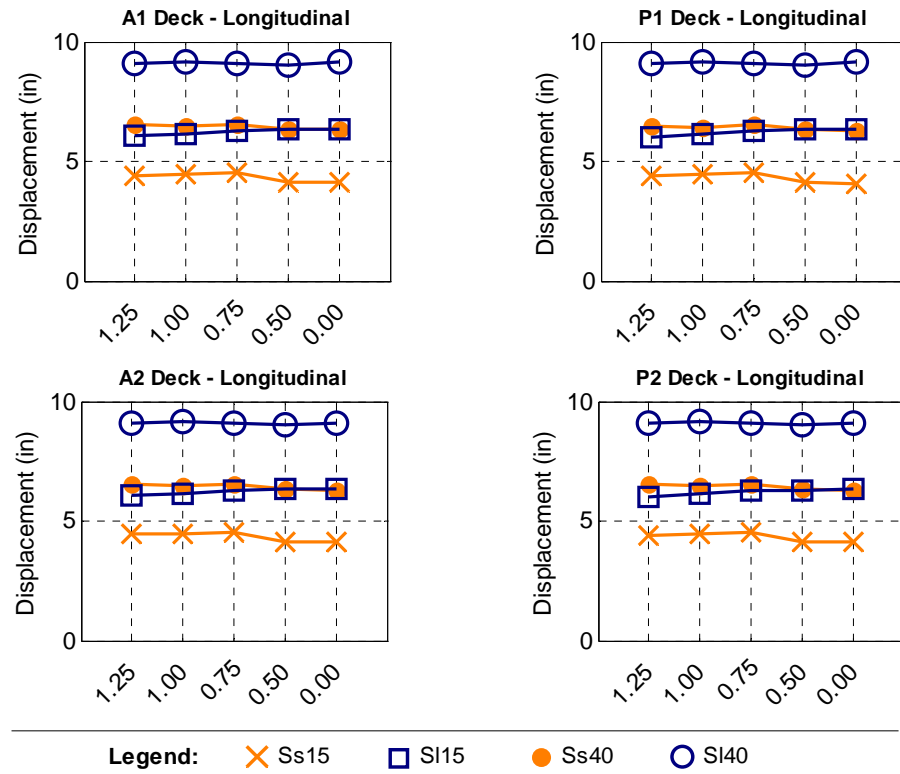


Figure 5.2. Variations in Peak Longitudinal Superstructure Displacement

Table 5.1. Peak Longitudinal Global Base Shear (kips)

		Ss Bridges		SI Bridges	
		15 ft Pier	40 ft Pier	15 ft Pier	40 ft Pier
Anchor Bolt Dia. (in.)	1.25	1392	1444	1444	1262
	1.00	1417	1591	1458	1255
	0.75	1389	1490	1445	1270
	0.50	1293	1401	1448	1259
	0.00	1268	1378	1465	1246
	NFB	1502	1475	1510	1255

Table 5.2. Peak Longitudinal Superstructure Displacement (in.)

		Ss Bridges		SI Bridges	
		15 ft Pier	40 ft Pier	15 ft Pier	40 ft Pier
Anchor Bolt Dia. (in.)	1.25	4.43	6.53	6.05	9.12
	1.00	4.47	6.46	6.17	9.18
	0.75	4.54	6.54	6.29	9.12
	0.50	4.14	6.34	6.34	9.03
	0.00	4.11	6.31	6.36	9.13
	NFB	5.25	6.22	7.55	9.14

5.1.2 Abutment Bearings

Peak longitudinal Abutment 1 bearing displacements are reported in Table 5.3, and the Abutment 2 response was similar. Bearing displacements were always greater than zero, indicating the abutment bearings always slid on the substructure. The horizontal force data in Figure 5.3 also suggest a sliding response, because peak recorded forces were in close correlation with the predicted 77 kip and 110 kip breakaway friction force for Ss and SI abutment bearings, respectively (Section 3.2.4). The abutment bearing response was not sensitive to anchor bolt diameter, being more strongly influenced by the abutment backwall and pier configuration.

Table 5.3. Peak Longitudinal Bearing Displacement at Abutment 1 (in.)

		Ss Bridges		SI Bridges	
		15 ft Pier	40 ft Pier	15 ft Pier	40 ft Pier
Anchor Bolt Dia. (in.)	1.25	3.16	5.41	4.30	7.37
	1.00	3.16	5.50	4.42	7.50
	0.75	3.16	5.50	4.54	7.44
	0.50	3.00	5.23	4.56	7.39
	0.00	2.96	5.14	4.57	7.45
	NFB	4.28	5.20	5.91	7.30

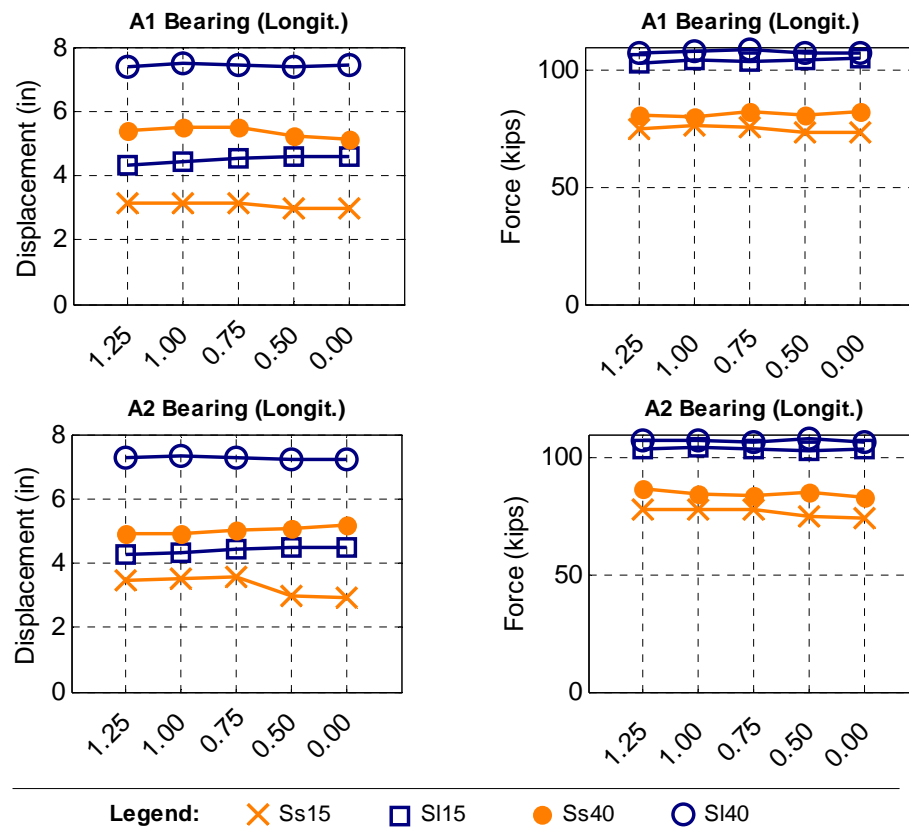


Figure 5.3. Variations in Peak Longitudinal Abutment Bearing Response

5.1.3 Pier 1 Elastomeric Bearings

Peak longitudinal displacements of the elastomeric bearings at Pier 1 are summarized in Table 5.4. Most bridges experienced little or no longitudinal bearing displacement, and like the abutment bearings, response was more sensitive to pier height than to anchor bolt diameter. The horizontal force response remained essentially constant with variations in anchor bolt diameter, as shown in Figure 5.4, and only the Ss bridge bearings developed sufficient force to begin

sliding. In Chapter 3 (Section 3.2.4), the breakaway friction force for these bearings was estimated at 205 kips, based on the superstructure dead load. In the dynamic analysis, sliding occurred at just 150 kips of horizontal force due to variations in the vertical load on the bearings. For the suite of 24 bridges, instantaneous vertical load on the Pier 1 bearings at the point of maximum horizontal bearing force ranged from 85% to 140% of the superstructure dead load.

Table 5.4. Peak Longitudinal Bearing Displacement at Pier 1 (in.)

		Ss Bridges		SI Bridges	
		15 ft Pier	40 ft Pier	15 ft Pier	40 ft Pier
Anchor Bolt Dia. (in.)	1.25	0.11	0.31	0.00	0.00
	1.00	0.22	0.27	0.00	0.00
	0.75	0.02	0.46	0.00	0.00
	0.50	0.07	0.35	0.00	0.00
	0.00	0.06	0.27	0.00	0.00
	NFB	0.38	0.25	0.00	0.00

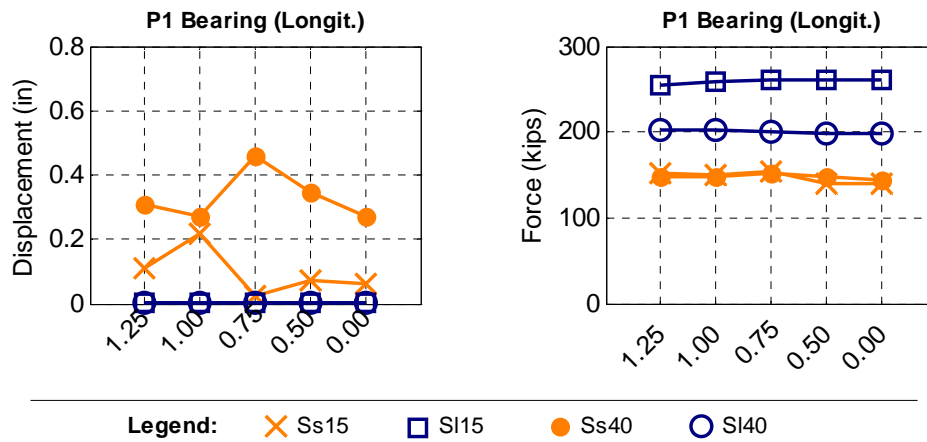


Figure 5.4. Variations in Peak Longitudinal Pier 1 Bearing Response

5.1.4 Pier 1 Columns

The Pier 1 column force, displacement, and strain data are shown in Figure 5.5; like the bearings, longitudinal column response was not sensitive to anchor bolt diameter. The strain plots provide peak compression strains in the confined core and peak tension strains in the longitudinal steel reinforcing. As discussed in Chapter 4 and summarized in Table 5.5, the columns began yielding when the first reinforcing bar yielded in tension ($\epsilon = 0.0023$) or the core concrete reached a compression strain of 0.002, and these limits are indicated in the plots with a dashed red line. The rebar strains were typically more critical than the concrete strains, and based

on the criteria in Table 5.5, all the piers yielded but were expected to remain serviceable. If the response to individual ground motions is considered instead of the average response shown in Figure 5.5, some of the S115 bridge columns sustained damage. The number of runs with yielding and damage is summarized for the full sensitivity study in Table 5.6.

Table 5.5. Column Performance Rubric

Performance Limit	Concrete Strain Limit (compression)	Steel Strain Limit (tension)	Columns with strains at or below this limit will be referred to as:
Yield	0.002	0.0023	Essentially Elastic
Serviceability	0.004	0.015	Serviceable / Lightly Damaged
Damage Control	0.018	0.060	Damaged
Life Safety	0.025	0.12	Severely Damaged

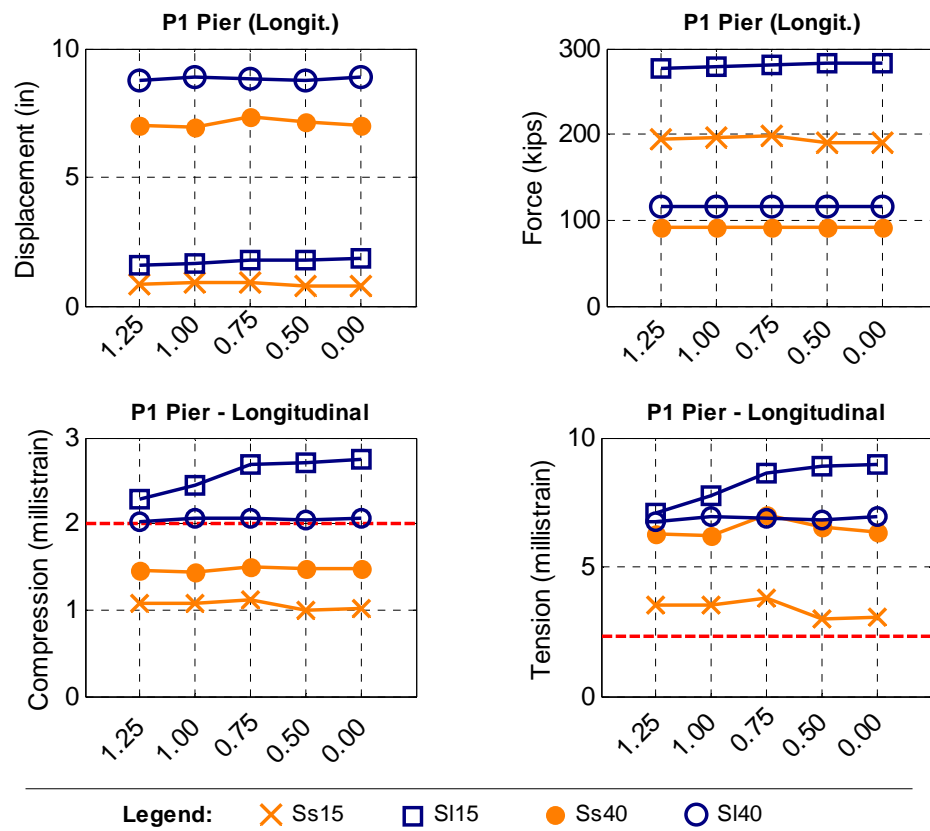


Figure 5.5. Variations in Peak Longitudinal Pier 1 Column Response

A comparison of the horizontal pier forces in Figure 5.5 with the horizontal bearing forces in Figure 5.4 reveals that peak pier force was slightly higher than peak bearing force for short-pier bridges, and the reverse was true of the tall-pier bridges. From a statics perspective,

this is counter-intuitive because one would expect parity of bearing and column demands. However, under dynamic earthquake loading the tall piers have a tendency to become out-of-phase with the bearings and superstructure, meaning that the accelerated column mass is producing a force that is opposite the bearing force. Results from the full sensitivity study show that, at the point of maximum horizontal pier force, the bearings and columns were displaced in the same direction for all short-pier runs, and in opposite directions for all tall-pier runs. At Pier 1, this tendency for out-of-phase column response appears to have reduced superstructure displacements, pier forces, and base shears, but this should not be relied upon in design until the nature and sensitivity of this dynamic response is better understood.

Table 5.6. Number of Longitudinal Runs with Yielding or Damage of Pier 1 Columns

		Short Steel (Ss) Superstructure				Long Steel (Sl) Superstructure			
		Short Pier (15 ft)		Tall Pier (40 ft)		Short Pier (15 ft)		Tall Pier (40 ft)	
		# Yield	# Dam.	# Yield	# Dam.	# Yield	# Dam.	# Yield	# Dam.
Anchor Bolt Dia. (in.)	1.25	8	n/a	9	n/a	10	1	9	n/a
	1.00	9	n/a	9	n/a	10	1	10	n/a
	0.75	9	n/a	8	n/a	10	2	10	n/a
	0.50	8	n/a	10	n/a	10	2	10	n/a
	0.00	8	n/a	10	n/a	10	2	10	n/a
	NFB	10	n/a	8	n/a	10	8	10	n/a

5.1.5 Pier 2 Fixed Bearings

The Pier 2 fixed bearings present the first instance of sensitivity to anchor bolt size. The summary of peak displacements in Table 5.7 shows that the fixed bearing anchor bolts responded in the elastic range at AB = 1.25, but fractured at AB = 0.50. For reference, based on related testing and analysis, the anchor bolt model defined yield and ultimate displacements as 10% and 100% of the anchor bolt diameter, respectively (Section 2.2).

The bearing force and displacement response are shown in Figure 5.6, accompanied by information for the column pier response and the global bridge response at Pier 2. Even though varying the anchor bolt diameter did alter the fixed bearing response, there was no appreciable change in global response, and little change in column response. The only exception was Ss15, where anchor rupture reduced peak pier displacement by 50% and greatly reduced the column damage level. In the other bridges, column yielding continued to dominate the Pier 2 response, even when the anchor bolts were completely removed. As illustrated for a single bridge and

ground motion in Figure 5.7, the horizontal fixed bearing force generated from friction alone was sufficient to yield the column. Table 5.8 summarizes the predicted and average recorded peak fixed bearing forces for the Ss bridges. Similar to the Pier 1 bearings, estimating friction force based on dead load was not a reliable method because vertical load on the Pier 2 bearings at the point of maximum horizontal bearing force ranged from 74% to 156% of the superstructure dead load.

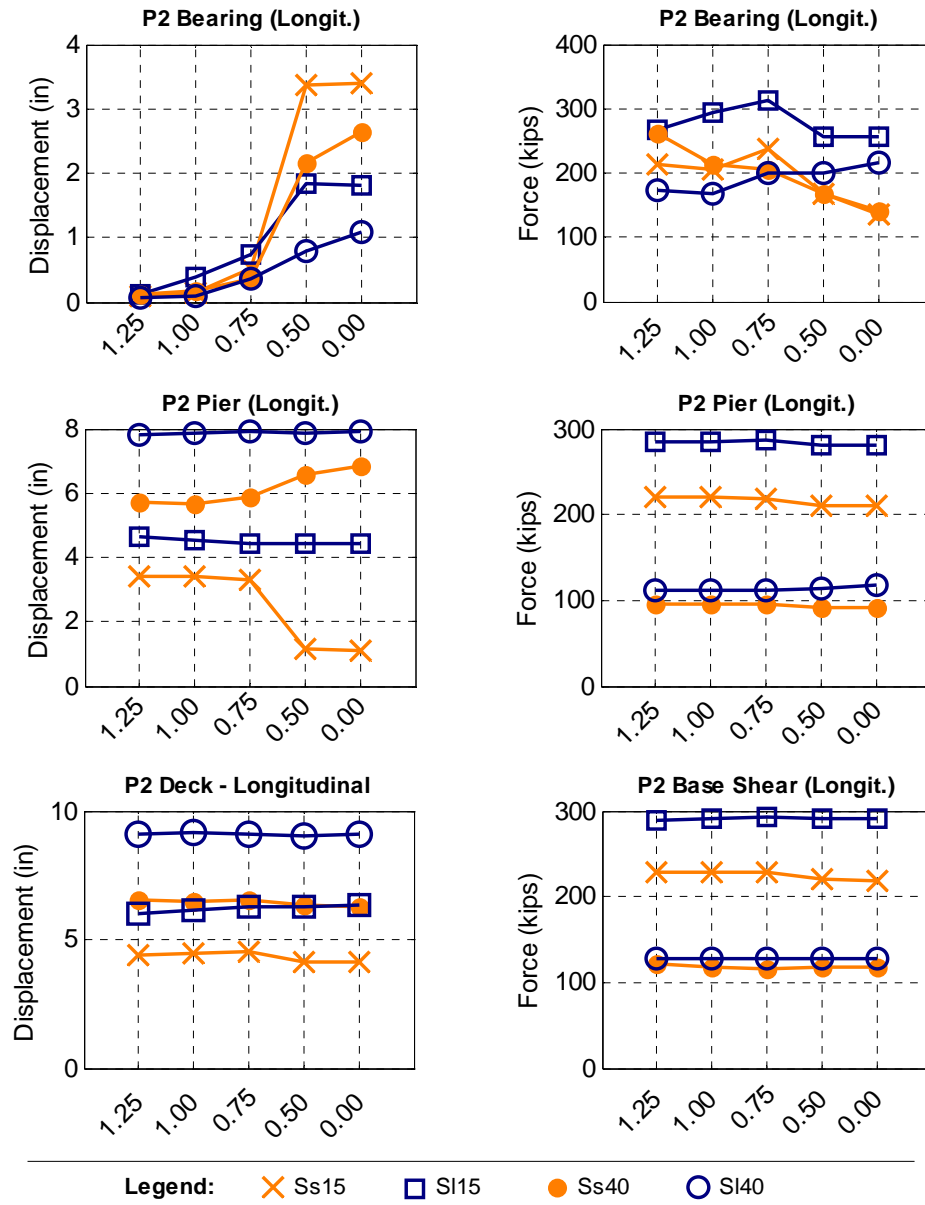


Figure 5.6. Variations in Peak Longitudinal Response at Pier 2

Table 5.7. Peak Longitudinal Fixed Bearing Displacement at Pier 2

		Ss Bridges		SI Bridges	
		15 ft Pier	40 ft Pier	15 ft Pier	40 ft Pier
Anchor Bolt Dia. (in.)	1.25	0.09	0.12	0.12	0.08
	1.00	0.15	0.17	0.40	0.10
	0.75	0.52	0.37	0.73	0.35
	0.50	3.38	2.17	1.85	0.79
	0.00	3.39	2.65	1.80	1.08
	NFB	0.27	0.13	0.00	0.00

Table 5.8. Actual Versus Predicted Peak Fixed Bearing Forces for the Ss Bridges

Bolt Dia (in.)	Qualitative Fixed Bearing Response	Avg Recorded Peak Bearing Force (kip)		Predicted Fuse Force (kip)		
		15 ft Pier	40 ft Pier	Elastomer Friction	Bolt Fracture	Total
1.25	Bolts Elastic	213	261	103	424	527
1.00	Bolts Elastic	205	212	103	271	374
0.75	Bolts Yield	336	203	103	153	256
0.50	Bolts Fracture, Brg Slides	168	168	103	68	171
0.00	Bearing Slides	135	142	103	0	103

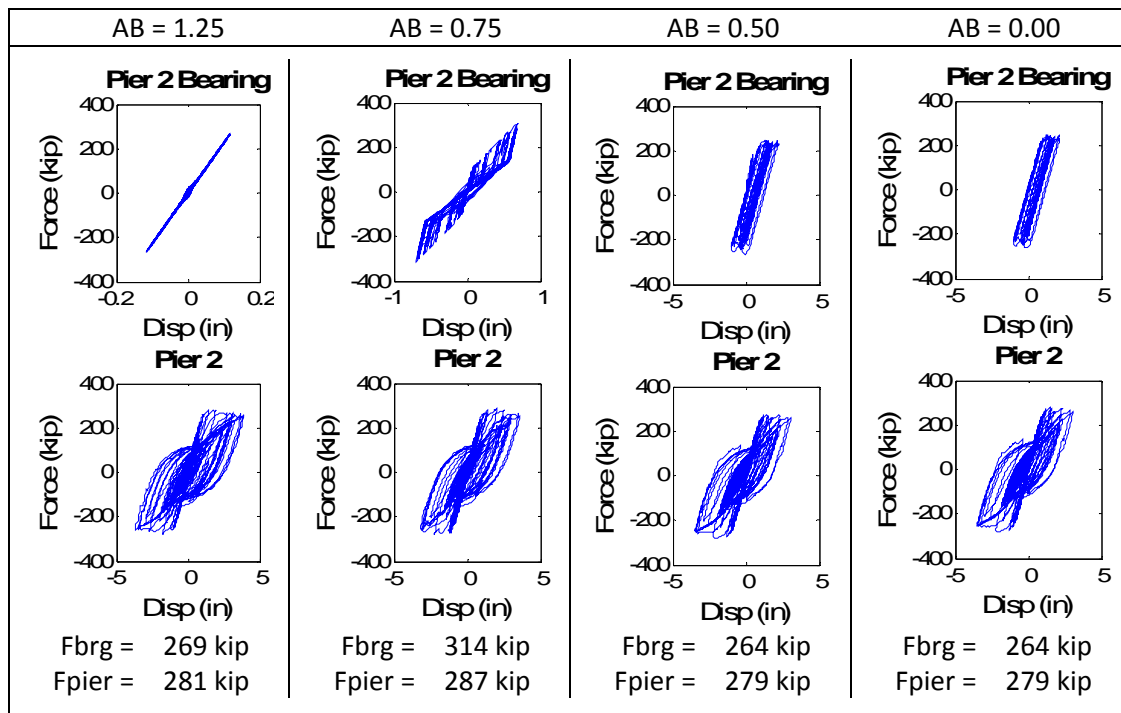


Figure 5.7. Longitudinal Response of SI15 Fixed Bearings and Columns to Ground Motion Pa04

5.1.6 Pier 2 Columns

As discussed in the previous section, only the Ss15 bridge showed response sensitivity to anchor bolt size. For Ss15, anchor bolt rupture at $AB = 0.5$ reduced column displacement by more than 50%, but for the other bridges, column displacement remained constant despite fusing of the fixed bearing anchor bolts. A comparison of the column forces in Figure 5.8 with the bearing forces in Figure 5.6 reveals similar forces for the short-pier bridges, however, for the tall-pier bridges, pier force is lower than bearing force. This is similar to the trend observed at Pier 1 and is likewise attributed to out-of-phase response of the 40 ft columns.

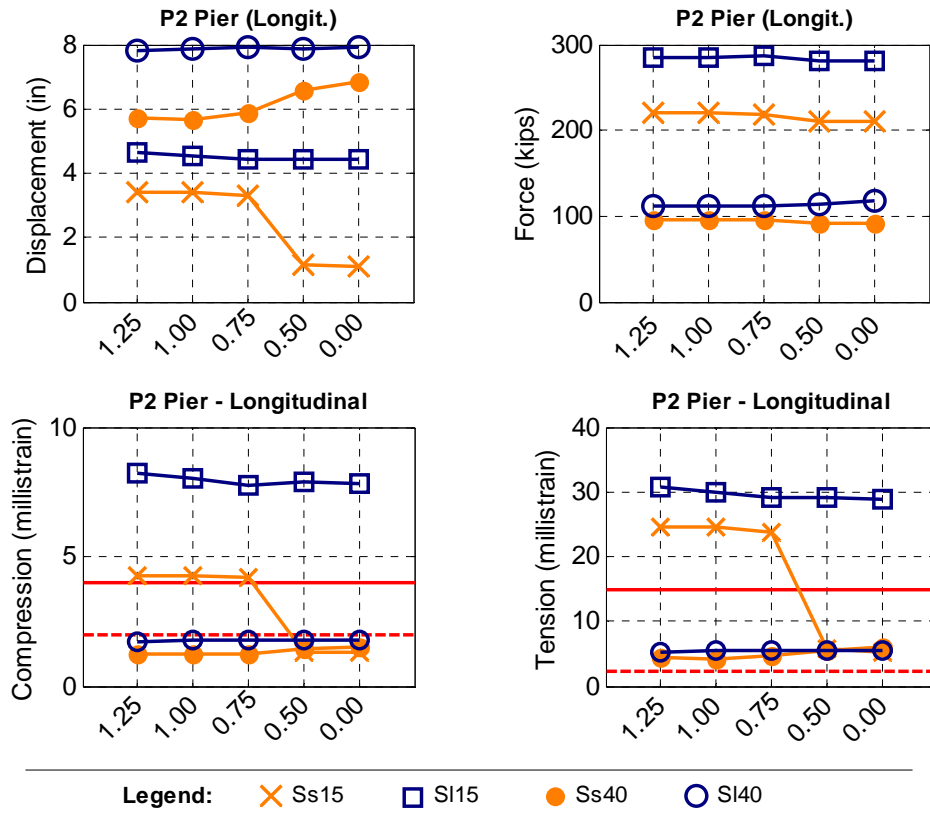


Figure 5.8. Variations in Peak Longitudinal Column Response at Pier 2

The strain plots included in Figure 5.8 provide peak compression strains in the confined core, and peak tension strains in the longitudinal steel reinforcing. As discussed in Chapter 4 and summarized in Table 5.5, the columns began yielding when the first reinforcing bar yielded in tension ($\epsilon = 0.0023$) or the core concrete reached a compression strain of 0.002. These yield limits are indicated in the plots with a dashed red line, the solid red line marks the serviceability limit and the damage limit is not shown. The Ss40 and SI40 bridge columns yielded but were

expected to remain serviceable, while the S115 bridges sustained damage for all anchor bolt sizes. In contrast, the Ss15 bridge was damaged for the three largest anchor bolt sizes, but anchor bolt rupture at $AB = 0.50$ produced a reduction in strains such that the columns remained serviceable. If the response to individual ground motions is considered instead of the average response shown in Figure 5.5, some of the S115 bridge columns sustained damage. The number of runs with yielding and damage is summarized for the full sensitivity study in Table 5.9. No instances of severe damage were recorded.

Table 5.9. Number of Longitudinal Runs with Yielding or Damage of Pier 2 Columns

		Short Steel (Ss) Superstructure				Long Steel (Sl) Superstructure			
		Short Pier (15 ft)		Tall Pier (40 ft)		Short Pier (15 ft)		Tall Pier (40 ft)	
		# Yield	# Dam.	# Yield	# Dam.	# Yield	# Dam.	# Yield	# Dam.
Anchor Bolt Dia. (in.)	1.25	9	n/a	10	2	10	n/a	10	2
	1.00	8	n/a	10	2	6	n/a	10	2
	0.75	n/a	n/a	10	n/a	n/a	n/a	10	3
	0.50	n/a	n/a	10	n/a	n/a	n/a	10	3
	0.00	n/a	n/a	10	n/a	n/a	n/a	10	2
	NFB	n/a	n/a	10	1	n/a	n/a	10	2

5.1.7 Summary of Longitudinal Response

Longitudinal response was largely insensitive to anchor bolt diameter. Figure 5.9 summarizes the limit states reached by each bridge, and there were very few instances where a change in anchor bolt diameter correlated with a change in the limit states.

The abutment bearings always slid, and the backwall (which always developed a full plastic hinge), was the critical bridge element that limited longitudinal superstructure movement. The elastomeric bearings at Pier 1 rarely slid, but the fixed bearings always fused for $AB = 0.50$ and $AB = 0.00$. The column piers always yielded, but generally remained serviceable. Instances of damage were marked with a * in Figure 5.9, and there were no instances of severe damage.

The two effects of the anchor bolt variations were to introduce the Fb limit state for the smaller bolt diameters, and reduce damage in the Pier 2 columns for Ss15. Clearly there are limitations on using anchor bolt diameter to calibrate longitudinal response, and while good results were achieved for the Ss15 bridge, bolt diameter may not be an effective calibration parameter for bridges with heavy superstructures or very tall piers.

		Short Steel (Ss) Superstructure									
		Short Pier (15 ft)					Tall Pier (40 ft)				
Anchor Bolt Dia. (in.)	1.25	EA Bw		P1 P2*			EA Bw EP		P1 P2		
	1.00	EA Bw EP		P1 P2*			EA Bw EP		P1 P2		
	0.75	EA Bw		P1 P2*			EA Bw EP		P1 P2		
	0.50	EA Bw	Fb P1 P2				EA Bw EP Fb P1 P2				
	0.00	EA Bw	Fb P1 P2				EA Bw EP Fb P1 P2				
	NFB	EA Bw EP Fb P1 P2					EA Bw EP		P1 P2		

		Long Steel (Sl) Superstructure									
		Short Pier (15 ft)					Tall Pier (40 ft)				
Anchor Bolt Dia. (in.)	1.25	EA Bw		P1 P2*			EA Bw		P1 P2		
	1.00	EA Bw		P1 P2*			EA Bw		P1 P2		
	0.75	EA Bw		P1 P2*			EA Bw		P1 P2		
	0.50	EA Bw	Fb P1 P2*				EA Bw	Fb P1 P2			
	0.00	EA Bw	Fb P1 P2*				EA Bw	Fb P1 P2			
	NFB	EA Bw		P1* P2*			EA Bw		P1 P2		

Column damage at Pier 1 (P1*) or Pier 2 (P2*)

Columns only lightly damaged, but neither the Pier 1 or Pier 2 bearings fused

Columns only lightly damaged and bearings at one or both piers fused

Figure 5.9. Limit States that Occurred Under Longitudinal Excitation

5.2 TRANSVERSE RESPONSE

5.2.1 Global Transverse Response

The transverse response of the overall bridge system was assessed through peak base shears at the supports and peak superstructure displacements of the deck relative to a point on the ground. Peak global base shears and superstructure displacements were both sensitive to anchor bolt diameter, as summarized in Table 5.10 and Table 5.11.

Unlike the longitudinal response where the backwalls provided most of the restraint and masked the influence of the anchor bolts, transverse restraint was provided directly by the retainer and fixed bearing anchor bolts. Thus, anchorage strength had a more pronounced correlation with system response. The concept is illustrated by the two schematic bridge piers in Figure 5.10. Bridge A employs the conventional ductile substructure ERS and the bolts are sized to remain elastic, while the quasi-isolated Bridge B uses bolts half this size, allowing rupture to

occur during the earthquake response. With smaller bolts, Bridge B has smaller fuse capacity than Bridge A, and the peak base shear is therefore expected to be smaller. However, this reduction in base shear is accompanied by an increase in displacement. In Bridge A the superstructure is restrained against sliding throughout the earthquake record, but the Bridge B superstructure is unrestrained after anchor rupture, and larger sliding displacements of the superstructure are expected.

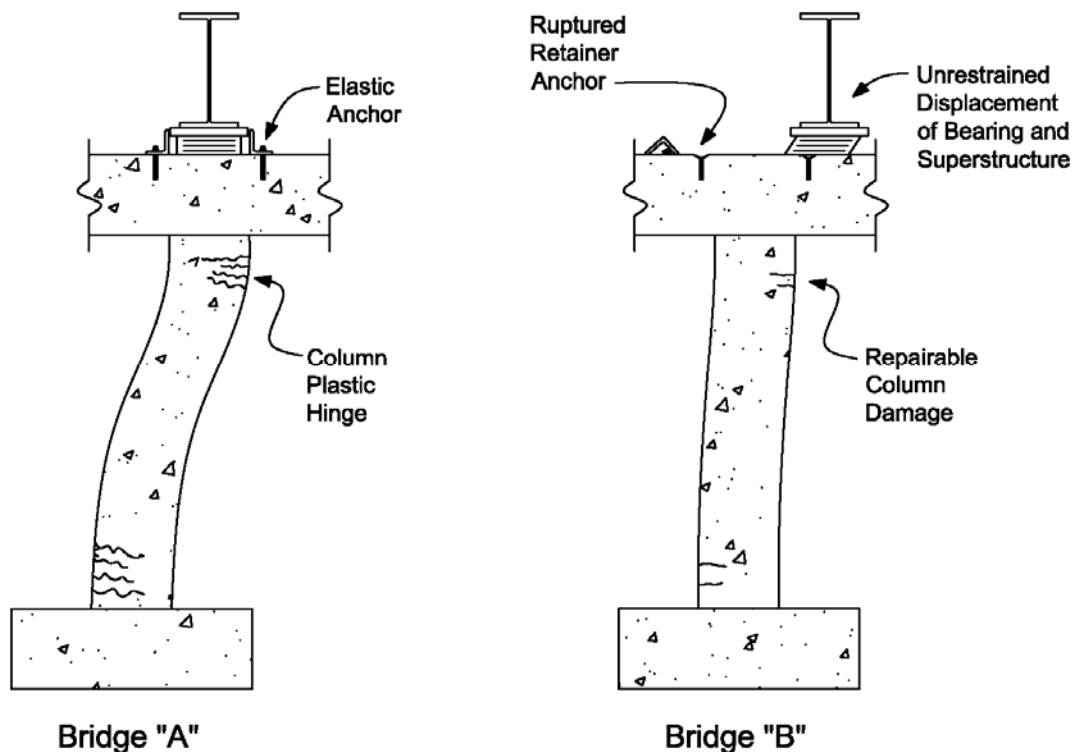


Figure 5.10. Idealized Response of Conventional and Quasi-Isolated Substructures

The base shear responses recorded for the short-pier bridges generally followed the trend anticipated for quasi-isolated bridges. As anchor bolt diameter was decreased, the peak base shears shown in Figure 5.11 decreased and the piers carried an increasing percentage of the global base shear. In tall-pier bridges, decreasing bolt diameter did lower base shears at the abutments, but the pier base shears were unchanged. At these piers, the response was governed by yielding of the columns rather than bearing fusing, so the base shear remained relatively constant.

Table 5.10. Peak Transverse Global Base Shear (kips)

		Ss Bridges		SI Bridges	
		15 ft Pier	40 ft Pier	15 ft Pier	40 ft Pier
Anchor Bolt Dia. (in.)	1.25	1296	1074	1629	1261
	1.00	1040	805	1149	900
	0.75	634	551	853	696
	0.50	506	530	846	690
	0.00	495	526	850	691
	NFB	591	532	1049	694

Table 5.11. Peak Transverse Superstructure Displacement (in.)

		Ss Bridges		SI Bridges	
		15 ft Pier	40 ft Pier	15 ft Pier	40 ft Pier
Anchor Bolt Dia. (in.)	1.25	2.95	12.90	9.32	14.16
	1.00	6.93	11.06	11.50	13.47
	0.75	7.64	13.60	11.68	13.49
	0.50	8.02	13.33	11.70	13.11
	0.00	8.76	13.09	11.80	13.16
	NFB	9.21	12.98	12.60	12.71

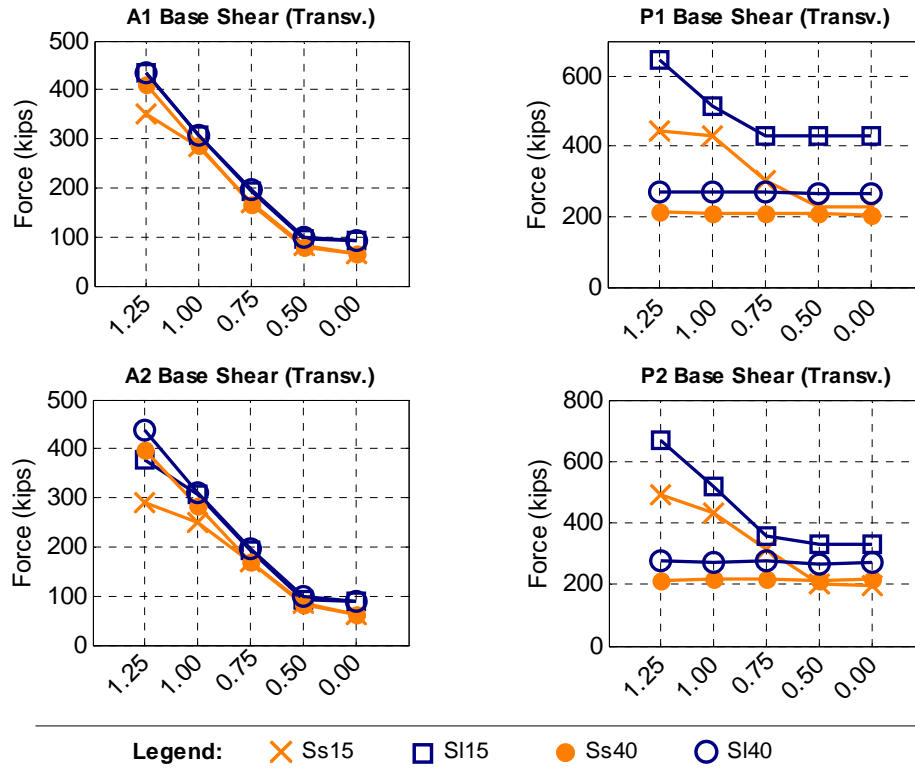


Figure 5.11. Variation in Peak Transverse Base Shear

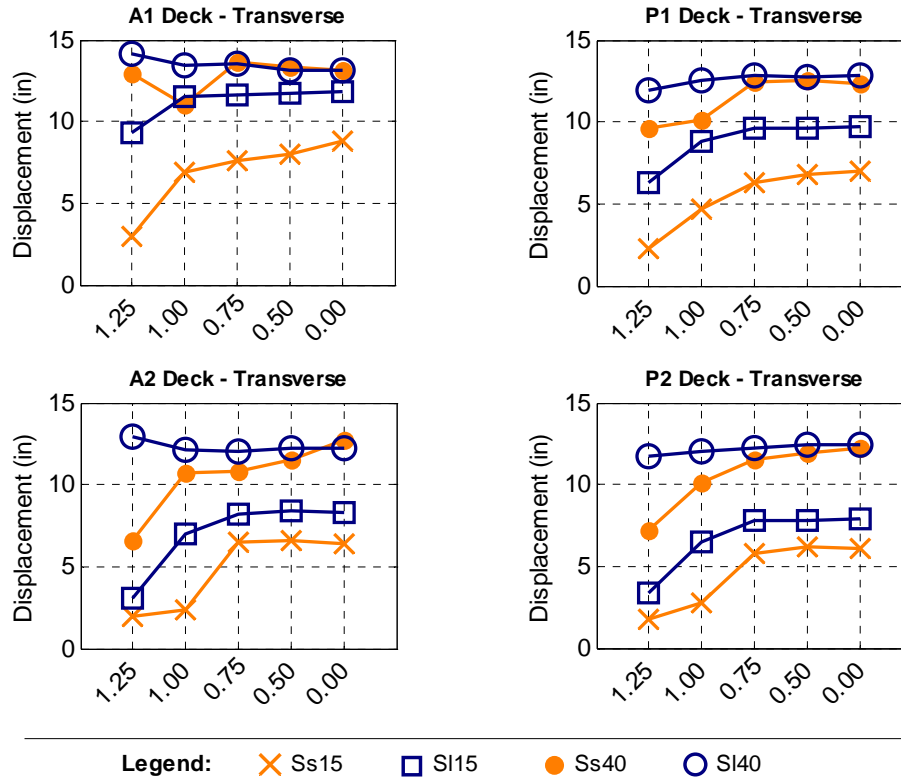


Figure 5.12. Variation in Peak Transverse Superstructure Displacement

As expected, the superstructure displacements shown in Figure 5.12 increased with the initial reduction in bolt diameter, but further reductions in diameter did not correspond to continually increasing superstructure displacements. Instead, the influence of subsequent bolt diameter reductions tapered off, and superstructure displacement for each bridge eventually remained constant by virtue of the horizontal friction force developed at the bearing sliding interface. Thus, even in cases without any positive anchorage (e.g., $AB = 0.00$) the superstructure was not truly unrestrained, and the horizontal friction force was sufficient to limit displacement at the level of seismic hazard expected in Illinois.

5.2.2 Abutment Bearings

When discussing transverse response, “fuse capacity” must be clearly defined because both elastomer friction and anchor bolt rupture contribute to the total capacity. Because the total capacity is what influences system response, any mention of “bearing capacity” or “fuse capacity” should be understood to include both the elastomer and retainer response. As needed, the elastomer or retainer components will be referenced explicitly.

The force response of the bearing assemblies was quite sensitive to anchor bolt diameter, as seen in Figure 5.13, and the displacement response followed similar trends as superstructure displacement. Comparison of the bearing assembly response in Figure 5.13 with the elastomer and retainer anchor responses in Figure 5.14 shows that assembly response resembled the retainer anchor behavior for larger bolt sizes, and then around $AB = 0.75$, transitioned to a response more similar to the elastomer friction behavior. The friction provided a lower bound on bearing capacity, and caused bearing displacement to stabilize rather than increase unchecked when the anchor bolts were removed at $AB = 0.00$.

Table 5.12 provides a comparison of recorded and predicted bearing forces for the Ss15 Abutment 2 bearings. In cases where the bolts ruptured, the recorded and predicted retainer values matched exactly because this ultimate capacity was explicitly defined in the bridge model (Section 2.2). Horizontal friction forces on the other hand, were estimated based on the superstructure dead load and a 0.6 coefficient of friction. In cases where the elastomer slid, the actual friction force was roughly 83% of predicted, for an effective coefficient of friction equal to 0.5. When predicting fuse capacity for the bearing assembly, the predicted peak elastomer and retainer forces were added, resulting in an overestimation of force capacity because these peak forces did not occur simultaneously. The recorded total bearing force was 40% to 70% of the value obtained by directly adding the recorded peak elastomer and retainer forces together.

Table 5.12. Recorded Versus Predicted Peak Transverse Bearing Forces (Abutment 2, Ss15 Bridge)

Bolt Dia (in)	Qualitative Fixed Bearing Response	Average Recorded Peak Transverse Bearing Force (kip)			Predicted Fuse Force (kip)		
		Elastomer	Retainer	Total Brg	Elastomer	Retainer	Total Brg
1.25	Bolts Yield	39	251	214	77	353	430
1.00	Bolts Yield	49	203	156	77	226	303
0.75	Bolts Fracture, Brg Slides	63	127	90	77	127	204
0.50	Bolts Fracture, Brg Slides	64	57	64	77	57	134
0.00	Bearing Slides	64	0	64	77	0	77

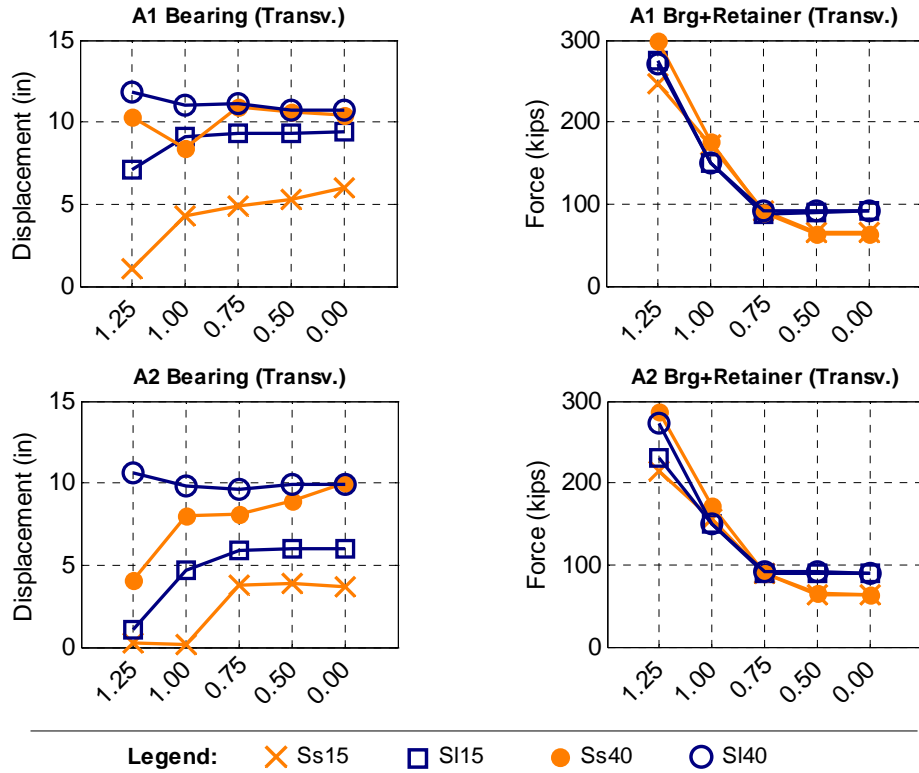


Figure 5.13. Variation in Peak Transverse Bearing Response at Abutments

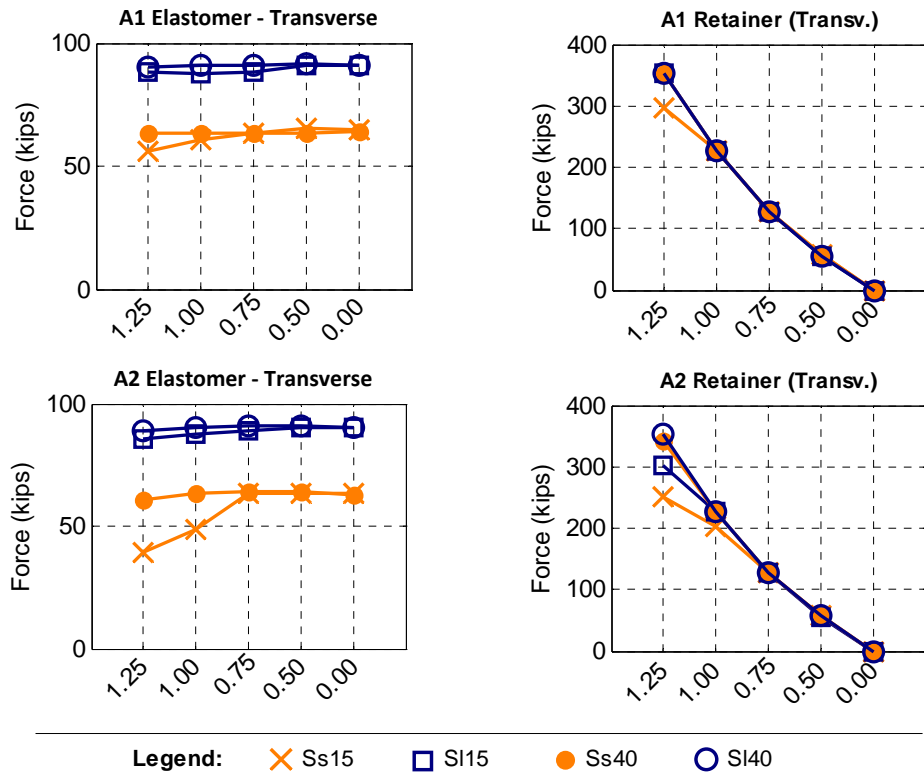


Figure 5.14. Variations in Peak Transverse Response of Abutment Bearing Components

5.2.3 Pier 1 Elastomeric Bearings

The transverse response of the elastomeric bearings at Pier 1 was affected by retainer anchor bolt diameter, but in contrast to the abutment bearings, the overall response was more dependent on the elastomer than the retainers. The relative importance of the elastomer is apparent from the similarities between bearing assembly response in Figure 5.15 and elastomer response in Figure 5.16.

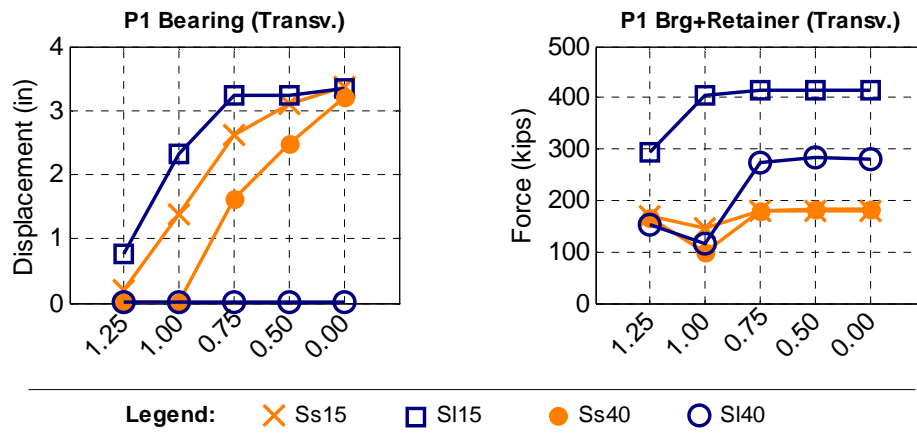


Figure 5.15. Variation in Peak Transverse Bearing Response at Pier 1

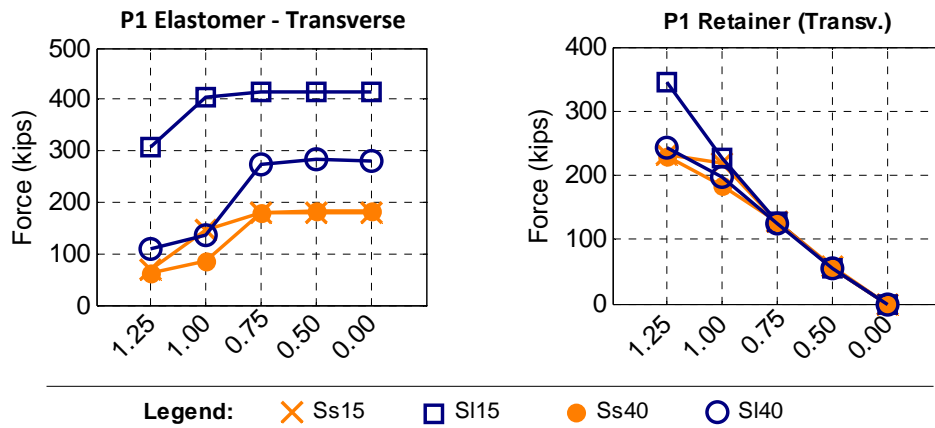


Figure 5.16. Variations in Peak Transverse Response of Pier 1 Bearing Components

The maximum anchor bolt diameter at which rupture could be achieved varied with bridge configuration. The SI15 anchors ruptured at AB = 1.25, followed by the Ss15 anchors at AB = 1.0 and finally the Ss40 and SI40 anchors at AB = 0.75. The post-rupture bearing response reflected purely elastic deformation for SI40, and a combination of deformation and sliding for the other bridges. The absence of a sliding response for SI40 was attributed to the effect of the

lower yield strength associated with the tall piers, and the high breakaway friction force required for the heavy SI superstructure. In combination, this created a pier system where the columns were likely to dominate the response rather than the bearings.

Table 5.13 provides a comparison of recorded and predicted peak bearing forces for the Ss15 Pier 1 bearings, and points to similar conclusions as Table 5.12 for the Abutment 2 bearings. Horizontal friction force was predicted based on the superstructure dead load and a 0.6 coefficient of friction. In cases where the elastomer slid, the actual friction force was roughly 87% of predicted, for an effective coefficient of friction equal to 0.53. Estimating total bearing fuse capacity as the sum of peak component capacities significantly overestimated capacity because these peak forces did not occur at the same time. The peak recorded total bearing force was 40% to 75% of the value obtained by directly adding the recorded peak elastomer and retainer forces together.

Table 5.13. Recorded Versus Predicted Peak Transverse Bearing Forces (Pier 1, Ss15 Bridge)

Bolt Dia (in)	Qualitative Fixed Bearing Response	Average Recorded Peak Transverse Bearing Force (kip)			Predicted Fuse Force (kip)		
		Elastomer	Retainer	Total Brg	Elastomer	Retainer	Total Brg
1.25	Bolts Yield	70	233	169	205	353	558
1.00	Bolts Fracture, Brg Slides	148	220	146	205	226	431
0.75	"	178	127	178	205	127	332
0.50	"	180	56	180	205	57	262
0.00	Bearing Slides	180	0	180	205	0	205

5.2.4 Pier 1 Columns

Force, displacement, and strain data for the Pier 1 column are shown in Figure 5.17, and with the exception of the SI40 bridge, variations in anchor bolt diameter modulated column performance. Taking the AB = 1.25 case as a starting point and working toward smaller diameter bolts, column demands noticeably decreased at the first anchor bolt size that allowed fracture. This trend was especially pronounced for the short-pier bridges. These columns initially had tension strains in excess of the rebar yield strain (indicated with a dashed red line in the strain plot), but following anchor bolt rupture, the strains dropped below the yield point and these columns were considered essentially elastic. This is an excellent response for the quasi-isolated

ERS, particularly given the relatively small 3 in. average sliding displacement shown in Figure 5.15.

The response of the Ss40 bridge was not quite as ideal, but anchor bolt fracture did result in reduced displacement and strain demands. As discussed in the previous section, the SI40 response was controlled by column yielding, and modifying anchor bolt diameter did not appreciably affect behavior. Though column yielding occurred in both the tall-pier bridges, the frequency and severity of damage was expected to be relatively low. The average response in Figure 5.17 falls within the serviceability strain limits, but when considering individual ground motions, some of the Ss40 and SI40 columns sustained damage. The number of runs with column yielding and damage is summarized in Table 5.14. No cases of severe damage were recorded, and overall, transverse column performance was quite good.

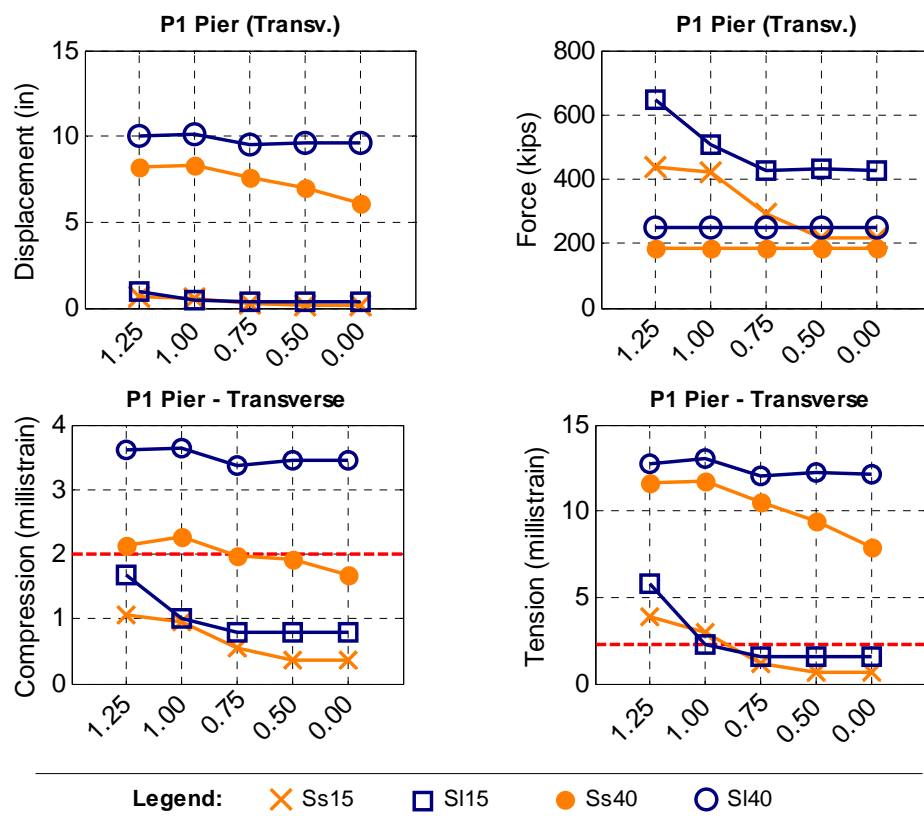


Figure 5.17. Variation in Peak Transverse Column Response at Pier 1

Table 5.14. Number of Transverse Runs with Yielding or Damage of Pier 1 Columns

		Short Steel (Ss) Superstructure				Long Steel (Sl) Superstructure			
		Short Pier (15 ft)		Tall Pier (40 ft)		Short Pier (15 ft)		Tall Pier (40 ft)	
		# Yield	# Dam.	# Yield	# Dam.	# Yield	# Dam.	# Yield	# Dam.
Anchor Bolt Dia. (in.)	1.25	9	n/a	10	2	10	n/a	10	2
	1.00	8	n/a	10	2	6	n/a	10	2
	0.75	n/a	n/a	10	n/a	n/a	n/a	10	3
	0.50	n/a	n/a	10	n/a	n/a	n/a	10	3
	0.00	n/a	n/a	10	n/a	n/a	n/a	10	2
	NFB	n/a	n/a	10	1	n/a	n/a	10	2

5.2.5 Pier 2 Fixed Bearings

Under transverse excitation, the fixed bearings at Pier 2 responded to anchor bolt variation with similar trends as the other transverse components discussed so far. When anchor bolt diameter was reduced, the fixed bearing anchors eventually fractured, accompanied by an increase in displacement and a reduction in force capacity. As shown in Figure 5.18, the short-pier bridges once again displayed the most pronounced response to bolt variation. The Ss40 bridge, with its taller columns did not experience anchor bolt fracture until AB = 0.5, after which the relatively light Short Steel superstructure made for a significant increase in sliding displacement at AB = 0.0. With the Sl40 bridge, anchor fracture was likewise delayed until AB = 0.5, but the much heavier Long Steel superstructure limited the magnitude of sliding. Recall that at Pier 1, no bearing sliding occurred for Sl40. The sliding observed at Pier 2 was only possible because the 0.6 friction coefficient used at Pier 1 to represent elastomer-on-concrete was reduced to 0.3, representing steel-on-neoprene for the fixed bearings.

Table 5.15. Peak Transverse Fixed Bearing Displacements (in.)

		Ss Bridges		Sl Bridges	
		15 ft Pier	40 ft Pier	15 ft Pier	40 ft Pier
Anchor Bolt Dia. (in.)	1.25	0.62	0.11	2.48	0.25
	1.00	2.48	0.15	6.14	0.40
	0.75	5.70	0.23	7.52	0.58
	0.50	6.13	1.38	7.50	1.18
	0.00	5.99	6.05	7.61	1.20
	NFB	5.61	2.48	6.45	0.00

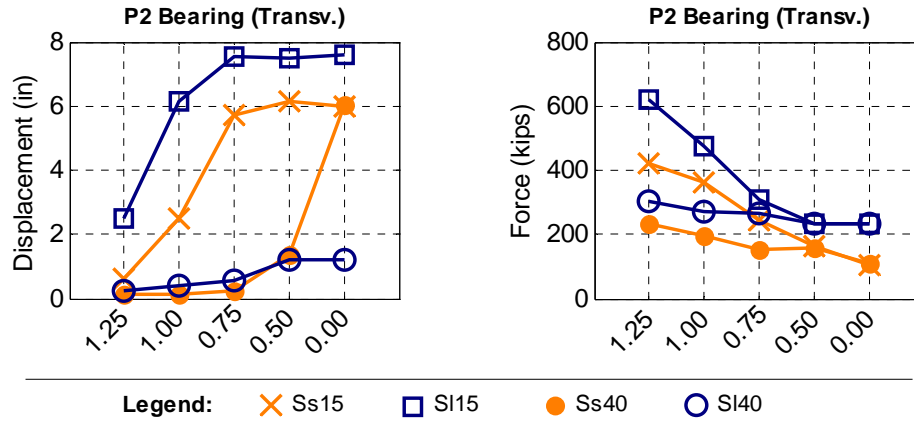


Figure 5.18. Variations in Peak Transverse Fixed Bearing Response at Pier 2

5.2.6 Pier 2 Columns

At Pier 2, the column response in short-pier bridges was strongly influenced by the anchor bolts used with the fixed bearings. This is suggested in part by the strong correlation between the Ss15 and SI15 bearing forces in Figure 5.18 with the column forces shown in Figure 5.19. Reductions in bolt diameter (and therefore bolt force capacity) produced an in-kind reduction of column forces, providing some capacity protection for the column. In contrast, reducing or even removing anchor bolts was insufficient to modify the Ss40 and SI40 column response, and these columns yielded in all cases.

The strain plots provide peak compression strains in the confined core and peak tension strains in the longitudinal steel reinforcing. The yield limit is shown with a red dashed line, and the damage limit, discussed in Chapter 4, is indicated with a solid red line. The short-pier bridges remained essentially elastic for all but AB = 1.25 whereas the SI40 bridge columns were at the damage limit. The Ss40 response was somewhere in between these two extremes. For AB = 1.25 through AB = 0.75, the fixed bearing anchors remained intact, requiring the column to accommodate all displacement. At these first three points then, column displacement approximately matched the superstructure displacement shown in Figure 5.12. Beyond AB = 0.75, superstructure displacement continued to increase, but the fixed bearing anchors had fractured, so some of the displacement was accommodated with the bearing element. The net effect was a beneficial reduction in column demands. Table 5.16 provides a summary of the number of runs with column yielding or damage, and for the Ss40 bridge, the number of runs

with damage dropped almost to zero after anchor bolts fracture. No instances of severe column damage were recorded.

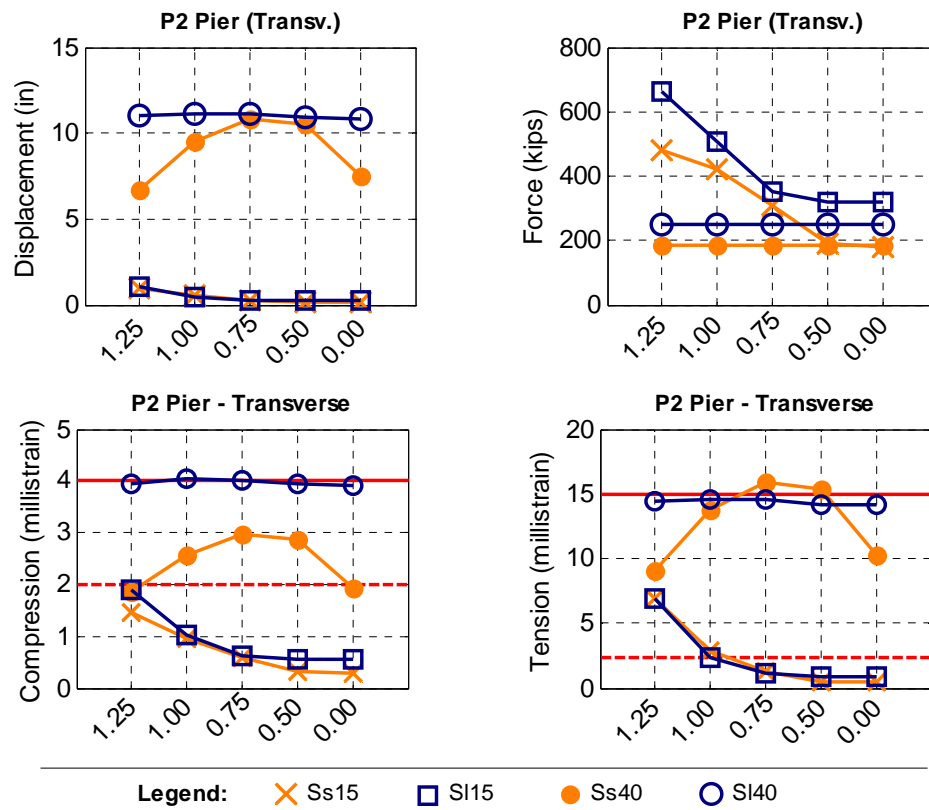


Figure 5.19. Variation in Peak Transverse Column Response at Pier 2

Table 5.16. Number of Transverse Runs with Yielding or Damage of Pier 2 Columns

		Short Steel (Ss) Superstructure				Long Steel (SI) Superstructure			
		Short Pier (15 ft)		Tall Pier (40 ft)		Short Pier (15 ft)		Tall Pier (40 ft)	
		# Yield	# Dam.	# Yield	# Dam.	# Yield	# Dam.	# Yield	# Dam.
Anchor Bolt Dia. (in.)	1.25	10	n/a	10	n/a	10	n/a	10	3
	1.00	8	n/a	10	4	5	n/a	10	5
	0.75	n/a	n/a	10	6	n/a	n/a	10	5
	0.50	n/a	n/a	10	4	n/a	n/a	10	5
	0.00	n/a	n/a	10	1	n/a	n/a	10	5
	NFB	n/a	n/a	10	1	n/a	n/a	10	2

5.2.7 Transverse Response Summary

Transverse response was much more influenced by anchor bolt diameter than the longitudinal response. Figure 5.20 summarizes the limit states reached by each bridge, and reduction in anchor bolt size frequently altered the occurrence of limit states.

		Short Steel (Ss) Superstructure														
		Short Pier (15 ft)						Tall Pier (40 ft)								
Anchor Bolt Dia. (in.)	1.25	EA	EP		P1	P2		EA	RA			P1	P2			
	1.00	EA	RA	EP	RP	Fb	P1	P2		EA	RA			P1	P2	
	0.75	EA	RA	EP	RP	Fb				EA	RA	EP	RP		P1	P2*
	0.50	EA	RA	EP	RP	Fb				EA	RA	EP	RP	Fb	P1	P2*
	0.00	EA	—	EP	---	Fb				EA	—	EP	---	Fb	P1	P2
	NFB	EA	—	EP	---	Fb				EA	—	EP	---	Fb	P1	P2

		Long Steel (Sl) Superstructure														
		Short Pier (15 ft)						Tall Pier (40 ft)								
Anchor Bolt Dia. (in.)	1.25	EA	RA	EP	RP	Fb	P1	P2		EA	RA				P1	P2
	1.00	EA	RA	EP	RP	Fb				EA	RA				P1	P2
	0.75	EA	RA	EP	RP	Fb				EA	RA		RP		P1	P2
	0.50	EA	RA	EP	RP	Fb				EA	RA		RP		P1	P2
	0.00	EA	—	EP	---	Fb				EA	—		---		P1	P2
	NFB	EA	—	EP	---	Fb				EA	—		---		P1	P2

Column damage at Pier 1 (P1*) or Pier 2 (P2*)

Columns only lightly damaged, but neither the Pier 1 or Pier 2 bearings fused

Columns only lightly damagedand bearings at one or both piers fused

Figure 5.20. Limit States that Occurred Under Transverse Excitation

For short-pier bridges (Ss15 and Sl15) the use of smaller anchor bolts was very effective at reducing column damage. Normally, full fusing of all retainers and fixed bearing anchors was achieved, followed by sliding on the concrete substructure. The friction between the bearings and substructure (or bearings and leveling pads in the case of fixed bearings) provided restraint that helped limit bearing sliding displacement, and sliding never led to bearing unseating or a risk of span loss.

The tall-pier bridges (Ss40 and Sl40) did not perform quite as well. Pier column yielding often dominated the response regardless of what anchor bolt size was selected. Full fusing of all

retainers and fixed bearings was less common than with the short-pier bridges, leading to more frequent and more severe pier damage. With that said, column strains never exceeded the upper bound of the damage limit state, so the life safe/no collapse criterion was always considered satisfied.

CHAPTER 6

CONCLUSIONS

This research investigated the sensitivity of quasi-isolated highway bridge seismic performance to variations in anchorage strength. The set of 24 analyzed bridges incorporated variations in substructure height, superstructure configuration, and bearing anchorage strength. Nonlinear numerical models developed for the earlier parametric study were used to represent the IDOT bearings and the full bridge system. The response of the bridge models to pure longitudinal and transverse excitation was assessed through nonlinear dynamic time-history analyses in OpenSees.

6.1 CONCLUSIONS FROM THE SENSITIVITY STUDY

The data from the sensitivity study point toward the following conclusions and observations:

6.1.1 General Observations

- For the Type I bearings used in the sensitivity study, bearing sliding never led to unseating or a risk of span loss.
- Yielding of the pier columns always occurred in the longitudinal direction and frequently occurred in the transverse direction. This was not the ideal response for quasi-isolation, particularly given that the column yielding often dominated the nonlinear response. The intent of the ERS was to use substructure yielding as a tertiary fuse following anchor fracture and bearing sliding, but in many of the sensitivity study runs, column yielding appeared to be the primary fuse. However, while some columns were damaged, all columns were expected to maintain sufficient structural integrity to satisfy the life safety/no collapse criterion.
- Bridges with heavy superstructures or tall piers were least influenced by anchor bolt variation. The columns tended to dominate the pier response, even when anchor bolts were completely removed. The friction at the bearing sliding interface was, by itself, often sufficient to transfer inertial forces from the superstructure that were large

enough to yield the piers. In this situation, the column strength, rather than the bearing anchorage strength, was the critical variable in system performance.

6.1.2 Longitudinal Observations

- Longitudinal response was largely insensitive to anchor bolt diameter and therefore, longitudinal performance calibration via anchorage strength has limited applicability.
- The backwall was a critical element in the longitudinal response, providing strength and stiffness that limited longitudinal displacements, but also limited the potential impact of anchorage strength on system behavior. The backwall and backfill were modeled with a simple flexural hinge and nonlinear spring. Given the degree of influence the backwalls had on longitudinal response, limitations of the current model should be kept in mind when interpreting the longitudinal data.
- Bridges with a light superstructure and short piers (i.e., Ss15) were responsive to anchor bolt calibration. Reducing the bolt diameter eventually allowed the fixed bearing anchors to fracture, and this significantly reduced column damage at the fixed bearing pier. Thus, for bridges similar to Ss15, longitudinal performance calibration via anchorage strength may have potential.

6.1.3 Transverse Observations

- Transverse response was much more influenced by anchor bolt diameter than the longitudinal response, and offers greater potential for calibration.
- In the transverse direction, once all retainer and fixed bearing anchors fused, the friction between the bearings and the substructure provided restraint that helped limit bearing sliding displacement.
- Bridges with short piers (i.e., Ss15 and Sl15) were responsive to anchor bolt calibration, and the use of smaller anchor bolts was effective at reducing column damage

6.2 FUTURE RESEARCH

Research into the seismic response of quasi-isolated highway bridge is ongoing, and some of the identified research needs are summarized below.

- The true backwall system involves complex structural interactions between the superstructure, backwall, wingwalls, approach slab, and fill. Consider evaluating longitudinal performance of the current OpenSees model through a sensitivity study focused on the backwall and backfill elements. This would be beneficial in interpreting the current results, and would provide insight into whether more detailed modeling of the backwall or backfill is advisable.
- Several bridges, particularly those with tall piers or heavy substructures, experienced column yielding regardless of anchor bolt diameter. A sensitivity study that introduced column diameter or column section properties as additional variables would determine the potential to achieve ideal quasi-isolated behavior in a broader range of bridge configurations.
- The response of the column elements was an essential aspect of system performance. Currently, the columns are modeled with lumped mass at the top and bottom. Consider a more refined representation where the mass is distributed to nodes along the column length.
- The 15 ft and 40 ft piers selected for this research were intended to represent the lower and upper bound of common bridge configurations in Illinois. Given the fairly significant differences in the response of short and tall-pier systems, consider introducing an intermediate pier height as a variable.
- This study focused on extremely regular bridge configurations, and future research should consider introducing some of the irregularities (e.g., skew) that commonly appear in practice.

REFERENCES

- American Association of State Highway and Transportation Officials (AASHTO). 2008. *LRFD Bridge Design Specifications*, Washington, DC: AASHTO.
- American Association of State Highway and Transportation Officials (AASHTO). 2009. *Guide Specifications for LRFD Seismic Bridge Design*, Washington, DC: AASHTO.
- Berry, Michael P., Dawn E. Lehman, and Laura N. Lowes. 2008. "Lumped-Plasticity Models for Performance Simulation of Bridge Columns." *ACI Structural Journal* 105 (3) (May 1): 270-279.
- Barth, K.E., and H. Wu. 2006. "Efficient Nonlinear Finite Element Modeling of Slab on Steel Stringer Bridges." *Finite Elements in Analysis and Design* 42(14–15):1304–1313.
- Buckle, I., M. Constantinou, M. Dicleli, and H. Ghasemi. 2006. *Seismic Isolation of Highway Bridges*. Special Report MCEER06-SP07. Buffalo, NY: Multidisciplinary Center for Earthquake Engineering Research.
- Building Seismic Safety Council (BSSC), 2000. *Prestandard and Commentary for the Seismic Rehabilitation of Buildings, FEMA-356*. Washington, DC: Federal Emergency Management Agency.
- Chang, C., and D. White. 2008. "An Assessment of Modeling Strategies for Composite Curved Steel I-Girder Bridges." *Engineering Structures* 30(11):2991–3002.
- Constantinou, M., A. Mokha, and A. Reinhorn. 1990. "Teflon Bearings in Base Isolation II: Modeling." *Journal of Structural Engineering* 116(2):455–474.
- Elwood, K.J., and M.O. Eberhard. 2006. "Effective Stiffness of Reinforced Concrete Columns." *PEER Research Digest* 2006(1).
- Fernandez, J.A., and G.J. Rix. 2008. "Seismic Hazard Analysis and Probabilistic Ground Motions in the Upper Mississippi Embayment." *Geotechnical Earthquake Engineering and Soil Dynamics Geotechnical Special Publication n181*. American Society of Civil Engineers.
- Filipov, E.T., L.A. Fahnestock, J.S. Steelman, J.F. Hajjar, J.M. LaFave, D.A. Foutch. 2013a. "Evaluation of Quasi-Isolated Seismic Bridge Behavior Using Nonlinear Bearing Models." *Engineering Structures* 49: 168-181.
- Filipov, E.T., J.R. Revell, L.A. Fahnestock, J.M. LaFave, J.F. Hajjar, D.A. Foutch, J.S. Steelman. 2013b. "Seismic Performance of Highway Bridges with Fusing Bearing Components for Quasi-Isolation." *Earthquake Engineering and Structural Dynamics*.

- Filipov, E.T. 2012. Nonlinear Seismic Analysis of Quasi-Isolation Systems for Earthquake Protection of Bridges. MS Thesis, University of Illinois at Urbana-Champaign, Urbana, IL.
- Ibarra, I.F., R.A. Medina, and H. Krawinkler. 2005. "Hysteretic Models That Incorporate Strength and Stiffness Deterioration." *Earthquake Engineering & Structural Dynamics* 34(12):1489–1511.
- Illinois Department of Transportation (IDOT), *Bridge Manual*. 2012. Springfield, IL: IDOT.
- Kowalski, M.J.. 2000. "Deformation Limit States for Circular Reinforced Concrete Bridge Columns." *Journal of Structural Engineering* 126:869-878.
- LaFave, J., Fahnestock, L., Foutch, D., Steelman, J., Revell, J., Filipov, E., and Hajjar, J. (2013a). *Experimental Investigation of the Seismic Response of Bridge Bearings*. Research Report No. ICT-13-002. Illinois Center for Transportation, University of Illinois at Urbana-Champaign.
- LaFave, J., Fahnestock, L., Foutch, D., Steelman, J., Revell, J., Filipov, E., and Hajjar, J. (2013b). *Seismic Performance of Quasi-Isolated Highway Bridges in Illinois*. Research Report No. ICT-13-015. Illinois Center for Transportation, University of Illinois at Urbana-Champaign.
- McKenna, F., S. Mazzoni, and G.L. Fenves. 2011. Open System for Earthquake Engineering Simulation (OpenSees) Software Version 2.2.0. University of California, Berkeley, CA. Available from <http://opensees.berkeley.edu/>.
- Mackie, K.R., K.J. Cronin, and B.G. Nielson. 2011. "Response Sensitivity of Highway Bridges to Randomly Oriented Multi-Component Earthquake Excitation." *Journal of Earthquake Engineering* 15(6):850–876.
- Mander, J.B., M.J.N. Priestley, R. Park. (1988). "Theoretical Stress-Strain Model for Confined Concrete." *Journal of Structural Engineering* 114(8):1804–1825.
- Roeder, C.W., and J.F. Stanton. 1991. "State of the Art Elastomeric Bridge Bearing Design." *ACI Structural Journal* 88(1):31–41.
- Scott, M.H., and G.L. Fenves. 2006. "Plastic Hinge Integration Methods for Force-Based Beam-Column Elements." *Journal of Structural Engineering* 132(2):244–252.
- Shamsabadi, A., K.M. Rollins, and M. Kapuskar. 2007. "Nonlinear Soil-Abutment-Bridge Structure Interaction for Seismic Performance-Based Design." *Journal of Geotechnical and Geoenvironmental Engineering* 133(6):707–720.
- Somerville, P., N. Smith, S. Punyamurthula, and J. Sun. 1997 (Oct.). *Development of Ground Motion Time Histories for Phase 2 of the FEMA/SAC Steel Project*. SAC/BD-97/04, Sacramento, CA: SAC Joint Venture.

- Steelman, J., L. Fahnestock, E. Filipov, J. LaFave, J. Hajjar, and D. Foutch. (2012). "Shear and Friction Response of Non-Seismic Laminated Elastomeric Bridge Bearings Subject to Seismic Demand." *Journal of Bridge Engineering* p.290.
- Vamvatsikos, D., and C.A. Cornell. 2002. "Incremental Dynamic Analysis." *Earthquake Engineering & Structural Dynamics* 31(3):491–514.
- Wilson, P., and A. Elgamal. 2010. "Bridge-Abutment-Backfill Dynamic Interaction Modeling Based on Full Scale Tests." In *Proceedings of the 9th U.S. National and 10th Canadian Conference on Earthquake Engineering*. EERI Publication. Toronto, ON, July 25–29, 2010.

APPENDIX A

NUMERICAL RESULTS

The organization of all tables in this appendix is outlined below for convenience. The tables present numerical results at $SF = 1.0$ for the 48 bridge variants in the parametric study. Results were tabulated for the longitudinal and transverse directions. As discussed in Chapter 4, each value in these tables was obtained by extracting the peak response from a set of individual time history runs, and then averaging the peak response over all ground motions in a suite. Supplemental information regarding interpretation of data in specific tables is given below.

Table No.	Content
1 - 2	Superstructure Displacement
3 - 10	Bearing Displacement
11 - 14	Pier Displacement
15 - 26	Pier Column Strain
27 - 36	Base Shear

Tables 1-2 Superstructure Displacement

Superstructure displacements were reported at Abutment 1, and measured as indicated in Figure A.2.

Tables 3-10 Bearing Displacement

Relative displacements were reported for bearing elements as defined in Figure A.2. This meant that elastic deformation was subtracted from total deformation to obtain a sliding displacement at either the elastomer on concrete cap interface (Type I) or top plate on PTFE pad interface (Type II – not included in sensitivity study). This calculation was not performed for the fixed bearings because there was relatively little elastic deformation. Instead, the total bearing displacement was directly reported.

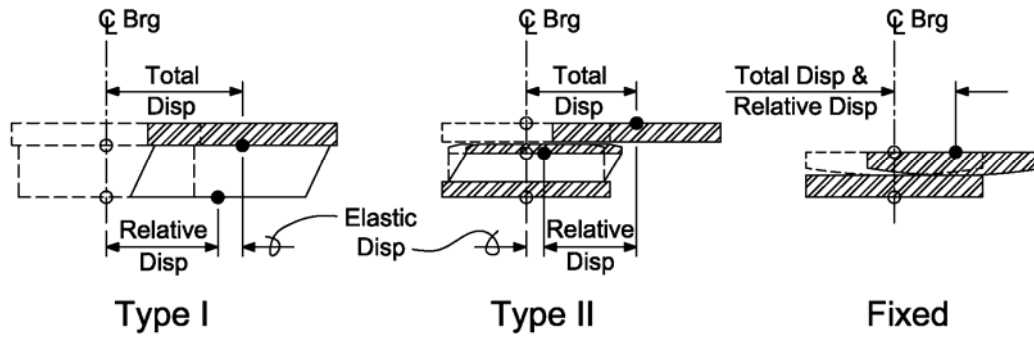


Figure A.1. Definitions of relative bearing displacement.

Tables 11-14 Pier Displacement

Relative pier displacement (Figure A.2) was reported as the top of pier displacement relative to bottom of pier displacement less any translation caused by rotation of the foundation element or the pier cap element.

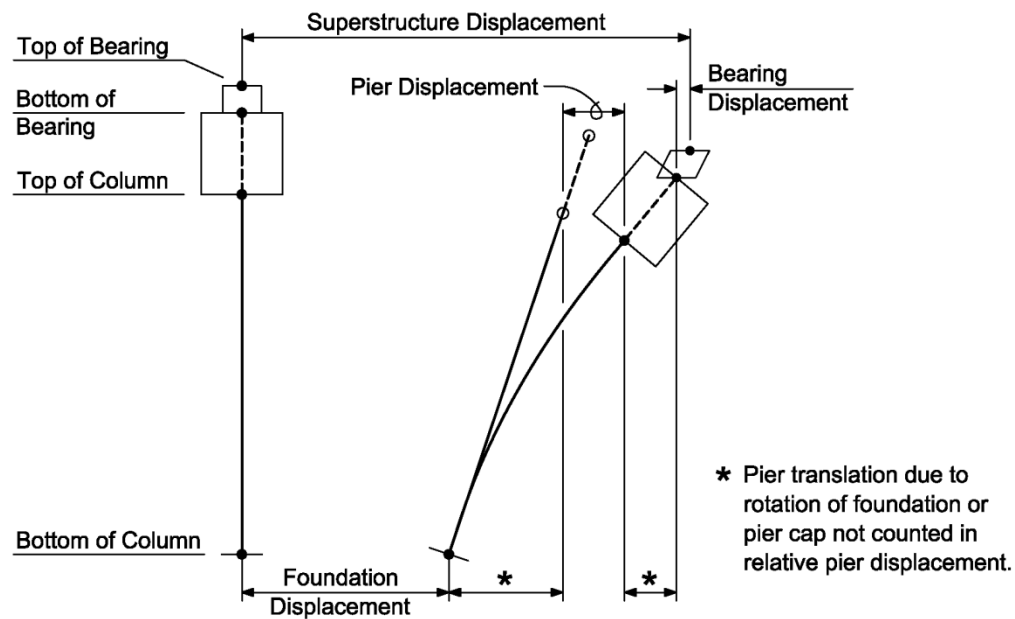


Figure A.2. Displacement definitions.

Table A.1. Peak Longitudinal Superstructure Displacement (in.)

		Short Steel (Ss) Superstructure				Long Steel (Sl) Superstructure			
		Short Pier (15 ft)		Tall Pier (40 ft)		Short Pier (15 ft)		Tall Pier (40 ft)	
		Avg	StdDev	Avg	StdDev	Avg	StdDev	Avg	StdDev
Anchor Bolt Dia. (in.)	1.25	4.43	0.55	6.53	0.44	6.05	0.82	9.12	0.74
	1.00	4.47	0.55	6.46	0.52	6.17	0.80	9.18	0.72
	0.75	4.54	0.50	6.54	0.68	6.29	0.81	9.12	0.70
	0.50	4.14	0.61	6.34	0.60	6.34	0.73	9.03	0.75
	0.00	4.11	0.61	6.31	0.71	6.36	0.78	9.13	0.79
	NFB	5.25	0.48	6.22	0.38	7.55	0.76	9.14	0.75

Table A.2. Peak Transverse Superstructure Displacement (in.)

		Short Steel (Ss) Superstructure				Long Steel (Sl) Superstructure			
		Short Pier (15 ft)		Tall Pier (40 ft)		Short Pier (15 ft)		Tall Pier (40 ft)	
		Avg	StdDev	Avg	StdDev	Avg	StdDev	Avg	StdDev
Anchor Bolt Dia. (in.)	1.25	2.95	0.64	12.90	3.54	9.32	2.95	14.16	3.29
	1.00	6.93	2.70	11.06	3.08	11.50	1.98	13.47	1.48
	0.75	7.64	2.14	13.60	2.37	11.68	2.34	13.49	1.50
	0.50	8.02	1.92	13.33	2.26	11.70	2.72	13.11	1.35
	0.00	8.76	2.73	13.09	1.73	11.80	2.52	13.16	1.56
	NFB	9.21	2.71	12.98	2.20	12.60	2.74	12.71	1.93

Table A.3. Peak Longitudinal Abutment 1 Bearing Displacement (in.)

		Short Steel (Ss) Superstructure				Long Steel (Sl) Superstructure			
		Short Pier (15 ft)		Tall Pier (40 ft)		Short Pier (15 ft)		Tall Pier (40 ft)	
		Avg	StdDev	Avg	StdDev	Avg	StdDev	Avg	StdDev
Anchor Bolt Dia. (in.)	1.25	3.16	0.75	5.41	0.92	4.30	0.58	7.37	0.62
	1.00	3.16	0.80	5.50	1.01	4.42	0.60	7.50	0.70
	0.75	3.16	0.82	5.50	0.83	4.54	0.62	7.44	0.72
	0.50	3.00	0.75	5.23	0.79	4.56	0.57	7.39	0.73
	0.00	2.96	0.81	5.14	0.73	4.57	0.64	7.45	0.80
	NFB	4.28	0.74	5.20	0.90	5.91	0.59	7.30	0.83

Table A.4. Peak Longitudinal Abutment 2 Bearing Displacement (in.)

		Short Steel (Ss) Superstructure				Long Steel (Sl) Superstructure			
		Short Pier (15 ft)		Tall Pier (40 ft)		Short Pier (15 ft)		Tall Pier (40 ft)	
		Avg	StdDev	Avg	StdDev	Avg	StdDev	Avg	StdDev
Anchor Bolt Dia. (in.)	1.25	3.46	0.52	4.93	0.54	4.25	0.80	7.29	0.71
	1.00	3.51	0.52	4.92	0.45	4.33	0.70	7.32	0.63
	0.75	3.59	0.55	5.04	0.94	4.45	0.74	7.28	0.69
	0.50	2.99	0.61	5.07	0.69	4.50	0.66	7.20	0.74
	0.00	2.93	0.59	5.16	0.72	4.51	0.67	7.21	0.79
	NFB	4.40	0.50	4.86	0.50	5.65	0.91	7.20	0.75

Table A.5. Peak Longitudinal Pier 1 Bearing Displacement (in.)

		Short Steel (Ss) Superstructure				Long Steel (Sl) Superstructure			
		Short Pier (15 ft)		Tall Pier (40 ft)		Short Pier (15 ft)		Tall Pier (40 ft)	
		Avg	StdDev	Avg	StdDev	Avg	StdDev	Avg	StdDev
Anchor Bolt Dia. (in.)	1.25	0.11	0.23	0.31	0.72	0.00	0.00	0.00	0.00
	1.00	0.22	0.28	0.27	0.61	0.00	0.00	0.00	0.00
	0.75	0.02	0.07	0.46	0.67	0.00	0.00	0.00	0.00
	0.50	0.07	0.22	0.35	0.57	0.00	0.00	0.00	0.00
	0.00	0.06	0.20	0.27	0.62	0.00	0.00	0.00	0.00
	NFB	0.38	0.41	0.25	0.48	0.00	0.00	0.00	0.00

Table A.6. Peak Longitudinal Pier 2 Bearing Displacement (in.)

		Short Steel (Ss) Superstructure				Long Steel (Sl) Superstructure			
		Short Pier (15 ft)		Tall Pier (40 ft)		Short Pier (15 ft)		Tall Pier (40 ft)	
		Avg	StdDev	Avg	StdDev	Avg	StdDev	Avg	StdDev
Anchor Bolt Dia. (in.)	1.25	0.09	0.01	0.12	0.01	0.12	0.01	0.08	0.01
	1.00	0.15	0.03	0.17	0.03	0.40	0.04	0.10	0.02
	0.75	0.52	0.07	0.37	0.08	0.73	0.13	0.35	0.06
	0.50	3.38	0.44	2.17	0.56	1.85	0.20	0.79	0.28
	0.00	3.39	0.44	2.65	0.74	1.80	0.21	1.08	0.25
	NFB	0.27	0.37	0.13	0.20	0.00	0.00	0.00	0.00

Table A.7. Peak Transverse Abutment 1 Bearing Displacement

		Short Steel (Ss) Superstructure				Long Steel (Sl) Superstructure			
		Short Pier (15 ft)		Tall Pier (40 ft)		Short Pier (15 ft)		Tall Pier (40 ft)	
		Avg	StdDev	Avg	StdDev	Avg	StdDev	Avg	StdDev
Anchor Bolt Dia. (in.)	1.25	1.06	0.71	10.28	3.59	7.10	2.94	11.78	3.29
	1.00	4.29	2.66	8.36	3.10	9.14	1.98	11.06	1.48
	0.75	4.91	2.13	10.91	2.37	9.32	2.35	11.11	1.52
	0.50	5.29	1.91	10.59	2.23	9.35	2.71	10.72	1.38
	0.00	6.03	2.73	10.38	1.73	9.45	2.52	10.76	1.57
	NFB	6.48	2.72	10.26	2.21	10.25	2.75	10.33	1.90

Table A.8. Peak Transverse Abutment 2 Bearing Displacement

		Short Steel (Ss) Superstructure				Long Steel (Sl) Superstructure			
		Short Pier (15 ft)		Tall Pier (40 ft)		Short Pier (15 ft)		Tall Pier (40 ft)	
		Avg	StdDev	Avg	StdDev	Avg	StdDev	Avg	StdDev
Anchor Bolt Dia. (in.)	1.25	0.26	0.31	4.09	3.09	1.11	0.55	10.61	4.68
	1.00	0.19	0.21	8.04	1.75	4.67	2.16	9.79	2.12
	0.75	3.80	1.62	8.13	2.01	5.88	2.84	9.61	2.31
	0.50	3.88	2.75	8.88	2.24	5.99	2.62	9.87	2.21
	0.00	3.65	2.06	10.06	1.99	5.95	2.67	9.88	2.17
	NFB	6.48	2.72	10.26	2.21	10.25	2.75	10.33	1.90

Table A.9. Peak Transverse Pier 1 Bearing Displacement

		Short Steel (Ss) Superstructure				Long Steel (Sl) Superstructure			
		Short Pier (15 ft)		Tall Pier (40 ft)		Short Pier (15 ft)		Tall Pier (40 ft)	
		Avg	StdDev	Avg	StdDev	Avg	StdDev	Avg	StdDev
Anchor Bolt Dia. (in.)	1.25	0.21	0.25	0.00	0.00	0.76	1.63	0.00	0.00
	1.00	1.39	1.63	0.00	0.00	2.33	1.95	0.00	0.00
	0.75	2.62	1.62	1.63	1.93	3.23	2.11	0.00	0.00
	0.50	3.09	1.97	2.49	1.57	3.23	2.32	0.00	0.00
	0.00	3.36	2.31	3.21	1.76	3.35	2.36	0.00	0.00
	NFB	5.61	2.76	2.48	1.71	6.45	2.76	0.00	0.00

Table A.10. Peak Transverse Pier 2 Bearing Displacement

		Short Steel (Ss) Superstructure				Long Steel (Sl) Superstructure			
		Short Pier (15 ft)		Tall Pier (40 ft)		Short Pier (15 ft)		Tall Pier (40 ft)	
		Avg	StdDev	Avg	StdDev	Avg	StdDev	Avg	StdDev
Anchor Bolt Dia. (in.)	1.25	0.62	0.17	0.11	0.02	2.48	1.60	0.25	0.06
	1.00	2.48	1.30	0.15	0.02	6.14	1.68	0.40	0.03
	0.75	5.70	1.66	0.23	0.03	7.52	2.16	0.58	0.05
	0.50	6.13	2.49	1.38	1.67	7.50	1.99	1.18	0.12
	0.00	5.99	2.09	6.05	1.60	7.61	2.15	1.20	0.12
	NFB	5.61	2.76	2.48	1.71	6.45	2.76	0.00	0.00

Table A.11. Peak Longitudinal Pier 1 Relative Pier Displacement (in.)

		Short Steel (Ss) Superstructure				Long Steel (Sl) Superstructure			
		Short Pier (15 ft)		Tall Pier (40 ft)		Short Pier (15 ft)		Tall Pier (40 ft)	
		Avg	StdDev	Avg	StdDev	Avg	StdDev	Avg	StdDev
Anchor Bolt Dia. (in.)	1.25	0.87	0.19	6.98	1.33	1.56	0.64	8.77	1.23
	1.00	0.88	0.18	6.93	1.13	1.66	0.64	8.88	1.24
	0.75	0.91	0.19	7.34	1.36	1.78	0.74	8.85	1.26
	0.50	0.80	0.16	7.14	1.32	1.81	0.69	8.78	1.25
	0.00	0.80	0.16	7.03	1.47	1.82	0.76	8.89	1.35
	NFB	1.13	0.22	6.38	0.79	3.23	0.77	8.36	1.20

Table A.12. Peak Longitudinal Pier 2 Relative Pier Displacement (in.)

		Short Steel (Ss) Superstructure				Long Steel (Sl) Superstructure			
		Short Pier (15 ft)		Tall Pier (40 ft)		Short Pier (15 ft)		Tall Pier (40 ft)	
		Avg	StdDev	Avg	StdDev	Avg	StdDev	Avg	StdDev
Anchor Bolt Dia. (in.)	1.25	3.44	0.46	5.70	0.41	4.67	0.66	7.80	0.66
	1.00	3.43	0.45	5.67	0.48	4.55	0.63	7.87	0.65
	0.75	3.33	0.42	5.86	0.70	4.44	0.64	7.89	0.69
	0.50	1.15	0.26	6.59	0.61	4.45	0.63	7.89	0.69
	0.00	1.10	0.25	6.84	0.85	4.43	0.61	7.94	0.79
	NFB	1.17	0.26	6.32	0.77	3.23	0.77	8.34	1.21

Table A.13. Peak Transverse Pier 1 Relative Pier Displacement (in.)

		Short Steel (Ss) Superstructure				Long Steel (Sl) Superstructure			
		Short Pier (15 ft)		Tall Pier (40 ft)		Short Pier (15 ft)		Tall Pier (40 ft)	
		Avg	StdDev	Avg	StdDev	Avg	StdDev	Avg	StdDev
Anchor Bolt Dia. (in.)	1.25	0.63	0.20	8.21	2.04	0.94	0.24	10.00	1.88
	1.00	0.51	0.09	8.35	2.83	0.47	0.04	10.14	1.83
	0.75	0.26	0.06	7.56	1.92	0.36	0.04	9.51	2.50
	0.50	0.16	0.02	6.96	2.27	0.36	0.03	9.63	2.25
	0.00	0.16	0.02	6.08	1.70	0.35	0.03	9.60	2.48
	NFB	0.17	0.01	7.34	2.01	0.37	0.02	9.58	2.62

Table A.14. Peak Transverse Pier 2 Relative Pier Displacement (in.)

		Short Steel (Ss) Superstructure				Long Steel (Sl) Superstructure			
		Short Pier (15 ft)		Tall Pier (40 ft)		Short Pier (15 ft)		Tall Pier (40 ft)	
		Avg	StdDev	Avg	StdDev	Avg	StdDev	Avg	StdDev
Anchor Bolt Dia. (in.)	1.25	0.99	0.40	6.74	1.86	1.08	0.16	10.99	2.85
	1.00	0.51	0.09	9.56	2.02	0.47	0.04	11.12	1.89
	0.75	0.28	0.04	10.83	2.09	0.27	0.02	11.13	2.28
	0.50	0.13	0.01	10.52	2.67	0.24	0.01	10.89	2.13
	0.00	0.12	0.01	7.45	1.57	0.24	0.02	10.85	2.15
	NFB	0.17	0.01	7.34	2.01	0.37	0.02	9.58	2.62

Table A.15. Peak Longitudinal Pier 1 Cover Concrete Compression Strain (millistrain)

		Short Steel (Ss) Superstructure				Long Steel (Sl) Superstructure			
		Short Pier (15 ft)		Tall Pier (40 ft)		Short Pier (15 ft)		Tall Pier (40 ft)	
		Avg	StdDev	Avg	StdDev	Avg	StdDev	Avg	StdDev
Anchor Bolt Dia. (in.)	1.25	1.45	0.33	2.07	0.48	3.06	1.83	2.74	0.54
	1.00	1.46	0.30	2.05	0.43	3.29	1.86	2.81	0.57
	0.75	1.52	0.31	2.18	0.49	3.63	2.19	2.79	0.58
	0.50	1.34	0.30	2.13	0.43	3.68	2.05	2.76	0.57
	0.00	1.35	0.30	2.13	0.55	3.73	2.26	2.80	0.61
	NFB	1.89	0.37	1.86	0.27	7.54	2.32	2.59	0.54

Table A.16. Peak Longitudinal Pier 1 Core Concrete Compression Strain (millistrain)

		Short Steel (Ss) Superstructure				Long Steel (Sl) Superstructure			
		Short Pier (15 ft)		Tall Pier (40 ft)		Short Pier (15 ft)		Tall Pier (40 ft)	
		Avg	StdDev	Avg	StdDev	Avg	StdDev	Avg	StdDev
Anchor Bolt Dia. (in.)	1.25	1.07	0.20	1.45	0.29	2.28	1.34	2.02	0.35
	1.00	1.08	0.18	1.44	0.27	2.44	1.36	2.07	0.37
	0.75	1.11	0.18	1.49	0.29	2.69	1.61	2.06	0.38
	0.50	1.00	0.21	1.48	0.24	2.71	1.51	2.04	0.37
	0.00	1.01	0.21	1.48	0.33	2.75	1.65	2.06	0.39
	NFB	1.33	0.23	1.32	0.16	5.45	1.72	1.92	0.35

Table A.17. Peak Longitudinal Pier 1 Steel Reinforcing Tensile Strain (millistrain)

		Short Steel (Ss) Superstructure				Long Steel (Sl) Superstructure			
		Short Pier (15 ft)		Tall Pier (40 ft)		Short Pier (15 ft)		Tall Pier (40 ft)	
		Avg	StdDev	Avg	StdDev	Avg	StdDev	Avg	StdDev
Anchor Bolt Dia. (in.)	1.25	3.53	1.41	6.30	2.33	7.08	4.65	6.75	2.05
	1.00	3.55	1.36	6.22	1.99	7.78	4.65	6.97	2.06
	0.75	3.81	1.44	7.02	2.37	8.65	5.38	6.91	2.11
	0.50	3.00	0.94	6.56	2.33	8.86	5.06	6.81	2.09
	0.00	3.03	0.96	6.37	2.48	8.98	5.60	6.97	2.22
	NFB	5.59	1.81	5.28	1.38	19.80	5.65	6.13	1.97

Table A.18. Peak Longitudinal Pier 2 Cover Concrete Compression Strain (millistrain)

		Short Steel (Ss) Superstructure				Long Steel (Sl) Superstructure			
		Short Pier (15 ft)		Tall Pier (40 ft)		Short Pier (15 ft)		Tall Pier (40 ft)	
		Avg	StdDev	Avg	StdDev	Avg	StdDev	Avg	StdDev
Anchor Bolt Dia. (in.)	1.25	6.66	1.36	1.71	0.16	11.45	2.06	2.30	0.27
	1.00	6.66	1.33	1.69	0.18	11.14	1.98	2.33	0.26
	0.75	6.48	1.27	1.74	0.22	10.83	2.06	2.33	0.29
	0.50	1.88	0.40	1.99	0.23	10.97	2.06	2.34	0.27
	0.00	1.82	0.40	2.11	0.31	10.87	1.98	2.40	0.37
	NFB	1.97	0.48	1.83	0.26	7.52	2.36	2.58	0.54

Table A.19. Peak Longitudinal Pier 2 Core Concrete Compression Strain (millistrain)

		Short Steel (Ss) Superstructure				Long Steel (Sl) Superstructure			
		Short Pier (15 ft)		Tall Pier (40 ft)		Short Pier (15 ft)		Tall Pier (40 ft)	
		Avg	StdDev	Avg	StdDev	Avg	StdDev	Avg	StdDev
Anchor Bolt Dia. (in.)	1.25	4.26	1.00	1.25	0.10	8.22	1.55	1.73	0.19
	1.00	4.27	0.99	1.23	0.11	8.00	1.50	1.75	0.18
	0.75	4.18	0.95	1.26	0.12	7.78	1.57	1.75	0.19
	0.50	1.30	0.21	1.42	0.14	7.90	1.59	1.75	0.18
	0.00	1.28	0.21	1.50	0.19	7.82	1.51	1.80	0.26
	NFB	1.38	0.29	1.31	0.16	5.43	1.76	1.92	0.36

Table A.20. Peak Longitudinal Pier 2 Steel Reinforcing Tensile Strain (millistrain)

		Short Steel (Ss) Superstructure				Long Steel (Sl) Superstructure			
		Short Pier (15 ft)		Tall Pier (40 ft)		Short Pier (15 ft)		Tall Pier (40 ft)	
		Avg	StdDev	Avg	StdDev	Avg	StdDev	Avg	StdDev
Anchor Bolt Dia. (in.)	1.25	24.60	3.40	4.36	0.65	30.71	4.58	5.18	0.92
	1.00	24.56	3.35	4.29	0.78	29.90	4.33	5.38	0.99
	0.75	23.63	3.07	4.57	1.15	29.08	4.41	5.39	1.09
	0.50	5.80	2.12	5.57	1.00	29.00	4.27	5.39	1.09
	0.00	5.32	2.07	5.94	1.38	28.92	4.18	5.56	1.22
	NFB	5.84	2.25	5.18	1.30	19.77	5.60	6.11	1.98

Table A.21. Peak Transverse Pier 1 Cover Concrete Compression Strain (millistrain)

		Short Steel (Ss) Superstructure				Long Steel (Sl) Superstructure			
		Short Pier (15 ft)		Tall Pier (40 ft)		Short Pier (15 ft)		Tall Pier (40 ft)	
		Avg	StdDev	Avg	StdDev	Avg	StdDev	Avg	StdDev
Anchor Bolt Dia. (in.)	1.25	1.45	0.37	3.26	1.03	2.30	0.49	4.96	1.06
	1.00	1.27	0.21	3.43	1.31	1.26	0.11	5.01	1.13
	0.75	0.69	0.14	2.99	0.77	0.99	0.10	4.64	1.57
	0.50	0.45	0.06	2.84	1.01	0.99	0.07	4.74	1.40
	0.00	0.45	0.05	2.46	0.66	0.98	0.07	4.73	1.55
	NFB	0.47	0.03	2.96	0.92	1.01	0.06	4.74	1.63

Table A.22. Peak Transverse Pier 1 Core Concrete Compression Strain (millistrain)

		Short Steel (Ss) Superstructure				Long Steel (Sl) Superstructure			
		Short Pier (15 ft)		Tall Pier (40 ft)		Short Pier (15 ft)		Tall Pier (40 ft)	
		Avg	StdDev	Avg	StdDev	Avg	StdDev	Avg	StdDev
Anchor Bolt Dia. (in.)	1.25	1.05	0.22	2.14	0.70	1.68	0.31	3.60	0.77
	1.00	0.95	0.14	2.28	0.86	0.99	0.08	3.63	0.84
	0.75	0.55	0.10	1.98	0.49	0.79	0.07	3.37	1.16
	0.50	0.37	0.05	1.91	0.66	0.79	0.05	3.45	1.03
	0.00	0.37	0.03	1.67	0.39	0.78	0.05	3.45	1.15
	NFB	0.38	0.03	1.98	0.59	0.81	0.05	3.45	1.20

Table A.23. Peak Transverse Pier 1 Steel Reinforcing Tensile Strain (millistrain)

		Short Steel (Ss) Superstructure				Long Steel (Sl) Superstructure			
		Short Pier (15 ft)		Tall Pier (40 ft)		Short Pier (15 ft)		Tall Pier (40 ft)	
		Avg	StdDev	Avg	StdDev	Avg	StdDev	Avg	StdDev
Anchor Bolt Dia. (in.)	1.25	3.89	1.64	11.58	3.30	5.80	1.93	12.76	2.95
	1.00	2.92	0.69	11.73	4.68	2.25	0.29	13.00	2.78
	0.75	1.18	0.35	10.48	3.29	1.57	0.22	12.08	3.74
	0.50	0.61	0.13	9.36	3.73	1.56	0.15	12.21	3.38
	0.00	0.60	0.09	7.94	2.88	1.54	0.16	12.14	3.72
	NFB	0.66	0.07	10.04	3.28	1.63	0.14	12.11	3.95

Table A.24. Peak Transverse Pier 2 Cover Concrete Compression Strain (millistrain)

		Short Steel (Ss) Superstructure				Long Steel (Sl) Superstructure			
		Short Pier (15 ft)		Tall Pier (40 ft)		Short Pier (15 ft)		Tall Pier (40 ft)	
		Avg	StdDev	Avg	StdDev	Avg	StdDev	Avg	StdDev
Anchor Bolt Dia. (in.)	1.25	2.16	0.73	2.75	0.85	2.62	0.32	5.46	1.88
	1.00	1.29	0.20	3.89	1.02	1.28	0.10	5.58	1.24
	0.75	0.75	0.11	4.53	1.26	0.76	0.05	5.54	1.44
	0.50	0.37	0.03	4.36	1.47	0.67	0.03	5.44	1.32
	0.00	0.35	0.03	2.95	0.78	0.68	0.04	5.41	1.32
	NFB	0.47	0.03	2.96	0.92	1.01	0.06	4.74	1.63

Table A.25. Peak Transverse Pier 2 Core Concrete Compression Strain (millistrain)

		Short Steel (Ss) Superstructure				Long Steel (Sl) Superstructure			
		Short Pier (15 ft)		Tall Pier (40 ft)		Short Pier (15 ft)		Tall Pier (40 ft)	
		Avg	StdDev	Avg	StdDev	Avg	StdDev	Avg	StdDev
Anchor Bolt Dia. (in.)	1.25	1.46	0.42	1.85	0.57	1.90	0.20	3.95	1.42
	1.00	0.96	0.14	2.55	0.70	1.01	0.07	4.03	0.95
	0.75	0.59	0.08	2.98	0.93	0.62	0.04	4.00	1.07
	0.50	0.31	0.02	2.86	1.04	0.55	0.03	3.94	0.98
	0.00	0.29	0.03	1.95	0.53	0.55	0.03	3.91	0.98
	NFB	0.38	0.03	1.98	0.59	0.81	0.05	3.45	1.20

Table A.26. Peak Transverse Pier 2 Steel Reinforcing Tensile Strain (millistrain)

		Short Steel (Ss) Superstructure				Long Steel (Sl) Superstructure			
		Short Pier (15 ft)		Tall Pier (40 ft)		Short Pier (15 ft)		Tall Pier (40 ft)	
		Avg	StdDev	Avg	StdDev	Avg	StdDev	Avg	StdDev
Anchor Bolt Dia. (in.)	1.25	6.94	3.36	9.00	3.08	6.85	1.36	14.40	4.14
	1.00	2.95	0.63	13.82	3.23	2.29	0.24	14.55	2.76
	0.75	1.34	0.26	15.87	3.13	1.09	0.10	14.63	3.35
	0.50	0.47	0.06	15.38	4.18	0.93	0.07	14.20	3.18
	0.00	0.42	0.06	10.32	2.47	0.93	0.08	14.15	3.20
	NFB	0.66	0.07	10.04	3.28	1.63	0.14	12.11	3.95

Table A.27. Peak Longitudinal Abutment 1 Base Shear (kips)

		Short Steel (Ss) Superstructure				Long Steel (Sl) Superstructure			
		Short Pier (15 ft)		Tall Pier (40 ft)		Short Pier (15 ft)		Tall Pier (40 ft)	
		Avg	StdDev	Avg	StdDev	Avg	StdDev	Avg	StdDev
Anchor Bolt Dia. (in.)	1.25	642	48	818	199	496	55	553	109
	1.00	665	57	932	394	506	52	570	114
	0.75	642	43	799	176	499	43	572	127
	0.50	632	37	769	159	491	38	571	109
	0.00	634	33	776	137	503	55	582	150
	NFB	686	66	817	197	523	73	570	93

Table A.28. Peak Longitudinal Abutment 2 Base Shear (kips)

		Short Steel (Ss) Superstructure				Long Steel (Sl) Superstructure			
		Short Pier (15 ft)		Tall Pier (40 ft)		Short Pier (15 ft)		Tall Pier (40 ft)	
		Avg	StdDev	Avg	StdDev	Avg	StdDev	Avg	StdDev
Anchor Bolt Dia. (in.)	1.25	643	55	709	112	489	40	591	155
	1.00	662	58	724	121	491	40	570	139
	0.75	650	50	821	290	490	44	586	133
	0.50	651	77	743	108	495	53	576	136
	0.00	619	39	733	83	502	69	564	103
	NFB	705	93	809	196	527	81	598	146

Table A.29. Peak Longitudinal Pier 1 Base Shear (kips)

		Short Steel (Ss) Superstructure				Long Steel (Sl) Superstructure			
		Short Pier (15 ft)		Tall Pier (40 ft)		Short Pier (15 ft)		Tall Pier (40 ft)	
		Avg	StdDev	Avg	StdDev	Avg	StdDev	Avg	StdDev
Anchor Bolt Dia. (in.)	1.25	201	21	122	13	282	9	134	17
	1.00	202	19	122	13	284	8	134	16
	0.75	205	17	119	11	286	7	134	16
	0.50	196	27	121	12	288	7	134	15
	0.00	197	26	121	10	288	7	134	16
	NFB	216	15	117	11	292	4	128	9

Table A.30. Peak Longitudinal Pier 2 Base Shear (kips)

		Short Steel (Ss) Superstructure				Long Steel (Sl) Superstructure			
		Short Pier (15 ft)		Tall Pier (40 ft)		Short Pier (15 ft)		Tall Pier (40 ft)	
		Avg	StdDev	Avg	StdDev	Avg	StdDev	Avg	StdDev
Anchor Bolt Dia. (in.)	1.25	229	10	121	8	289	8	128	14
	1.00	229	9	118	11	292	7	128	12
	0.75	228	9	116	7	293	7	128	9
	0.50	220	9	118	8	291	7	128	8
	0.00	219	8	118	10	291	6	129	12
	NFB	216	15	117	11	292	4	128	9

Table A.31. Peak Longitudinal Global Bridge Base Shear (kips)

		Short Steel (Ss) Superstructure				Long Steel (Sl) Superstructure			
		Short Pier (15 ft)		Tall Pier (40 ft)		Short Pier (15 ft)		Tall Pier (40 ft)	
		Avg	StdDev	Avg	StdDev	Avg	StdDev	Avg	StdDev
Anchor Bolt Dia. (in.)	1.25	1392	77	1444	179	1444	85	1262	147
	1.00	1417	79	1591	370	1458	73	1255	142
	0.75	1389	82	1490	301	1445	68	1270	124
	0.50	1293	96	1401	142	1448	66	1259	124
	0.00	1268	74	1378	123	1465	85	1246	127
	NFB	1502	118	1475	184	1510	78	1255	124

Table A.32. Peak Transverse Abutment 1 Base Shear (kips)

		Steel short (Ss) superstructure				Steel long (Sl) superstructure			
		Short (15 ft)		Tall (40 ft)		Short (15 ft)		Tall (40 ft)	
		Avg	StdDev	Avg	StdDev	Avg	StdDev	Avg	StdDev
Anchor Bolt Dia. (in.)	1.25	351	35	411	1	436	2	436	2
	1.00	284	2	286	4	308	3	308	2
	0.75	171	9	168	7	191	7	196	8
	0.50	83	11	78	0	94	6	98	16
	0.00	65	1	64	1	91	1	91	2
	NFB	63	1	63	1	89	1	92	2

Table A.33. Peak Transverse Abutment 2 Base Shear (kips)

		Short Steel (Ss) Superstructure				Long Steel (Sl) Superstructure			
		Short Pier (15 ft)		Tall Pier (40 ft)		Short Pier (15 ft)		Tall Pier (40 ft)	
		Avg	StdDev	Avg	StdDev	Avg	StdDev	Avg	StdDev
Anchor Bolt Dia. (in.)	1.25	289	32	397	17	379	24	437	3
	1.00	250	28	284	4	307	4	311	2
	0.75	169	7	168	6	193	8	196	8
	0.50	85	14	83	10	92	1	98	15
	0.00	64	2	63	1	90	2	91	2
	NFB	63	1	63	1	89	1	92	2

Table A.34. Peak Transverse Pier 1 Base Shear (kips)

		Short Steel (Ss) Superstructure				Long Steel (Sl) Superstructure			
		Short Pier (15 ft)		Tall Pier (40 ft)		Short Pier (15 ft)		Tall Pier (40 ft)	
		Avg	StdDev	Avg	StdDev	Avg	StdDev	Avg	StdDev
Anchor Bolt Dia. (in.)	1.25	444	40	213	13	648	32	269	9
	1.00	430	30	210	12	515	29	268	11
	0.75	301	40	208	13	432	34	269	9
	0.50	230	25	208	18	431	24	267	14
	0.00	229	20	204	15	428	26	267	13
	NFB	238	12	211	8	442	22	267	14

Table A.35. Peak Transverse Pier 2 Base Shear (kips)

		Short Steel (Ss) Superstructure				Long Steel (Sl) Superstructure			
		Short Pier (15 ft)		Tall Pier (40 ft)		Short Pier (15 ft)		Tall Pier (40 ft)	
		Avg	StdDev	Avg	StdDev	Avg	StdDev	Avg	StdDev
Anchor Bolt Dia. (in.)	1.25	490	23	214	16	669	15	276	12
	1.00	430	28	218	9	517	25	271	9
	0.75	317	35	216	12	355	19	274	9
	0.50	201	16	213	10	331	16	268	13
	0.00	194	15	215	13	332	19	269	12
	NFB	238	12	211	8	442	22	267	14

Table A.36. Peak Transverse Global Bridge Base Shear (kips)

		Short Steel (Ss) Superstructure				Long Steel (Sl) Superstructure			
		Short Pier (15 ft)		Tall Pier (40 ft)		Short Pier (15 ft)		Tall Pier (40 ft)	
		Avg	StdDev	Avg	StdDev	Avg	StdDev	Avg	StdDev
Anchor Bolt Dia. (in.)	1.25	1296	153	1074	83	1629	172	1261	96
	1.00	1040	124	805	100	1149	102	900	65
	0.75	634	105	551	46	853	67	696	28
	0.50	506	59	530	25	846	54	690	30
	0.00	495	40	526	26	850	54	691	27
	NFB	591	25	532	19	1049	45	694	28

APPENDIX B

GROUND MOTIONS

Results of time history analyses are, in general, markedly dependent on ground motion characteristics. Thus, every effort was made to select ground motions and scaling methods appropriate for southern Illinois. Table B.1 summarizes key ground motion characteristics, including the scale factor applied to the original record to produce the input ground motion at the design earthquake. Figures B.1 through B.10 show the soil (Pa) ground motions as scaled to the design earthquake. Among the ten ground motions, there were noticeable differences in duration, total number of cycles, and number of extreme cycles. These ground motion characteristics can be an important factor in determining seismic response of a nonlinear system.

Table B.1. Ground Motion Characteristics

Record ID	Record Length (s)	Scale Factor at SF = 1.0	Unscaled PGA	Scaled to SF = 1.0			V_{\max}/A_{\max}	Significant Duration (s)
				PGA (g)	PGV (in/s)	PGD (in)		
Pa01	43	1.86	0.45	0.83	41.7	41.0	0.13	19.7
Pa02	88	1.74	0.33	0.58	30.4	20.1	0.14	33.2
Pa03	58	1.81	0.39	0.70	27.7	14.4	0.10	29.7
Pa04	85	1.94	0.35	0.67	24.2	21.8	0.09	29.5
Pa05	88	1.92	0.32	0.62	29.5	96.8	0.12	28.6
Pa06	58	1.87	0.37	0.70	30.4	47.8	0.11	29.8
Pa07	45	1.52	0.39	0.59	29.8	15.6	0.13	19.8
Pa08	49	1.55	0.37	0.58	29.8	10.2	0.13	23.8
Pa09	42	1.34	0.51	0.68	25.8	14.5	0.10	22.9
Pa10	42	1.91	0.35	0.67	34.3	19.7	0.13	21.8

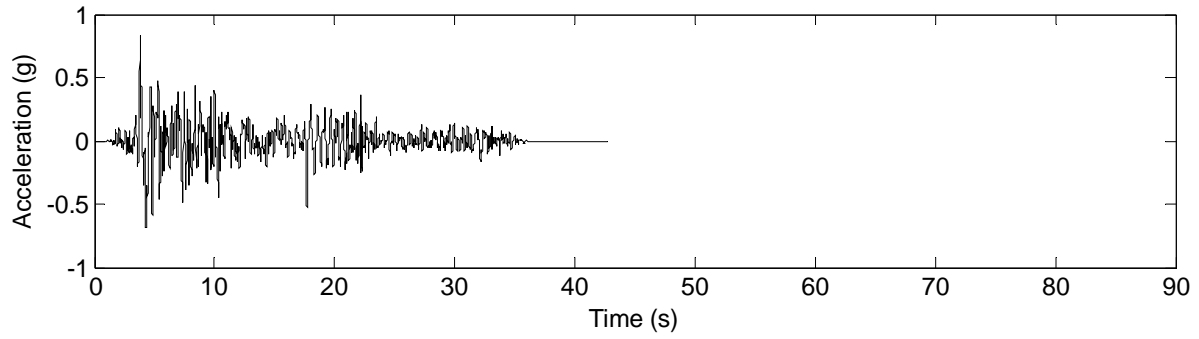


Figure B.1. Paducah 01 Ground Motion

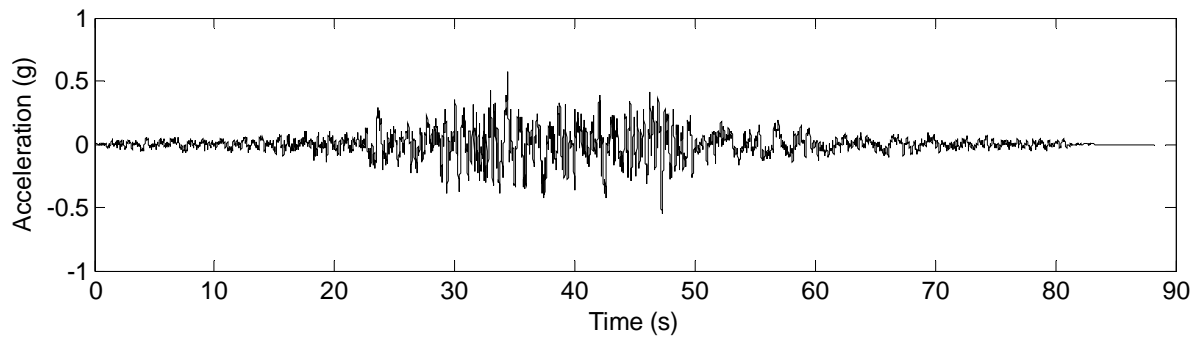


Figure B.2. Paducah 02 Ground Motion

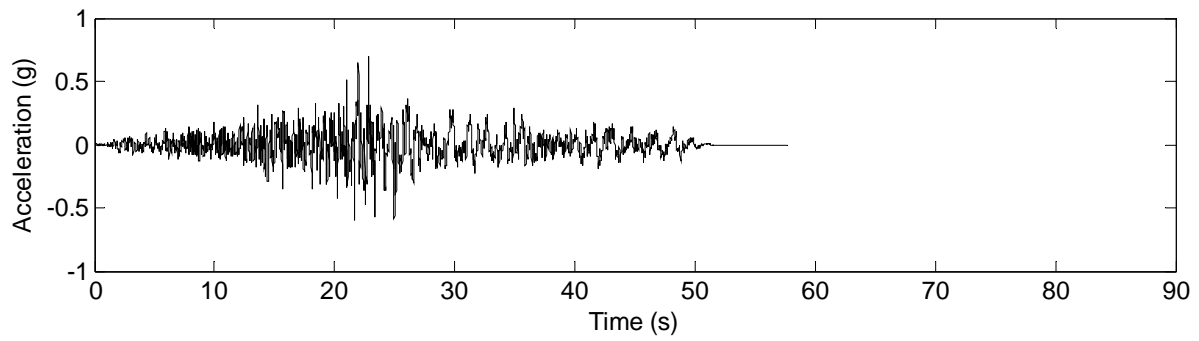


Figure B.3. Paducah 03 Ground Motion

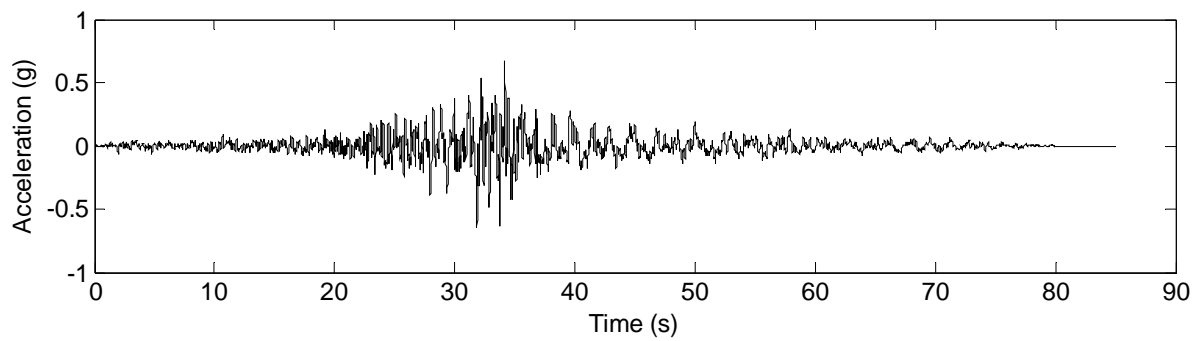


Figure B.4. Paducah 04 Ground Motion

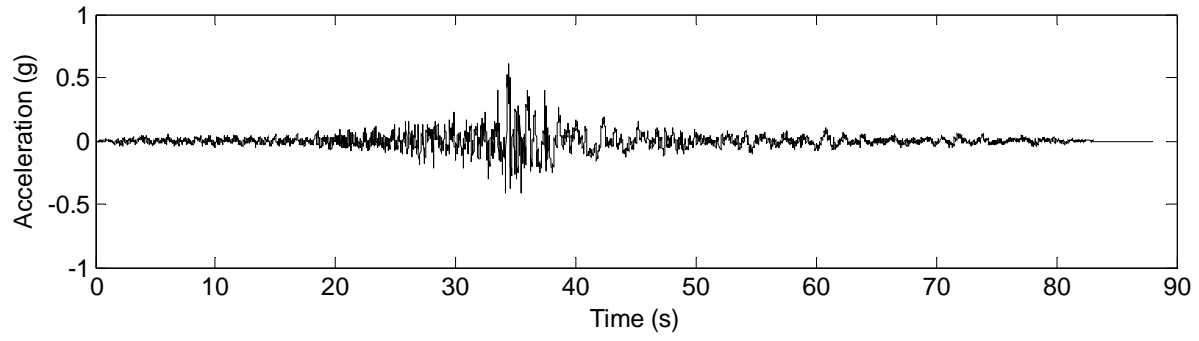


Figure B.5. Paducah 05 Ground Motion

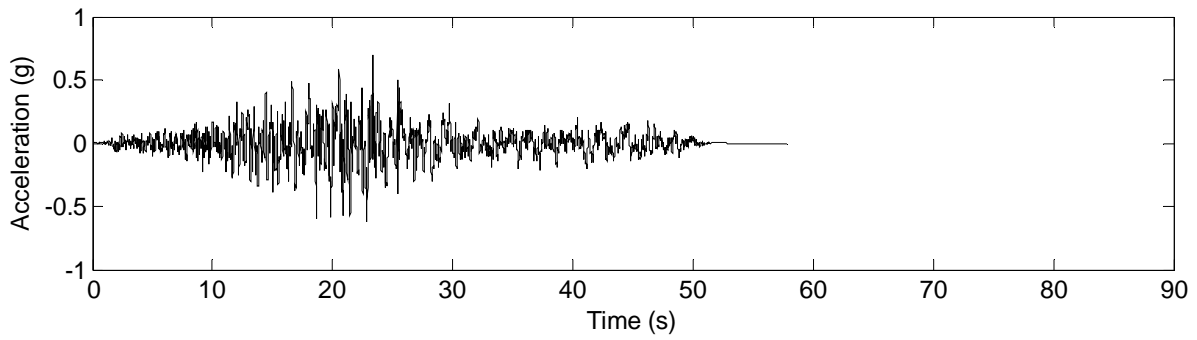


Figure B.6. Paducah 06 Ground Motion

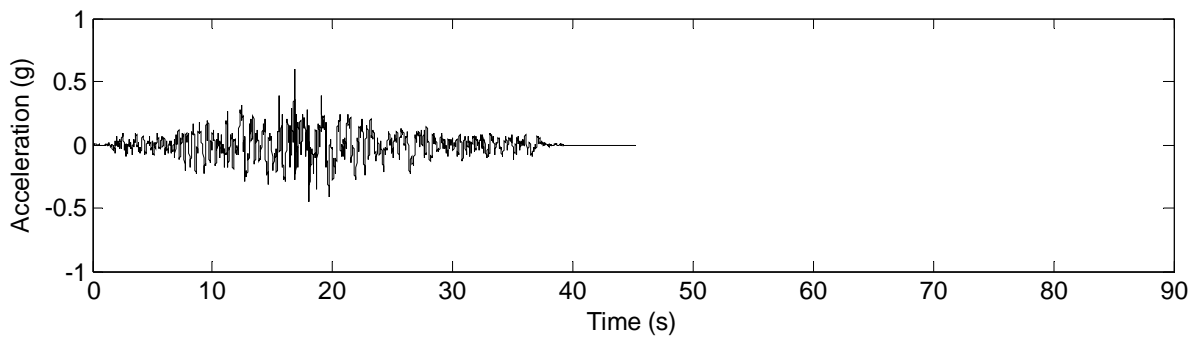


Figure B.7. Paducah 07 Ground Motion

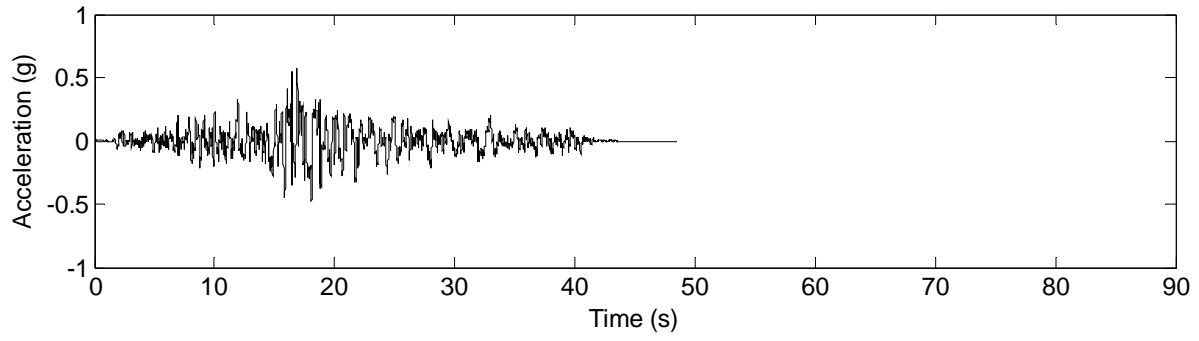


Figure B.8. Paducah 08 Ground Motion

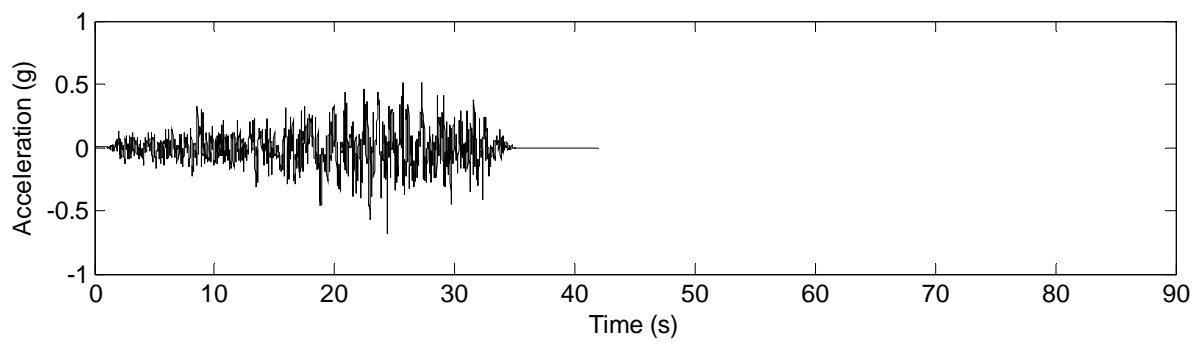


Figure B.9. Paducah 09 Ground Motion

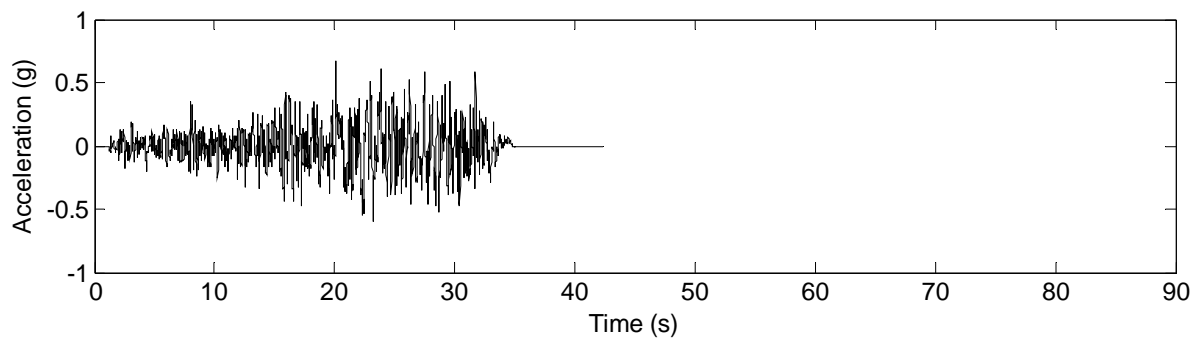


Figure B.10. Paducah 10 Ground Motion